



Hamburg University of Applied Sciences

Faculty of Life Sciences

Performance Optimization of Bifacial Module PV Power Plants Based on Simulations and Measurements

Master Thesis in Renewable Energy Systems

Submitted by

Míriam Guari Borrull

Matriculation number: XXXXXXXXXX

Hamburg, on 20th of May 2019

Reviewer (HAW- Hamburg): Prof. Dr. Timon Kampschulte

Reviewer (Enerparc AG): B.Sc. Armin Scherl

The thesis was created and supervised
in cooperation with Enerparc AG

Abstract

In contrast to monofacial photovoltaic (PV) systems, bifacial PV systems are able to harvest sunlight from both front and rear side, hence increasing the generated energy yield. The biggest contribution to the additional generated energy comes from the ground reflected irradiance, which depends on the module installation design. In this work, the optimum geometry of system design for bifacial PV power plants is found. For this objective, the individual and combined effect of the installation parameters on the energy yield of bifacial were studied through simulations and measurements. To empirically validate the used simulation model, measurements for different tilt angles were carried out and compared with the simulation results. In addition, a compilation of published data of the bifacial gain for bifacial PV plants with different system design geometry was done.

Analyzing the variance of the results of the simulations, it was found that the parameter that has the biggest contribution on the bifacial gain in energy (BGE) is the reflection of the ground surface. To study this effect, short-term measurements for different reflecting surfaces are carried out and compared with calculations based on the view factor. It was found that the BGE is directly dependent on the albedo of the surface by a factor of 0.40. Carried out simulations yielded bifacial gains of up to 30 % for a stand-alone module. For big scale power plants with a distance between rows of 2.3 m, bifacial gains of 4 % were yielded and by using a white reflective cover underneath the modules, BGE could be increased up to 8 %. It was also found that modules in large scale systems generate comparably lower energy levels up to 12 % less bifacial gain in comparison to neighboring modules due to large shadowing areas.

Declaration

To the best of my knowledge, I do hereby declare that this thesis is entirely the result of my own work. Information derived from published or unpublished work of others has been acknowledged in the bibliography.

Hamburg, 20th of May 2019

Signature:

Míriam Guari Borrull

Acknowledgments

Firstly, I would like to express my sincere gratitude to my professor and advisor Prof. Dr. Kampschulte, for training and caring for the new generation of engineers in the renewable energy systems field and for the continuous support, insights, and guidance for writing this thesis.

I would also like to thank Stefan Müller for giving me the opportunity to work in Enerparc AG and to Armin Scherl for his motivation, encouragement, and trust in my work, allowing this thesis to be my own work, but steering me in the right direction whenever I needed it.

Very special gratitude goes out to all my colleagues from Enerparc AG, who have always been open to help me in my work and for all the fun we have working together. It has been fantastic to write this thesis in such a supportive and friendly environment.

Finally, I must express my very profound gratitude to my family, for their moral and emotional support throughout my years of study and through the process of researching and writing this thesis. This accomplishment would not have been possible without you. Thank you.

Table of contents

1.	Introduction	12
1.1.	Objective	12
1.2.	Experimental approach.....	12
1.3.	Context	13
1.4.	Scope of work.....	13
1.5.	Motivation	13
2.	Bifacial solar technology.....	14
2.1.	Bifacial cell technology.....	14
2.2.	Bifacial module technology.....	15
2.3.	Definition of bifacial gain	16
2.4.	Bifacial market	17
3.	Applications for bifacial PV modules	19
3.1.	Small-scale bifacial PV tests	19
3.1.1.	Examples of small-scale bifacial PV tests.....	20
3.2.	Vertical bifacial PV systems	23
3.2.1.	Dual use applications.....	24
3.2.2.	Example of vertical bifacial PV system	25
3.3.	Horizontal floating bifacial PV systems.....	27
3.3.1.	Example for floating PV system.....	28
3.4.	Large-scale bifacial PV systems.....	28
3.4.1.	Example of large scale bifacial system.....	29
3.5.	Horizontal single-axis tracked bifacial systems	32
3.5.1.	Example for single-axis tracked bifacial PV system.....	32
3.6.	Recapitulation.....	33
4.	System design considerations.....	35
4.1.	Albedo	35
4.2.	Height	37
4.3.	Azimuth.....	38
4.4.	Size of the System	40
4.5.	Tilt angle.....	40
4.6.	Pitch.....	40
4.7.	Mounting structure	41

4.8.	Inverter sizing.....	42
5.	Indoor measurements	44
5.1.	General considerations	44
5.2.	Determination of bifaciality coefficient	45
5.3.	Indoor power generation gain measurement	48
6.	Outdoor measurements.....	50
6.1.	Long term measurements	50
6.1.1.	Location and setup.....	50
6.1.2.	Data Acquisition System	52
6.1.3.	Data Analysis	54
6.2.	Short term measurements	56
6.2.1.	Location and setup.....	56
6.2.2.	Data Acquisition System - HelioScale ϕ	57
6.2.1.	Data Acquisition System – HT I-V400W.....	58
6.2.2.	Methodology for the analysis of the short-term measurements.....	58
6.2.3.	Verification of the STC extrapolation from the HT I-V 400 W	59
6.2.4.	Effect of the size of the system in the bifacial gain.....	60
6.2.1.	Albedo measurement	63
6.2.1.	Effect of the reflective surface	65
6.2.2.	Effect of different tilt angle	69
7.	Simulations.....	73
7.1.	Parameters contribution rate.....	73
7.2.	Combined effect of the design elements.....	74
8.	Summary	79
9.	Bibliography.....	81
	Appendix A: Bifacial module LR6-60BP 290M datasheet.....	86
	Appendix B: Monofacial reference module REC Twinpeak 290 datasheet.....	87
	Appendix C: Helios Scale Phi	88
	Appendix D: I-V 400 W	89
	Appendix E: Measurements Table	90
	Appendix F: Simulations.....	91

List of Figures

Figure 2.1. Structure of a mono-facial solar cell (upper left), a mono-facial PV module (upper right), bifacial solar cell (lower left) and a bifacial PV module (lower right) [Guo13].	14
Figure 2.2. Cumulative bifacial PV installed capacity [Chu18].	18
Figure 3.1.a)-c) possible applications for bifacial modules and d) resulting in daily power generation curves compared to monofacial ones in the same configuration [Cze18].	19
Figure 3.2 Photograph showing the setup of monofacial and bifacial modules installed at the Prism Solar test, in Albuquerque [Ste17].	21
Figure 3.3 Field test site during summer. The white area of under the left array is crushed scallops' shells [Sug13].	22
Figure 3.4.a) Field test site during winter. Both arrays are practically under the same conditions. b) Under heavy snow conditions, snow gets stacked on the surface of the module [Sug13]	22
Figure 3.5 Simulated electricity output of a solar module in three different configurations:south-north-facing monofacial module ($MONO_{SN}$) at 37° , south-north-facing bifacial (Bi_{SN}) at 48° , and east-west-facing bifacial (Bi_{EW}) at 90° tilt angle on a minute-by-minute basis. [Sun18].	24
Figure 3.6 Pilot test of 28 kW vertical bifacial E-W oriented PV system in Saarland, Germany by Next2Sun [Hil17].	25
Figure 3.7 Energy yield for the small scale vertical bifacial East-West oriented bifacial PV plant in Saarland (Next2Sun) a) comparison of the specific monthly yield between vertical bifacial East-West oriented and a monofacial system South oriented; b) specific hourly energy yield [Hil17].	26
Figure 3.8 Fresnel reflection curve for the air-water interface at different incident angles [Lib18].	27
Figure 3.9 Pilot test of 5.5 kWp Bifacial PV system Sunfloat [Kre17].	28
Figure 3.10 Installed accumulated capacity of bifacial PV plant since 2011 [Kop16]	28
Figure 3.11 Large-scale power plant for fixed tilt angle, 1.25 MW, "Hokuto", Japan, by PVG Solutions [Ish16].	29
Figure 3.12 Large-scale power plant for fixed tilt angle, 2.5 MW, "La Hormiga", Chile, by MegaCell Group [Kop18]	30
Figure 3.13.a) Horizontal East-West oriented 400 kWp (front side only) bifacial PV plant b) System design parameters for the power plant [Ver17].	31
Figure 3.14.a) Power plant of 1.7 MW with single axis tracking in La Silla, Chile and b) portrait configuration of trackers with bifacial modules [Biz17].	32
Figure 3.15 Simulated electricity output of a solar module in two configurations: south-north-facing bifacial (Bi_{SN}) at 48° , and east-west-facing bifacial (Bi_{EW}) at 90° tilt angle on a minute-by-minute basis. [Sun18]	34
Figure 4.1 Effect of ground material albedo on bifacial gain of energy [Chu18].	35
Figure 4.2 Global albedo map from April 7-22, 2002. NASA [NAS02]	36
Figure 4.3 Evolution of ground Global horizontal irradiance (GHI), ground reflected Irradiance (GRI) and albedo (white pebbles) measurement by the albedometer on a 2-day period (01/04/16 to 02/04/16) in the Sandia National Laboratories in Albuquerque [Ste17].	36
Figure 4.4 Total irradiance on module rear side for elevations a) 1 m and b) 10 cm. [Sho15]	37
Figure 4.5 Effect of the height of the lowest side of the modules above the ground on the bifacial gain based on internal simulations of Longi Solar [Win18].	38

Figure 4.6 a) South facing horizontal module and b) East-West facing vertical module [Kha17].....	38
Figure 4.7 Global map showing energy yield ratio of optimally tilted Bi_{EW} over Bi_{SN} for three different scenarios: a) ground mounted with an albedo of 25%, b) ground mounted with an albedo of 50%, and c) 1 m elevated with an albedo of 0.5 [Sun18]. Tilted angles are optimized for all scenarios i.e. for Bi_{EW} is tilt angle 90° ; for Bi_{SN} optimum tilt angle is 48° according to Sun, Khan et al. [Sun18]	39
Figure 4.8 Simulated bifacial gain (%) of all modules in a field in El Gouna with an albedo of 50% [Sho15].	40
Figure 4.9 Effect of the GCR of the bifacial PV plant on the bifacial gain based on internal simulations of LG. Simulations were done for 1 MW system with fixed tilt structure and 2 rows of modules in landscape [LG].....	41
Figure 4.10 Idealized energy yield curves of photovoltaic systems with monofacial and bifacial modules [Ame17].	42
Figure 5.1. Setup for the indoor measurements at the University of Applied Sciences Hamburg.	44
Figure 5.2. Measured simulator's non-uniformity of irradiance on different points of the bifacial module to be tested.	45
Figure 5.3. Front- and rear-side set-up for indoor characterization of bifaciality [DIN17].....	45
Figure 5.4. Measured I-V curve for the front and the rear side of the bifacial module.	46
Figure 5.5. Measured spectral response of a bifacial solar module, front and rear side [Bon19a].....	47
Figure 5.6. P_{max} as a function of irradiance level on the rear side G_R or its 1-side equivalent irradiance G_E	49
Figure 6.1. Schematic showing the setup of monofacial and bifacial modules installed at Dornstedt in Germany for the long-term measurements. Red represents bifacial modules, green represents monofacial modules (Enerparc AG).....	51
Figure 6.2. Photograph showing part of the setup of monofacial and bifacial modules installed at Dornstedt in Germany (Enerparc AG)	51
Figure 6.3. Single line diagram for both bifacial a) and monofacial b) modules (Enerparc AG).....	52
Figure 6.4. Placement of the tables (Enerparc AG).....	52
Figure 6.5. Module temperature sensor	53
Figure 6.6. Ambient temperature sensor	53
Figure 6.7. Monthly specific energy yield for the entire time of generation of the power plant in Dornstedt (N 51.4179). The PV plant has a fixed tilt angle of 20° , pitch of 3.5 m, an elevation of 0.8 m and an estimated albedo of 18 %	54
Figure 6.8. Effect of the amount of snow underneath the modules in the bifacial gain. Measurements from a power plant in Dornstedt (N 51.4179) with a fixed tilt angle of 20° , pitch of 3.5 m, an elevation of 0.8 m and an estimated albedo of 18 % when there is no snow and 80 % with snow.....	55
Figure 6.9. Schematic showing the structure designed to carry out the short-term measurements a) without modules b) with modules. (Enerparc AG).	56
Figure 6.10. Structure used for the short-term outdoor measurements. Structure designed with four poles in the middle of the width and with four straps at each side in order to modify the tilt angle. a) without modules b) with modules.	56
Figure 6.11. Rotating Shadowband Irradiometer (RSI) from Hukseflux	57
Figure 6.12. Set up for the albedo measurement from Hukseflux, composed of two pyranometers; one facing the sky and the other facing the ground.....	58
Figure 6.13. Experimental set-up for the measurements for quantifying the effect of the neighboring modules.	61

Figure 6.14. Experimental set-up for the measurements of the power output of just the front side of the bifacial module.	61
Figure 6.15. Measured bifacial gain for each module of the measurements table on a sunny day at 15:00 h.	62
Figure 6.16. Measured bifacial gain for each module of the measurements table on a sunny day at 10:00 h.	63
Figure 6.17 Albedometer SRA20 [HUK18].	64
Figure 6.18. Used covers for the measurement of the effect of the albedo of the ground reflecting material and set-up for the albedo measurement.	65
Figure 6.19. Experimental set-up for the measurements of the effect of different albedos in the bifacial gain.	66
Figure 6.20. Function of the effect of the albedo in the bifacial gain for a single module with no shadow underneath it.	66
Figure 6.21. View factor between two surfaces.	67
Figure 6.22. The components of the reflected radiation to the rear side [Cha18].	68
Figure 6.23. Calculated and Measured power output (W) of a single module with 15 ° tilt angle and for different albedo values.	69
Figure 6.24. Measured power output during an entire day of a bifacial module with a front side power of 290 Wp and measured irradiance level for the same day.	70
Figure 6.25. Measured and simulated power output for a single module with a front side power of 290 Wp a) for 10° tilt angle and b) for 20° tilt angle.	70
Figure 6.26. Simulated yearly specific energy yield (kWh/kWp) for a single bifacial module with 290 Wp front side power output. With an elevation of 2 m, albedo of 44 % and different tilt angles.	71
Figure 6.27. Simulated yearly specific energy yield (kWh/kWp) for a power plant in Marlow (Germany) with an albedo of 44 %, a height between the lower side of the module and the ground of 0.7 m, a distance between rows of 2.3 m and different tilt angles [0°,90°].	72
Figure 7.1. Yearly specific energy yield (kWh/kWp) for different tilt angles of a bifacial power plant installed in Marlow (Germany) with different distances between rows and different number of module-rows per table, a ground albedo of 44 % and a height between the lowest side of the table and the ground of 0.7 m.	75
Figure 7.2. Measured and simulated power output for a single module with a front side power of 290 Wp a) for 10° tilt angle and b) for 20° tilt angle.	76
Figure 7.3 Effect of the tilted angle on a) energy yield and b) bifacial gain of energy. Data obtained from several simulations done with the program PVSyst for the period of a whole year for a 766 kWp PV plant located in Marlow (Germany) for south-north orientation, 6 modules per row, 2.3 m of distance between rows and different albedos and heights.	77

List of Tables

Table 2.1 Different advanced bifacial cell technologies and their respective bifaciality coefficient and efficiency [Chu18].....	15
Table 3.1 Most relevant properties for bifacial installations with “typical” installation conditions (south orientation, fixed tilt).....	20
Table 3.2 Description of the different setup configurations used at the Prism Solar test [Ste17, Gul18]	21
Table 3.3 Results of bifacial gain in energy (BGE) for snowy and non-snowy seasons and for different albedos [Sug13].....	23
Table 3.4 Description of the characteristics of the Pilot test of 28 kW vertical bifacial E-W oriented PV system Next2Sun [Hil17].	26
Table 3.5 Description of the characteristics of the large-scale power plant for a fixed tilt angle, 1.25 MW, “Hokuto”, Japan, by PVG Solutions [Lib18].....	29
Table 3.6 Description of the characteristics of the large-scale power plant for fixed tilt angle, 2.5 MW, “La Hormiga”, Chile, by MegaCell Group [Lib18].	30
Table 3.7 Description of the characteristics of the 400 kWp power plant with East-West orientation by Tempress [Ver17].....	31
Table 3.8 Description of the characteristics of the 1.7 MW power plant with single axis tracking in “La Silla”, Chile by Enel [Lib18].....	33
Table 3.9 Bifacial gains for various installation geometries.....	33
Table 5.1 Electrical characteristics of the bifacial module used for the indoor measurements from the datasheet of the fabricant and from the laboratory measurements (LR6-60BP 290M).....	44
Table 5.2 Electrical characteristics of the bifacial module used for the indoor measurements from the datasheet of the fabricant and from the indoor measurements (LR6-60BP 290M).....	46
Table 6.1 Type of modules in the PV plant.....	50
Table 6.2. Empirically determined temperature difference between the cell and the module back surface as a function of the module type mounting structures [Boy04]	60
Table 6.3. Pmax under STC comparison between the I-V curve tracer software and the calculated values.....	60
Table 6.4. Raw results of the measurements carried out to measure the impact of the shadowing of the neighboring modules for the power output and the bifacial gain.	62
Table 6.5. Measured albedos for each covering material used for the experiments.	65
Table 6.6. Measured bifacial gains for a single module with different covering materials underneath and a tilt angle of 15 ° on a sunny day.	66
Table 7.1. Analysis of variance (ANOVA).	73
Table 7.2. Simulated optimum tilt angle for different distances between rows and different number of module-rows with landscape orientation on the table. The simulated power plant has a nominal front-side-power of 766 kWp, an albedo of 44 % and a height over the ground of 0.7 m.	75
Table 7.3. Simulated bifacial gain for different distances between rows and different number of module-rows with landscape orientation on the table. The simulated power plant has a nominal front-side-power of 766 kWp, an albedo of 44 % and a height over the ground of 0.7 m.	75

Abbreviations

AC	Alternating Current	A
AG	Arbeitsgemeinschaft	
BGE	Bifacial Gain in Energy	%
Bifi	Bifacial	
BSTC	Bifacial Standard Test Conditions	
DC	Direct Current	A
DOE	Department Of Energy	
EEX prices	European Energy Exchange	
EGP	Enel Green Power	
EPEX	European Power Exchange	
EUPVSEC	European PV Solar Energy Conference	
GCR	Ground Coverage Ratio	%
GDP	Gross Domestic Product	
HJT	Heterojunction cell architecture	
HSAT	Horizontal Single-Axis Tracking	
IBC	Integrated Back Contact	
IEC	International Electrotechnical Commission	
ISC	International Solar Energy Research Center Konstanz	
LCOE	Levelized Cost Of Energy	€/kWh
NASA	National Aeronautics and Space Administration	
PERC	Passivated Emitter and Rear Cell	
PERT	Passivated Emitter Rear Totally Diffused	
PV	Photovoltaic	
RTC	Regional Test Centers	
STC	Standard Test Conditions	
SWCT	Smart Wire Connection Technology	

Symbols

φ	Bifaciality	%
η	Efficiency	%
g_{bifacial}	Bifacial gain	
e_{bifacial}	Specific energy yield with bifacial modules	kWh/kWp
$e_{\text{monofacial}}$	Specific energy yield with monofacial modules	kWh/kWp
Mon_{SN}	South-North facing monofacial module	
Bi_{SN}	South-North facing bifacial module	
Bi_{EW}	East-West facing bifacial module	
A_{module}	Module area	m ²
$A_{\text{entire surface}}$	Land surface area	m ²
V_{oc}	Open circuit voltage	V
I_{sc}	Short circuit current	A
P_{mpp}	Maximum power point power	W
I_{mpp}	Maximum power point current	A
φ_{Isc}	Short circuit current bifaciality coefficient	%
I_{sc_r}	Short-circuit current when the device is illuminated only on the rear side, at STC	A
I_{sc_f}	Short-circuit current when the device is illuminated only on the front side, at STC	A
P_{BSTC}	Power at BSTC	W
G_{rear}	Rear irradiance	W/m ²
G_{Ei}	1-side equivalent irradiance	W/m ²
rdg	Reading	
dgt	Digit	

1. Introduction

Bifacial technology is a new promising concept in the PV industry. In contrast to the monofacial modules, the bifacial technology can absorb light from both module sides, which can decrease the Levelized Cost Of Energy (LCOE) of photovoltaics. This cost reduction is caused by the additional energy gained from the extra reflected irradiance reaching the rear side of the modules. In order to determine the LCOE of bifacial modules and thus their profitability, it is necessary to determine exactly the energy gain. The determination of the gain in energy production for bifacial modules is more complex than the one for monofacial modules since besides from the tilt angle and the distance between module rows, it also depends on the module installation elevation, the ground albedo and the self-shadowing of the modules on the ground.

1.1. Objective

Bifacial modules is currently a largely discussed topic in the photovoltaics (PV) industry. The current bifacial's main challenge is the lack of standards to quantify the gain of this technology in comparison to monofacial technology. Moreover, there is also no guide to design bifacial plants optimally.

The aim of this work is to identify the optimal installation conditions for a bifacial power plant. Therefore, different installation scenarios for bifacial PV power plants are empirically examined to show the energy gain of each scenario. This provides general indicators for the design of a plant and helps engineers and practitioners to decide between bifacial or monofacial modules.

1.2. Experimental approach

After an introduction in the bifacial technology in chapter 2, a compilation of published data was done in order to get an overview of the state of the art and common practices for bifacial modules in chapter 3, identifying the significant design parameters to be analyzed. In chapter 4, literature for each of the significant design parameters and its effect in the bifacial gain was reviewed.

For measurements, a type of bifacial module was used as an example. In chapter 5, the properties of the used module were obtained through indoor measurements carried out in a laboratory. The indoor measurements provide information such as the bifaciality of the module and the power output under Bifacial Standard Test Conditions (BSTC).

Once analyzed the module that was used for the outdoor measurements, the yearly bifacial gain for a power plant with no artificial albedo and a distance between rows of 3.5 m was measured for a long term period in chapter 6. Bifacial gain could be calculated thanks to a monofacial reference system installed in the same power plant where measurements were carried out. Bifacial gains up to 6 % for the winter period and a yearly bifacial gain of 4 % were measured for an estimated albedo of 17 %.

Then, in order to identify the individual effect of certain installation parameters such as the size of the system and the ground albedo, short term outdoor measurements were carried out. For the analysis of the tilt angle, since it varies with the sun's latitude and direction of incidence, which vary during the entire year, the analysis of the optimum tilt angle and the impact of it combined with other system design parameters was done by several simulations. To validate the simulation model, this was compared with measurements taken for different tilt angles.

Finally, the combined effect of all parameters was summarized and interpreted in chapter 7, where additionally, conclusions on the optimal installation conditions for a bifacial power plant were drawn.

1.3. Context

With more than 2.5 GW of installed PV power, Enerparc AG has been for many years working in the technological and commercial evolution of solar energy systems. In the still growing photovoltaic industry, Enerparc AG is always upgrading and optimizing its solar power plants in order to maximize the installed capacity.

In recent years, bifacial technology has gained much attention in the PV industry. Hence, it is of great interest to the company to get to know this technology and how much more power output is to be expected out of it. Bifacial PV modules and systems have the clear potential to surpass monofacial ones as there are many conditions where the total amount of light on both sides leads to higher energy generation than a monofacial module installed with the optimum tilt angle. Nevertheless, the field performance of bifacial modules is highly dependent on the system design.

In the future, Enerparc AG might start using bifacial solar modules instead of monofacial. Therefore, it is of great importance to find out the best system design according to the company standards.

1.4. Scope of work

The gain in energy production for bifacial modules can be expressed as a function of the irradiance reaching the rear side of the module, which depends on the module installation height, the tilt angle, the ground albedo, the distance between module rows and the self-shadowing of the modules on the ground. In this work, the individual and combined impact of those parameters on the gain in energy is investigated.

1.5. Motivation

A nation's Gross Domestic Product (GDP) and therefore, its economic growth and prosperity, are directly connected to its energy consumption. Currently, according to the International Energy Agency [IEA19], almost 80 % of the global energy consumption is based on fossil fuels. This high fossil fuel consumption is causing environmental and health problems due to the increase in CO₂, NO_x and SO₂ emissions. With the emergence of several developing economies and the exponential growth of the human population, the rising demand for energy cannot be sustainably met by fossil fuels.

Renewable energies offer an ecological alternative to fossil fuels and are already playing an important role in the energy market. Collecting the sun's energy and directly converting it into electricity using photovoltaic modules is expected to play a big role in the future. This can be explained due to the fact that, especially since 2008 [BSW19], photovoltaic systems have achieved a comparably lower Levelized Cost Of Energy (LCOE). Bifacial technology appears in this context as an evolution of the monofacial modules and pulled by the motivation of finding lower LCOE for PV systems.

2. Bifacial solar technology

Bifacial PV consists mainly of solar cells that are light sensitive on both sides. The optimization needed to make the rear side of a cell receptive for sunlight absorption is primarily printing a rear metallization pattern that is similar to the front side. The bifacial concept also requires some changes at the module level; the key effort is to replace the traditional opaque backsheet either with a transparent backsheet or with glass. Figure 2.1 shows an example of mono and bifacial solar cell and their corresponding module structure.

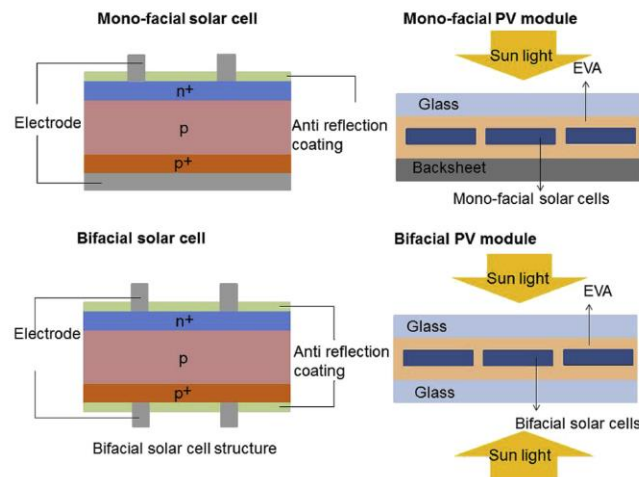


Figure 2.1. Structure of a mono-facial solar cell (upper left), a mono-facial PV module (upper right), bifacial solar cell (lower left) and a bifacial PV module (lower right) [Guo13].

In Figure 2.1 the depicted bifacial solar cell example has a p-PERC architecture, besides from this one, there are more other types of cell architectures that are bifacial. In this chapter, an overview of bifacial solar technology is presented at the cell and module level, the system design level will be presented in further chapters. In addition, a short introduction to the bifacial market can also be found in this chapter.

2.1. Bifacial cell technology

Bifacial solar cells enable the absorption of sunlight from both sides. However, the amount of electrical power generation is not simply doubled since the front and the back side do not have the same efficiency. This happens because, in back illumination, most of the charge carriers are generated away from the junction, which is located in the top of the cell, hence collection efficiency is lower than the one of the front side [Dur12]. The ratio between the efficiency of the rear side over the efficiency of the front side is called the bifaciality coefficient.

The choices to go bifacial at the cell level are mainly among three commercial cell architectures: PERC, PERT, and heterojunction (HJT). Depending on the used materials and production tools, there are other several subsections coming out of these technologies. Even the IBC cell structure is a possible candidate for bifacial if some optimization is applied. Each of these advanced cell technologies exhibits a different bifaciality coefficient and efficiency. The higher the bifaciality factor and the efficiency of the cell, also the higher the production complexity and the costs. Table 2.1 summarizes the different advanced cell technologies and their respective bifaciality and efficiency.

Table 2.1 Different advanced bifacial cell technologies and their respective bifaciality coefficient and efficiency [Chu18]

Cell technology	Bifaciality (φ)	Efficiency (η_{cell})
PERC	~ 70-80 %	~ 16 %
IBC	> 80 %	~ 19 %
n-PERT	90 %	~ 20 %
HTJ	> 90%	~ 20 %

Even though PERC technology has the lowest bifaciality coefficient, it is the predominant one in the market since it is the most spread and almost has become a standard in the p-type monocrystalline industry. Moreover, in terms of production, there is no additional cost to turn monofacial PERC cell into a PERC bifacial cell, because it only requires to replace the aluminium back surface field with a rear contact grid [Chu18]. According to W. Wahl, Head of Product Management, Chief Engineer of LONGI Solar Technology GmbH, Mono p-PERC bifacial technology is the best choice for low LCOE [Wah19].

2.2. Bifacial module technology

At the module level, not many changes have to be applied to turn a standard module into a bifacial one. The major change to go bifacial is to make the rear cover transparent in order to facilitate the absorption of sunlight from the rear side. This can be done by using glass or transparent backsheets. While glass is the current state of the art, backsheets suppliers like DuPont are working hard to promote transparent backsheets. In addition, bifacial solar modules require a different junction box design. Moreover, implementing new suitable interconnection approaches helps to maximize the benefits of the bifacial architecture.

Glass-Glass

PV manufacturers are increasingly evaluating glass-glass configurations, which has given them the confidence to extend modules performance warranty. Several module manufacturers offer up to 30-year performance warranties for double glass modules. Another benefit from the double glass structure is that it enables to avoid the usage of the expensive aluminium frame.

However, even though eliminating the aluminium frame makes the module lighter, reduces the costs for module manufacturers and avoids dust accumulation, the absence of the frame increases the risk of module breakage during transportation and installation. Moreover, in comparison with the case of transparent backsheets, for glass-glass modules, there is no systematic installation method, which leads to higher installation costs. In addition, glass-glass modules are around 20 % heavier than monofacial modules [Chu18].

DuPont presented in the PV Operations Europe 2019, based on 1 GW data, that after 4 years of operation 35 % of glass-glass modules present defects such as delamination, cracking and yellowing [Gar19].

Transparent Backsheets

Manufacturers of transparent backsheet present it as a long-time proven solution for bifacial. The benefits of the usage of the transparent backsheet are that it weighs less and is easy to handle, like the monofacial modules with opaque backsheet. Moreover, the module fabrication process for bifacial technology with transparent backsheet does not change at all. For hot regions, it also makes sense to use the transparent backsheet since its heat dissipation is much better and it results in a lower cell operating temperature.

During the PVMagazine Webinar “New approach for bifacial modules and yield expectations”, A. Viaro from Jinko Solar affirmed that even though double glass modules have higher transparency than the alternative backsheet, both have the same bifaciality and that the price of both glass and transparent backsheet are very comparable.

Interconnection

Optimization for the interconnection of bifacial cells in a bifacial module is required especially regarding heating and cooling of the cell. The gain due to bifaciality mainly reflects in increased currents, which also increases the losses. Thus, the approach of half-cut cells is very effective for interconnecting bifacial cells, which reduce resistance losses by $1/4^{\text{th}}$, provides an instant power boost of [Chu19], lower operating temperature, lower sensitivity on inhomogeneous ground reflections and better partial shade performance [Wah19].

Shingles is an extrapolation of half-cut cells, both in manufacturing effort as well as power boost. It consists of interconnecting cells directly by placing them onto each other. Cells are sliced into a number of strips along the busbars, which reduces the current and thus reduces the load on the fingers [Chu19].

Advanced interconnection approaches such as multi busbars or Smart Wire Connection Technology (SWCT) offered by Meyer Burger, help in increasing bifaciality, in particular for PERC.

Junction Box

The junction box is recommended to be installed or moved so that it does not cover the cells rear side in bifacial modules. New junction box designs that can be placed at the corners are already commercially available.

2.3. Definition of bifacial gain

In the following chapters, the term “bifacial gain” will be used very often. It is one of the most useful ways to visualize the benefits of bifacial modules and, together with the total cost of installing and operating the bifacial PV system, determines the LCOE (€/kWh) and thus the economic viability of bifacial PV.

The bifacial gain means the difference in the energy yield between a bifacial and a monofacial device or system under identical installation configurations. The energy yield is typically analyzed in kWh/kWp. The kWp data usually reflects the STC front-side measurement of the bifacial module. In order to make the most direct comparison possible, devices of similar type and with the same front-side

efficiency are to be compared. Bifacial devices with the back side covered are also a good option to measure the bifacial gain, this comparison reveals precisely what additional energy yield is provided by the rear side only. Nevertheless, even if the monofacial solar cell has similar properties as the bifacial, it will lead to small deviations, as the white backsheet is causing additional reflection of the front-incoming light into the solar cell.

According to the research group from the International Solar Energy Research Center (ISC) Konstanz, the bifacial gain is calculated using the following equation:

$$g_{bifacial} [\%] = \left(\frac{(e_{bifacial} - e_{monofacial})}{e_{monofacial}} \right) \times 100 \quad (2.1)$$

With

- $g_{bifacial}$: bifacial gain (%)
- $e_{bifacial}$: specific energy yield (kWh/kWp) of the PV device or system with bifacial modules
- $e_{monofacial}$: specific energy yield (kWh/kWp) of the PV device or system with monofacial modules on the same site, with the same configuration and during the same time period.

As mentioned, it is very important that the monofacial reference device is as similar as possible to the bifacial device to be analyzed. The temperature coefficient is another important point and should be in consideration. Otherwise, if the bifacial module has a lower temperature coefficient than the monofacial reference module, a significant part of the bifacial gain could be attributed to bifaciality when it would be actually due to the reduced temperature losses.

2.4. Bifacial market

During the Bifacial PV World workshop 2018 in Denver, Kopecek R. *et al.* [Kop18] presented the market share for bifacial modules for 2018, which was 0.3%, but with a prediction of 5 % for 2021 and up to 40 % for 2027, with an LCOE of 3 ct/kWh for 2022 at a utility scale.

During the last two years, the bifacial installations have been growing exponentially; while the cumulative installations were 100 MW in 2016, in 2017 they have grown up to 700 MW, as it can be seen in Figure 2.2.

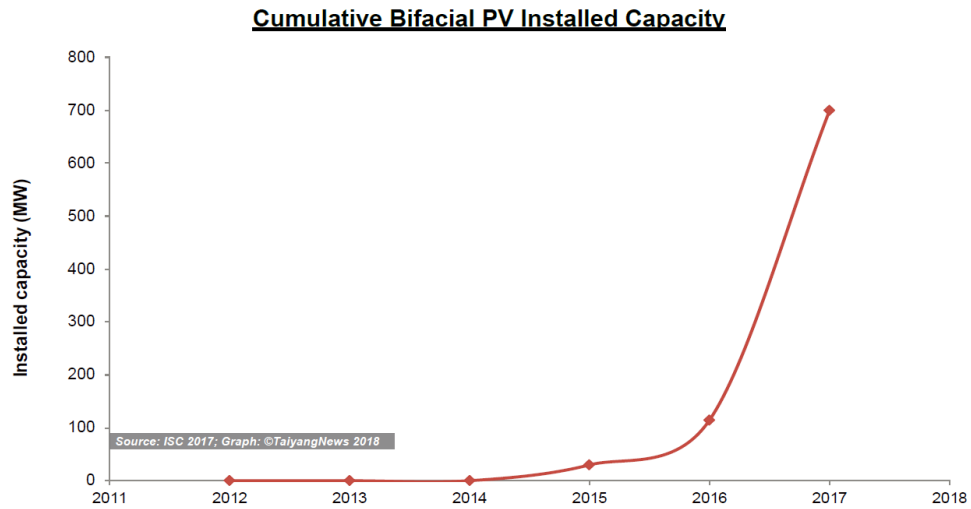


Figure 2.2. Cumulative bifacial PV installed capacity [Chu18].

Based on discussions with leading PV manufacturers and scientists, by the end of 2019, PERC based bifacial products would account for 10 to 20 % of the PERC capacity of the leading manufacturers [Chu19], such as LONGI and Jinko Solar.

3. Applications for bifacial PV modules

Many module companies, research institutes, and developers interested in bifacial technology are currently installing small- and large-scale systems under very different conditions (orientation, tilt angle, height, bifaciality, albedo...) in order to get more data on performance and reliability.

In this chapter, a compilation of published results from different bifacial PV configurations is given. The purpose of it is to understand the different possible applications for bifacial modules at the system level. Furthermore, it can also help to disclose the most significant properties that define a bifacial PV plant and allow a rough estimation of the bifacial gain to be expected for very differing systems. Figure 3.1 depicts the different possible applications for bifacial modules and the resulting daily power output.

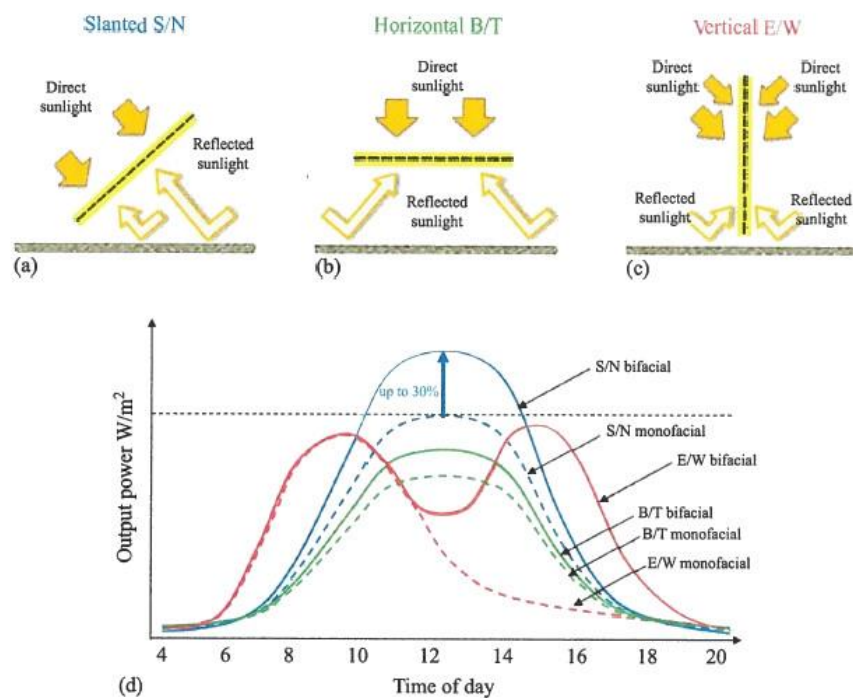


Figure 3.1.a-c) possible applications for bifacial modules and d) resulting in daily power generation curves compared to monofacial ones in the same configuration [Cze18].

3.1. Small-scale bifacial PV tests

As every very different setup of each system impedes direct comparisons, large deviations concerning the bifacial gain have to be expected. Therefore, in Table 3.1, data from publications with “typical” installation conditions (south orientation and limited tilt) and measurement duration of at least several months are considered. This compilation is done with the intention of register some of the more meaningful published data for different setups as possible concerning the bifacial gain.

Table 3.1 Most relevant properties for bifacial installations with “typical” installation conditions (south orientation, fixed tilt)

<i>Ref</i>	<i>Albedo [%]</i>	<i>Tilt [°]</i>	<i>Elevation lower module edge [m]</i>	<i>Bifaciality [%]</i>	<i>Bifacial gain [%]</i>	<i>“Normalized bifacial gain” [%]</i>
[Cas16]	10	30	1.3	95	17.7	18.6
[Sug13]	20	35	2.5	95	15.8	16.6
[Cas16]	22	20	0.2	95	12.3	13.0
[Com14]	30	20	1.0	90	22.3	24.8
[Sug13]	50	35	2.5	95	23.6	24.8
[Kre11]	50	30	0.7	71	16.0	22.5
[SAN16]	64	20	0.3	64	24.3	34.7
[Cas16]	68	20	0.2	95	19.6	20.6
[Cas16]	77	30	0.2	95	22.8	23.9
[Pod17]	80	45	0.1	93	13.0	14.0

In spite of the very different setups compiled in this chapter, for all small-scale systems bifacial gains above 10% are observed, with increasing values for higher albedos. Published bifacial gains are in a range between 10 % and 30 %. Nevertheless, it must not be forgotten that all those systems are small-scale systems. For bigger-scale systems, a lower bifacial gain is to be expected due to the shading produced in the rear side by the neighboring modules [Asg17].

The different bifaciality factors of each module used in each system also hinder a direct comparison. Thus, the concept “normalized bifacial gain” is defined as an approach to include the different bifaciality factors in the comparison. The assumption is that all modules have the same bifaciality of 100% and is defined by the following equation:

$$\text{“Normalized bifacial gain”} = \frac{\text{Bifacial gain}}{\text{Bifaciality}} \cdot 100\% \quad (3.1)$$

3.1.1. Examples of small-scale bifacial PV tests

Prism Solar test at the New Mexico Regional Test Center

In order to quantify the additional energy that bifacial PV arrays can generate under different conditions and orientations, the Sandia National Laboratories and the DOE PV Regional Test Centers (RTCs) for Solar Technologies installed the Prism Solar test at the New Mexico RTC, which is located at Sandia National Laboratories in Albuquerque (N35°). The Prism Solar test consists of five separate bifacial systems with its respective reference systems, i.e. same configuration with monofacial modules, at different configurations with different tilt angle, azimuth, and albedo of the ground cover. There is a total of 32 modules and each module is grid connected through a microinverter.

Monofacial modules are the Suniva OPT265-60-4-100 with a power of 265 W, as for the bifacial modules in the test, they are the Prism Bi60-343BST, with a front side power of 270 W. The Prism

bifacial modules are made from N-type silicon while the Suniva monofacial modules are made from P- type silicon. Table 3.2 and Figure 3.2 show the different setup configurations used.

Table 3.2 Description of the different setup configurations used at the Prism Solar test [Ste17, Gul18]

Label	Tilt [°]	Azimuth [°]	Ground surface
S15Wht	15	180 (South)	White gravel ~ 50 %
W15Wht	15	270 (West)	White gravel ~ 50 %
S30Nat	30	180 (South)	Natural – grey gravel ~ 20 %
S90Nat	90	180 (South)	Natural – grey gravel ~ 20 %
W90Nat	90	270 (West)	Natural – grey gravel ~ 20 %

The label of each array starts with the azimuth of the modules, “S” for South and “W” for West; afterward comes the tilt angle and then the ground surface, either “Wht” for white gravel or “Nat” for natural ground, which is grey gravel.



Figure 3.2 Photograph showing the setup of monofacial and bifacial modules installed at the Prism Solar test, in Albuquerque [Ste17].

After twelve months of data collection, one of the drawn conclusions are that bifacial gains are not consistent through the day; bifacial gains are larger in morning and afternoon periods when the power output is lower. Moreover, it was found that the highest bifacial gain was among the vertically tilted bifacial modules, especially the ones mounted with the west-orientation, whereas the highest amount of energy produced per module was seen on the south facing with 15 ° tilted system over white gravel.

It was also found that the bifacial gains changed between clear and cloudy conditions. In regards to west facing modules (W15Wht and W90Nat), bifacial gains were higher during clear periods, this is due to the fact that west-facing bifacial modules benefit from direct irradiance reaching the backside in the morning and evening. In contrast, the south-facing (S15Wht, S30Nat, and S90Nat) modules had larger bifacial gains during cloudy periods, this happens as the rear side could receive additional sky diffuse irradiance.

Solar installation in Kitami city, Hokkaido, Japan. PVG Solutions Inc.

Generally speaking, snowy regions are not suitable for PV systems; during the winter season, PV arrays can be covered with snow for several months, which may not only lead to power generation loss but also to damage to the PV system. A special type of PV systems with snow melting system is one of the

possible solutions. Bifacial PV systems with diagonally rotated modules in the module plane can be also a solution [Alt17]. First, because the inclination helps the snow to fall and not to get stacked on the module surface. Moreover, in case snow loads are very heavy and end up covering the module surface, the power output does not end up being zero thanks to the contribution of the rear side and the elevated albedo of the snow laying on the ground.

In 2013, PVG Solutions Inc. in order to demonstrate the power output characteristics of bifacial photovoltaic systems, installed a couple of 3kW bifi-PV systems at a northern snowy area located in Kitami city, Hokkaido, Japan. Both arrays were tilted 35 ° and oriented to the south. The modules used are the PST 254 EarthON60, manufactured with the “EarthOn” cells, which have a bifaciality factor over 95% at the mass production level [Sug13].

In Figure 3.3 the test set up can be seen for a non-snowy period. It can be seen that under one of the arrays, crushed scallops’ shells were laid down in order to obtain a higher albedo.



Figure 3.3 Field test site during summer. The white area of under the left array is crushed scallops’ shells [Sug13]

In Figure 3.4, it can be seen the test site in winter. Here scallops’ shells have no impact on the albedo and both arrays are practically under the same conditions.



Figure 3.4.a) Field test site during winter. Both arrays are practically under the same conditions. **b)** Under heavy snow conditions, snow gets stacked on the surface of the module [Sug13]

Thanks to the high tilt angle and the system with diagonally rotated modules in the module plane, snow did not get stacked on the module surface. Nevertheless, in January 2013, snow levels in Kitami city reached the 30 cm levels above the ground and this led to fully covered modules with snow (Figure 3.4.b).

About a half year operation results of bifi-PV demonstration field test system in a snowy area, it was obtained a bifacial gain from 8.6 % for the worst scenario (low albedo on summer) to 23.9 % for the best scenario (high albedo values during winter thanks to the fresh snow laying on the ground). It is important to remark for this example that no monofacial system was installed as a reference value for the analysis of the bifacial gain. Thus, monofacial power output was estimated from the front side irradiation, the module temperature was also estimated from the radiation and temperature loss (or gain) was calculated from the temperature coefficients. Therefore, bifacial gain values are not as reliable as if there had been a monofacial reference system. Table 3.3 shows the results of the test.

Table 3.3 Results of bifacial gain in energy (BGE) for snowy and non-snowy seasons and for different albedos [Sug13]

	<i>Albedo</i>	<i>BGE Summer</i>	<i>BGE Winter</i>
Bifacial gain for grass	~ 23 %	14.6 %	23.0 %
Bifacial gain for shells	~ 50 %	20.6 %	23.9 %

3.2. Vertical bifacial PV systems

Although the main purpose of bifacial PV systems is the extra energy yield, there are also applications that would not be possible to carry out with monofacial modules. Vertical mounting bifacial PV systems, typically in an east-west orientation, is one of the most considered applications. Vertical bifacial PV systems present particular benefits such as no sticking snow in snow-rich regions and minimized soiling and sand deposition for desert locations. Moreover, this type of installation avoids the maximum power generation peak at noon (“peak-shaving”) and instead contributes to a more consistent energy production throughout the day improving the alignment between electricity production and demand. However, vertically installed bifacial PV systems suffer from very pronounced shading and therefore, the energy yield will heavily depend on the specific lay-out of the PV plant.

In Figure 3.5 Sun, Khan *et al.* [Sun18] summarizes the different simulated electricity output that can be obtained out of one single module for south-north-facing monofacial module ($Mono_{SN}$), for south-north-facing bifacial module (Bi_{SN}), and for a bifacial module east-west-oriented (Bi_{EW}). All the simulated configurations are considered to be elevated 0.5 m above the ground and with an albedo of 0.5. The tilt angles are optimized for maximum production, i.e. $Mono_{SN}$ 37°, Bi_{SN} 48°, and Bi_{EW} 90° - angles optimized for Washington, DC (38.9° N, 77.03° W).

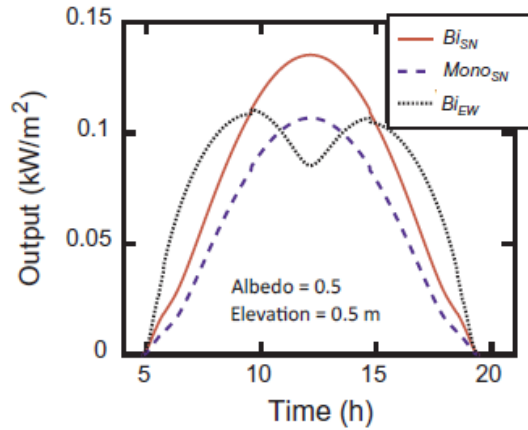


Figure 3.5 Simulated electricity output of a solar module in three different configurations: south-north-facing monofacial module ($Mono_{SN}$) at 37° , south-north-facing bifacial (Bi_{SN}) at 48° , and east-west-facing bifacial (Bi_{EW}) at 90° tilt angle on a minute-by-minute basis. [Sun18]

It can be seen in Figure 3.5 that, for Bi_{SN} the peak of electricity output is at 12:00 h and that, for Bi_{EW} , there are two peaks on the received daily radiation; one peak appears in the morning, and the other peak appears in the afternoon. This comes together with high electricity demand, so the additional power is very valuable and is lowering the need for storage options.

3.2.1. Dual use applications

In industrial countries, land use is becoming more and more restricted. Furthermore, land prices rise constantly. To overcome this challenge, vertical bifacial PV systems can allow the use of bifacial modules as integrated, “dual use” devices within functional structures in order to take the maximum advantage of the land. In this chapter, some of the dual-use applications will be presented.

Agro-PV

So-called “agrophotovoltaics-concepts”, which use the same area for farming and PV. The most popular height for Agro-PV is the elevated installation of PV modules at a minimum height and space between rows that enables agricultural machines to drive through and use the land underneath. Meyer, C. suggests a height of at least 3 m from the ground and a space between rows between 10 and 15 m [Mey18].

The new approach of vertical bifacial PV plants as Agro-PV-concept implies almost no coverage on the ground area and nearly no influence on the distribution of irradiation and rainfall.

Natural PV

Since a ground coverage ratio of more than 50 % can lead to a strong interference of nature and environment, conventional PV plants are usually in conflict with habitat protection. This problem can be solved or reduced by installing the modules vertically thanks to their low impact on the environment conditions.

PV integration into functional structures

There are many vertical structures that can be used for PV integration. Following examples are of particular relevance:

- Noise barriers
- Fences
- Railings
- Cooling effect in summer

Often, “dual-use” application into functional structures face problems such as the fact that functional requirements of the primary structure and additional PV generation differ, e.g. in the case of noise barriers, a rough surface for good absorption and high weight is needed for good barrier functionality. In contrast, solar modules are weight-oriented designed.

3.2.2. Example of vertical bifacial PV system

“Next2Sun”

In May 2015, the German start-up “Next2Sun” installed a facility near Merzig in the Saarland with 28 kWp and few module rows to prove the feasibility of the concept and the correctness of the yield forecast in a realistic test setup. Figure 3.6 show the vertical bifacial PV plant installed by “Next2Sun”.



Figure 3.6 Pilot test of 28 kW vertical bifacial E-W oriented PV system in Saarland, Germany by Next2Sun [Hil17].

Table 3.4 shows the characteristics of the PV plant.

Table 3.4 Description of the characteristics of the Pilot test of 28 kW vertical bifacial E-W oriented PV system Next2Sun [Hil17].

Characteristics	Description
Module type	Customized 66-cell double-glass module with n-type cells
Bifaciality	87 %
Albedo	~ 20 %
Pitch	10 m row spacing
Mutual row shading	5-10 % loss
Modules per row	2 x 16 modules in landscape orientation
Strings	12
Total height	3 m
Mounting system	Steel based post-and-beam construction

After three years of gathering data and experience, an analysis has been done and it has been noticed an annual energy gain of 10 % and an average price gain base on EEX prices of 7 % [Hil17]. The Energy yield for the small scale vertical bifacial East-West oriented bifacial PV plant in Saarland is depicted in Figure 3.7.

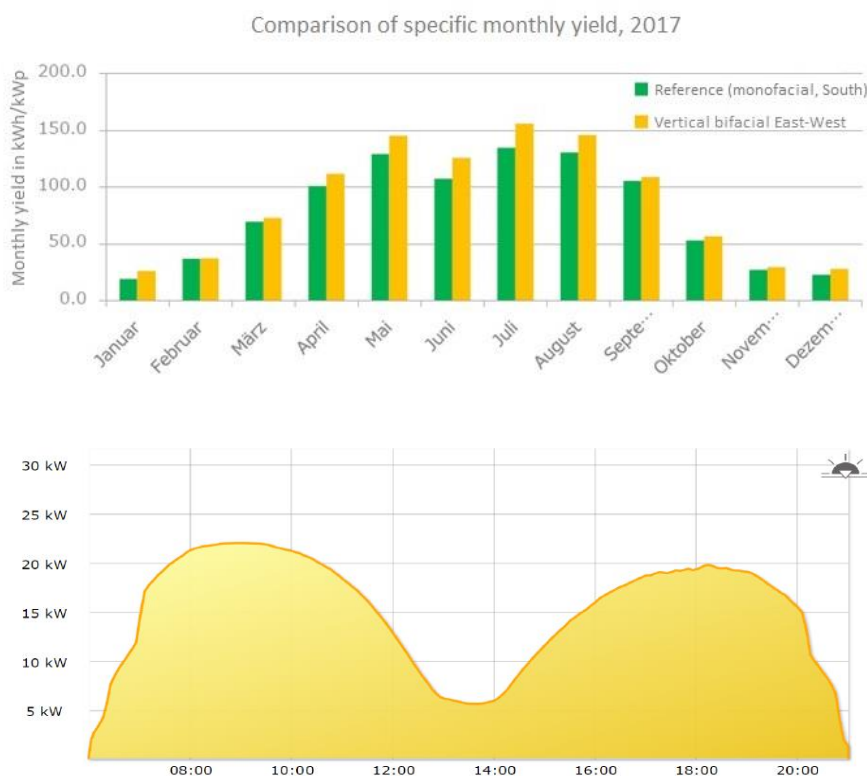


Figure 3.7 Energy yield for the small scale vertical bifacial East-West oriented bifacial PV plant in Saarland (Next2Sun) **a)** comparison of the specific monthly yield between vertical bifacial East-West oriented and a monofacial system South oriented; **b)** specific hourly energy yield [Hil17].

On the PV magazine of March 2019 [Lic19], Nicolai Zwosta, Managing Director of Next2Sun, announced that their third agro-photovoltaic project with 4 MWp in Donaueschingen should be by the end of the month completed. This power plant is also built with vertical east-west oriented modules. Zwosta conceded also that their first two solar parks with this technology (Saarland) could not be sold profitably and that they expect a change in this project.

3.3. Horizontal floating bifacial PV systems

Currently installed floating PV capacity amounts to over 500 MWp worldwide and about 90 % of the capacity was installed in Japan and China, in a small number of very large projects [Jon18]. However, the use of bifacial PV modules on water is still limited.

The main reason for floating PV is the land use of ground-mounted PV systems; in many areas of the world land is scarce or there simply is not enough usable land to supply renewable energy locally. A clear advantage is the potentially large scale of projects; as long as the original function of the water surface is not compromised, large patches of water are potentially available. Another advantage is the additional cooling effect thanks to the temperature inertia of the water mass. Besides from those advantages, bifacial modules add an extra and significant advantage which is the bifacial gain.

In general, water is regarded as a material that has a very low albedo of below 10 % [Vol16]. However, this water albedo value is valid at 0° incident angle, or perpendicular to the water surface. The Fresnel reflection function describes the reflection of a portion of incident light at a discrete interface and occurs at the air-glass or water interface. According to the Fresnel reflection function (Figure 3.8), at incident angles over 65° the Fresnel reflection increases from 0.05 for 0° incident angle up to 1 for 90°. Therefore, light reflection should be especially pronounced at low incident angles, i.e. at the edges of the day (dusk and dawn).

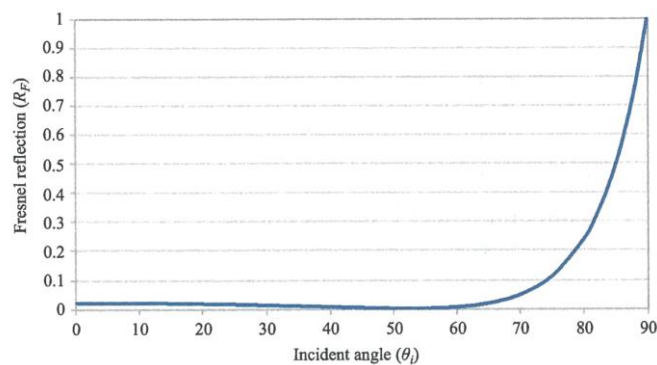


Figure 3.8 Fresnel reflection curve for the air-water interface at different incident angles [Lib18].

In the Fresnel reflection function, waves and fouling of the water are not taken into account. While waves lead to more diffuse reflection, floating particles in water cause light scattering in different directions [Lib18]. This could have an enhancing effect on the reflection of sunlight.

3.3.1. Example for floating PV system

“Sunfloat”

On 2017 Sunfloat developed a fixed south pilot floating system for bifacial modules in order to make solar PV on water the lowest cost and best-accepted PV technology as well as to provide wave-resistant commercially viable systems and face the corrosive conditions. What is remarkable from this pilot test set-up is that the floating structure is open to the water surface, i.e. no permanent shading or coverage. Figure 3.9 depicts the pilot test from “Sunfloat”.



Figure 3.9 Pilot test of 5.5 kWp Bifacial PV system Sunfloat [Kre17].

Experiments in the field show that, for flat light angles of the incident light, average bifacial energy gains of over 30 % can be reached with bifacial PV on water [Lib18].

3.4. Large-scale bifacial PV systems

In large-scale bifacial PV systems (> MW), the bifacial gain is lower than the one of small-scale bifacial systems due to the shadowing produced by the neighboring modules. As a consequence, it is necessary to prove on an economic basis that the bifacial gain is not annihilated by additional costs such as the extra costs of bifacial modules in comparison with monofacial modules, structure frame specificities to limit the rear shadowing and the ground preparation to increase the albedo.

Nevertheless, Kopecek, R. presented at the Bifacial PV Workshop in Miyazaki on 2016 a benchmark indicating the growth of the cumulated capacity of bifacial power plants, Figure 3.10. According to Kopecek, R., more than 95 % of the installed capacity is modules south oriented with a fixed tilt.

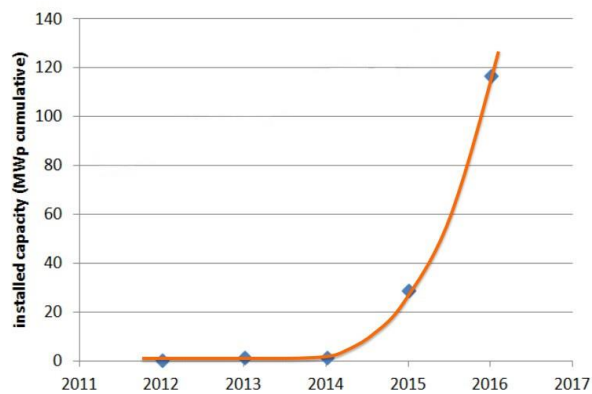


Figure 3.10 Installed acumulated capacity of bifacial PV plant since 2011 [Kop16]

3.4.1. Example of large scale bifacial system

“PVG Solutions”

In May 2013, the Japanese company PVG Solutions installed the first large scale 1.25 MW bifacial PV Power plant named Karuma. The Hokuto power plant is installed in a very snowy region in Asahikawa, Hokkaido and is specially adapted for these conditions. Figure 3.11 shows the large-scale bifacial PV power plant by “PVG Solutions”.



Figure 3.11 Large-scale power plant for fixed tilt angle, 1.25 MW, “Hokuto”, Japan, by PVG Solutions [Ish16].

As it can be seen in Figure 3.11, the mounting structure of this PV plant integrates metallic frames on the rear side, which may include additional shadowing on the rear side of the bifacial modules. Nevertheless, since the “Hokuto” is installed in a snowy region, the presence of the metallic frames on the rear side can be required for mechanical strength towards environmental impacts such as wind or snow. Table 3.5 summarizes the characteristics of the large-scale power plant by “PVG Solutions”. **Table 3.5** Description of the characteristics of the large-scale power plant for a fixed tilt angle, 1.25 MW, “Hokuto”, Japan, by PVG Solutions [Lib18].

Table 3.5 Description of the characteristics of the large-scale power plant for a fixed tilt angle, 1.25 MW, “Hokuto”, Japan, by PVG Solutions [Lib18].

<i>Characteristics</i>	<i>Description</i>
Total capacity	1.25 MW
Bifaciality	n.a.
Height	1.5 m
Albedo	Variable from 20 % (bare soil) up to 90 % (snow)
Module type	n-type mono-crystalline PST254EarthON60 254 Wp (front side)
Number of modules	~ 9.090 modules
Orientation	Landscape, south, fixed tilt
Tilt angle	40 °
Pitch	10.3 m
Rows	4 (~ 4 m)
Mounting system	The mounting structure is crossing under the modules

At the 3rd bifi Workshop in Miyazaki, Japan, Ishikawa, N. *et al.* presented the results of this power plant over a period of 32 months. An energy yield over 1.200 kW/year has been obtained despite a latitude of

43.5N and heavy snowfall in winter. Moreover, the bifacial gain of this power plant is considered to be over 20 % based on estimated generated power for a monofacial system at the given location [Ish16].

Another significant advantage of this power plant is the fact that it is installed in a snowy environment, which leads to a higher production on the rear side thanks to the higher albedo and the acceleration of the melting of the snow remaining on the front side of the module due to the rear irradiance (thermalization effect) [Lib18].

“MegaCell”/ “Imelsa”

MegaCell group installed a large-scale bifacial PV plant in La Hormiga, Chile. The PV plant has 2.5 MW total installed capacity with 9.090 bifacial modules installed in a tilt angle, north facing and landscape orientation.



Figure 3.12 Large-scale power plant for fixed tilt angle, 2.5 MW, “La Hormiga”, Chile, by MegaCell Group [Kop18]

Table 3.6 summarizes the main characteristics of the bifacial power plant “La Hormiga”, Chile.

Table 3.6 Description of the characteristics of the large-scale power plant for fixed tilt angle, 2.5 MW, “La Hormiga”, Chile, by MegaCell Group [Lib18].

<i>Characteristics</i>	<i>Description</i>
Total capacity	2.5 MW
Bifaciality	n.a.
Albedo	White quartz (~ 40 %)
Module type	BiSoN solar modules, front-side power in STC: 275 Wp
Number of modules	~ 9.090 modules
Orientation	Landscape, north, fixed tilt
Rows	3
Mounting system	The mounting structure is not under the modules

At the 25th Bifacial Workshop (2018) in Denver, USA, Kopecek, R. *et al.* showed that the PV plant La Hormiga, Chile, showed a bifacial gain of 20% [Kop18].

“Tempress Amtech Group”

The company Tempress Amtech Group installed in June 2017 a 400 kWp East-West oriented bifacial PV park to cover 80 % of their own electricity consumption.

a)



b)

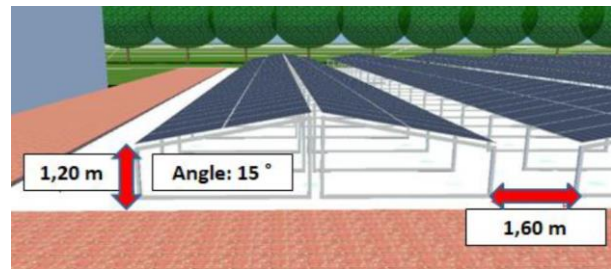


Figure 3.13.a) Horizontal East-West oriented 400 kWp (front side only) bifacial PV plant b) System design parameters for the power plant [Ver17].

In Figure 3.13 it can be seen the Tempress small-scale power plant and its system design parameters. This could be a good option for bifacial modules application since it combines the advantages of vertical bifacial power plants with east-west orientation and the advantages of horizontal bifacial power plants with south-north orientation; on one side, a higher power output can be obtained during mornings and evenings, which fits with the demand curve. On the other side, for such a low tilt angle and height there is a low effect for self-shadowing, which allows having a smaller distance between rows which leads to a higher ground coverage ratio. Table 3.7 summarizes the main characteristics of the bifacial power plant with East-West orientation by Tempress.

Table 3.7 Description of the characteristics of the 400 kWp power plant with East-West orientation by Tempress [Ver17].

<i>Characteristics</i>	<i>Description</i>
Total capacity	400 kWp (front side only)
Bifaciality	3300 m ²
Albedo	Pebbles ~ 40 %
Number of modules	1428 modules in portrait
Pitch	1,60 m
Tilt angle	15 °
Rows	2
Orientation	East-West

On the bifacial workshop 2017 in Konstanz, Tempress presented the results achieved with their power plant based on measurements carried out from July to September. It was achieved a bifacial gain between 15 and 19 % and more energy density (kWh/m²), according to Tempress, more than 3x than the south oriented [Ver17].

3.5. Horizontal single-axis tracked bifacial systems

During the last years, horizontal single-axis tracking (HSAT) has become a very important technology in regions close to the equator with the goal of maximizing the energy yield as well as to minimize the electricity generation costs (LCOE). And even though bifacial systems in combination with tracking has been for a long time thought not to be compatible [Lib18], recently companies such as MEGACELL and ENEL groups have realized that the combination of tracking with bifacial modules makes very much sense and lead to very high power generations.

Solar tracker markers such as NEXTTracker, ConvertItalia, and ArcTech are bringing to the market specially designed tracking models specially designed for bifacial modules. Arctech, for example, offers a single-row design called *SkySmart* which has two modules in portrait and has fewer posts and is perfect for bifacial modules [Sol18]. Furthermore, they also offer the *Arctracker Pro* which is a centralized tracker with a push-pull design that is very advisable for flat land. According to the article of Thurston C. W. published in the PV magazine of February 2018, single-axis trackers typically add 25 % to the normal bifacial gain, which results in a roughly estimated 12.5 % gain, compared with tracked systems using monofacial panels [Thu18].

3.5.1. Example for single-axis tracked bifacial PV system

“Enel”

Enel Green Power (EGP) installed in 2016 in La Silla (Chile) a 1.7 MW power plant with single-axis trackers with monofacial modules, bifacial modules, and electronic modules. The purpose of the PV plant is to test innovative technologies and in real operating conditions of utility-scale PV plants and compare them with traditional technologies.

a)



b)

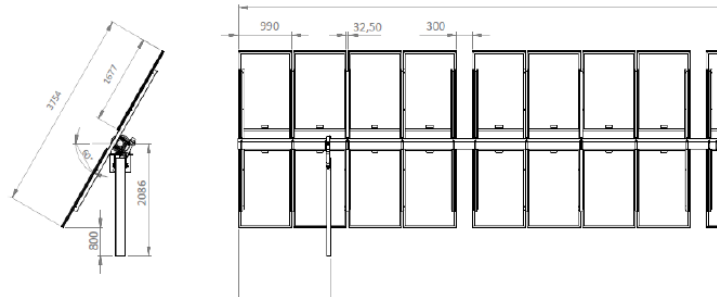


Figure 3.14.a) Power plant of 1.7 MW with single axis tracking in La Silla, Chile and b) portrait configuration of trackers with bifacial modules [Biz17]

Figure 3.14 b) depicts the configuration of the used trackers in the PV plant “La Silla” for bifacial modules. As it can be noticed, the structure leaves a free space between modules in order to maximize the bifacial effect and avoid the shadowing of nearby modules. The Table 3.8 summarizes the main characteristics of the bifacial power plant with single axis “La Silla”, Chile.

Table 3.8 Description of the characteristics of the 1.7 MW power plant with single axis tracking in “La Silla”, Chile by Enel [Lib18].

<i>Characteristics</i>	<i>Description</i>
Total capacity	1.7 MW
Bifaciality	> 85 %
Albedo	23 %
Module type	n-Pert BiSoN solar modules (MBA-GG60 280 Wp)
Modules per row	4 x 2 modules along horizontal and vertical axes in landscape orientation
Rows	3
Mounting system	Steel based post-and-beam construction

Enel Green Power presented at the EUPVSEC 2017 in Amsterdam [DiS17] and at the bifiPV workshop in Konstanz in 2017 [Biz17] the results from its La Silla project in Chile; during the 9-month monitoring period, an average energy yield gain from monofacial HSAT to bifacial HSAT of 12.8 % was observed.

Libal, J. *et al.* showed basing their calculations on theory how a combined two-axis (5 % more than single-axis [Lib18]) tracking with bifaciality and a ground albedo of around 0.5 could reach 57.5 % more power as compared to a monofacial fixed tilt. It is also mentioned in their book that, conditional to the additional costs for two-axis tracking systems and for artificially increasing the ground albedo, a system configuration such as the single-axis tracking combined with bifacial modules could lead to the lowest LCOEs achievable with a currently commercially available PV module technology.

Therefore, if an investment for a tracking system is planned, it makes sense to use bifacial modules in many cases e.g. for sandy desert regions, where the albedo is known to be between 20-40 %.

3.6. Recapitulation

This compilation of existing literature shows that performance capabilities of bifacial solar systems are affected by the rear face conditions. In order to have a clearer comparison of the most common geometries for bifacial modules power plants, a summary is done in Table 3.9.

Table 3.9 Bifacial gains for various installation geometries

<i>Ref</i>	<i>Type of PV plant</i>	<i>Albedo</i>	<i>Tilt angle</i>	<i>Elevation</i>	<i>BGE</i>
[Hil17]	Vertical installation (E-W)	20 %	90 °	1 m	10 %
[Ver17]	Slanted fixed (E-W)	~ 40 %	15 °	1.2 m	15 % – 19 %
[Lib18]	Slanted fixed (S-N)	20 %	40 °	1.5 m	> 20 %
[Biz17]	Single axis tracked (S-N)	23 %	-	-	40 % [Joa17]

As for the comparison between vertical and horizontal bifacial module PV plants, Figure 4.1 shows the simulated output power of one south-north-facing bifacial module (Bi_{SN}), and the same bifacial module east-west-oriented (Bi_{EW}). The simulations are done by Sun, Khan *et al.* [Sun18] and all the simulated configurations are considered to be elevated 0.5 m above the ground and with an albedo of 50 %. The

tilt angles are optimized by Sun, Khan *et al.* [Sun18] for maximum production, i.e. Bi_{SN} 48° , and Bi_{EW} 90° . Moreover, it also depicts the EPEX day-ahead hourly price average for 2018 in Germany [EPE19].

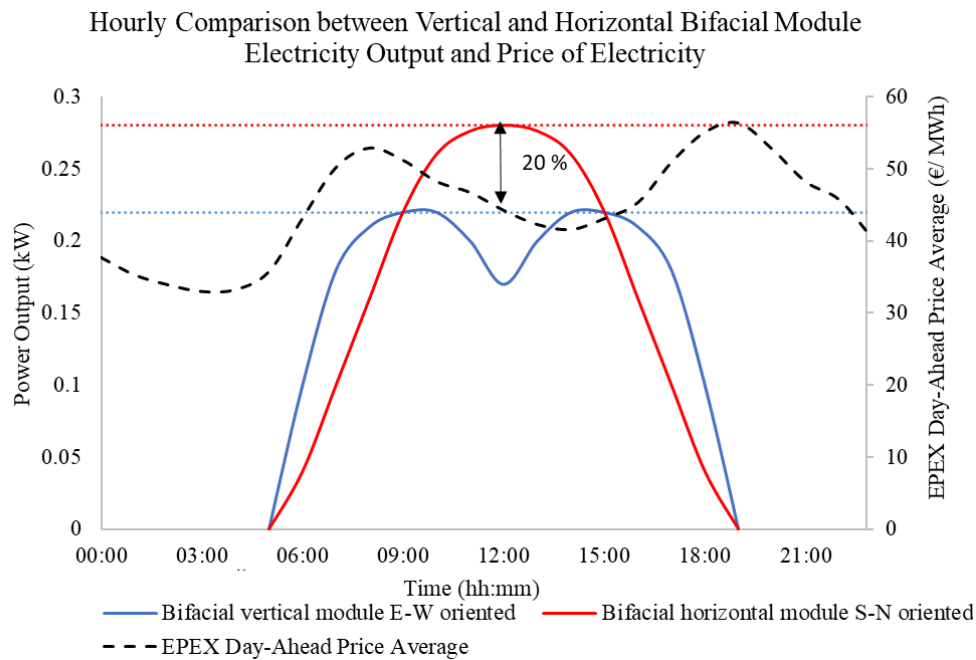


Figure 3.15 Simulated electricity output of a solar module in two configurations: south-north-facing bifacial (Bi_{SN}) at 48° , and east-west-facing bifacial (Bi_{EW}) at 90° tilt angle on a minute-by-minute basis. [Sun18]

Figure 3.15 depicts that, for Bi_{SN} the peak of electricity output is at 12:00 h and that, for Bi_{EW} , there are two peaks on the received daily radiation; one peak appears in the morning, and the other peak appears in the afternoon. This comes together with high electricity demand, so the additional power is very valuable and is lowering the need for storage options. Nevertheless, if the revenue for each orientation is compared, prices and electricity output compensate each other and no more revenue is obtained from any of the two orientations. Moreover, vertical modules have a very low Ground Coverage Ratio, which can increase dramatically the LCOE if compared with the horizontal modules, which need a shorter row spacing.

As for the comparison between slanted fixed system and single axis tracked system, M. Joanny *et al.* [Joa17] presented at the bifacial PV workshop 2017 in Konstanz the LCOE for the slanted fixed bifacial PV system “La Hormiga” in Chile, which is 6 US \$ct/ kWh and for the single axis tracked bifacial system “La Silla” also in Chile, which is 4.5 US \$ct/ kWh .

4. System design considerations

Performance of bifacial PV systems depends on the spatial distribution of the incident irradiance on the rear side of the module, which is strongly affected by several conditions such as albedo of the ground surface, module elevation, azimuth, tilt angle, size of the system, and the distance between module rows. In this chapter, the different published effects of the site-specific conditions on the annual bifacial gain for a horizontal bifacial PV system are presented.

4.1. Albedo

The albedo or ground reflectance is a property of a non-luminous surface that describes the capacity to reflect part of the solar radiation received. It is the ratio between the reflected radiation and the incident radiation on a surface. Increasing the albedo of the ground of the PV plant increases the intensity of the reflected radiation on the back side of the bifacial module and so does the system’s performance. Figure 4.1 shows the effect of the albedo on the bifacial gain.

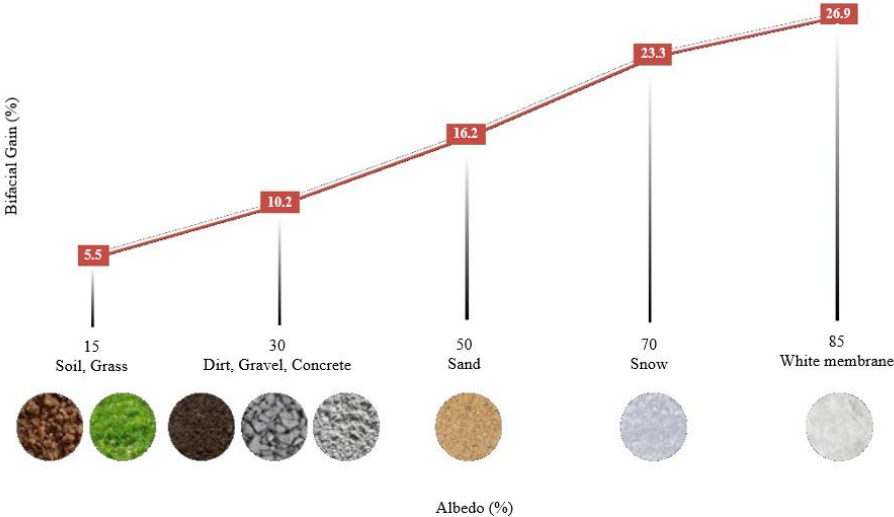


Figure 4.1 Effect of ground material albedo on bifacial gain of energy [Chu18].

As Figure 4.1 depicts, bifacial performance increases linearly with albedo. Albedo value for a site can change seasonally; for example, at high latitudes, winter conditions can introduce seasonal bifacial improvements as high albedos increase the intensity of irradiance reflection. In comparison, for desert locations or arid environments without foliage, the albedo will be constant and high. Figure 4.2 gives an example of NASA data during the month of April 2002 [NAS02].

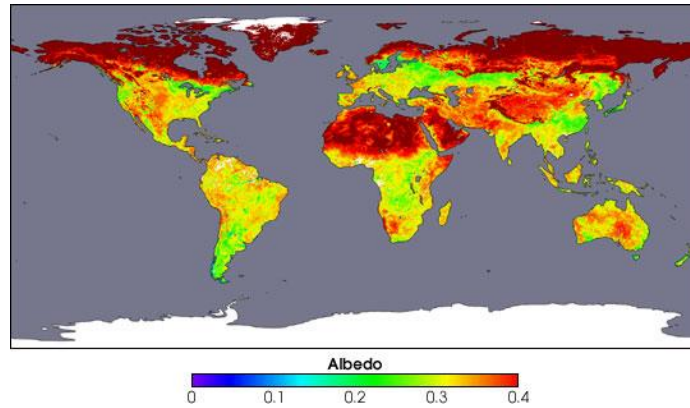


Figure 4.2 Global albedo map from April 7-22, 2002. NASA [NAS02]

As it depicts Figure 4.2, high albedo values can be found in desert areas such as Northern Africa, the Middle East, China, and Australia.

Even though snow and vegetation have a great seasonal impact, variations during the day should also be expected, e.g., during and after periods of rain. M. Chiodetti [Chi15] showed how the albedo can change over the day (Figure 4.3). In addition, F. Yang *et al.* proposed a model of albedo for snow-free ground in which two main factors could be noted for a given location: the solar zenith angle and the fraction of diffuse skylight [Yan08]. Sandia measured the albedo of the Prism Solar Installation at the New Mexico Regional Test Centre from March 9 – April 5, 2016. Besides from the shading on the ground surface observed during the late afternoon, the albedo measurements were consistent over both clear and cloudy days.

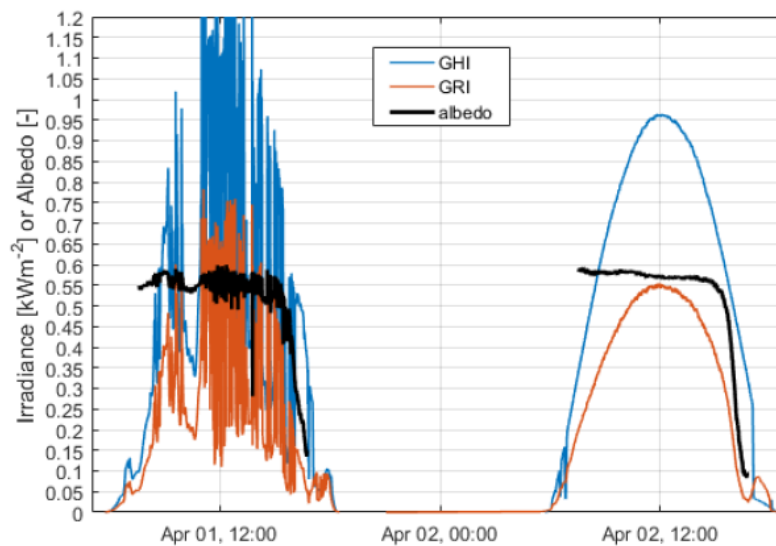


Figure 4.3 Evolution of ground Global horizontal irradiance (GHI), ground reflected Irradiance (GRI) and albedo (white pebbles) measurement by the albedometer on a 2-day period (01/04/16 to 02/04/16) in the Sandia National Laboratories in Albuquerque [Ste17].

4.2. Height

The module height (elevation) is defined as the distance between the bottom of the lowest part of the module and the ground surface. The height has a great impact on the energy yield; when the bifacial modules are installed very close to the ground, the reflected irradiance from the ground is affected by self-shadowing, whereas when increasing the height of the modules over the ground, the clearance of the ground increases and so does the backside irradiance. It is also of great importance being aware of the fact that due to higher wind loads, high module mounting structures are also more expensive and mechanically more challenging. Therefore, determining the optimal height of the modules is also a compromise between finding the height in which the modules are far enough from the shadow it casts, but not too far so that the wind loads are very high.

Figure 4.4 shows the influence of the height on the irradiance received on the back side of the bifacial module for a single module system in El Gouna based on simulations. As it can be noticed, the module mounted at a height of 10 cm does not only receive less irradiance on its rear side, but also the rear side irradiance is more inhomogeneous, due to the proximity of the module to the shadow on the ground.

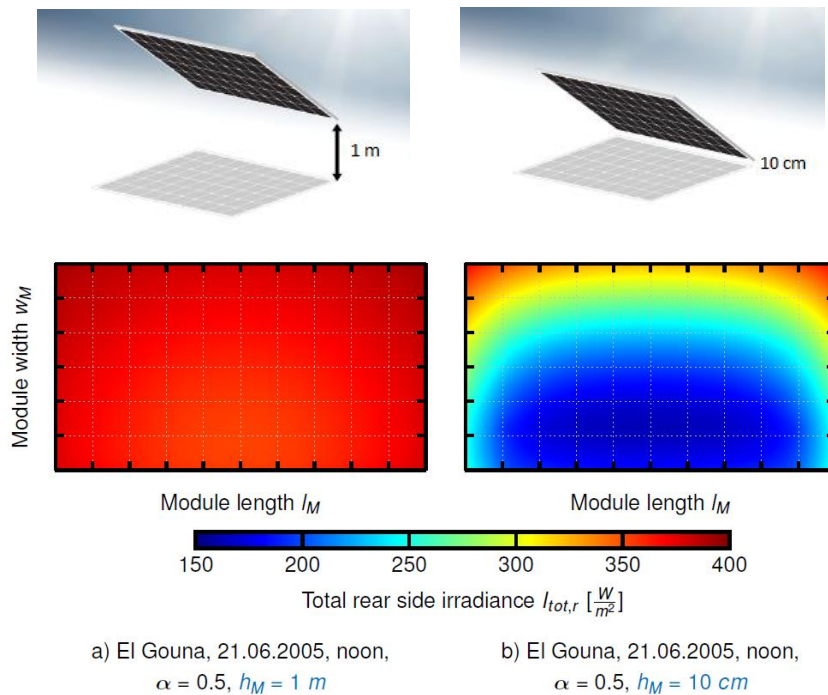


Figure 4.4 Total irradiance on module rear side for elevations a) 1 m and b) 10 cm. [Sho15]

In Figure 4.5, the impact of the height on the bifacial gain for a power plant with fixed tilt [Win18]. Plotted data has been obtained from internal simulations of Longi Solar.

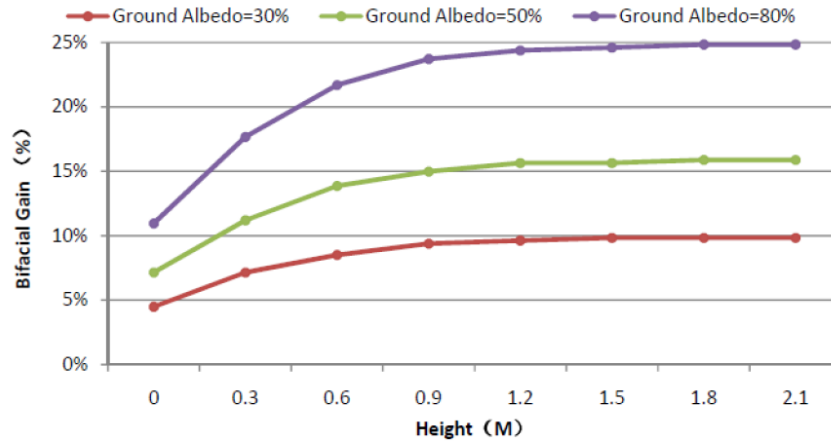


Figure 4.5 Effect of the height of the lowest side of the modules above the ground on the bifacial gain based on internal simulations of Longi Solar [Win18]

It can be observed that for high albedos bifacial gain increases with the height. However, the trend has a saturating effect. This phenomenon happens due to the fact that for certain heights the self-shadowing on backside irradiance is diminished and increasing the height does not increase the performance.

As that height up to certain value does not have a great impact on the energy yield, wind loads will prevail and minimum height that minimizes the self-shadowing effect and doesn't imply extra costs will be chosen.

4.3. Azimuth

Optimal orientation of bifacial modules is also to be determined. When analyzing the orientation of the modules two orientations must be confined: east-west-facing bifacial modules (Bi_{EW}) and south-north-facing bifacial modules (Bi_{SN}).

In Figure 4.7, a comparison of the performance between Bi_{EW} and Bi_{SN} for different scenarios is depicted. The tilt angle of both azimuth scenarios is optimized. According to Guo, Walsh *et al.* 2013 [Guo13], for Bi_{EW} the optimum tilt angle is found to be 90° i.e., vertical installation and in the case of Bi_{SN} , the optimum tilt angle for a single module is 48° .



Figure 4.6 a) South facing horizontal module and b) East-West facing vertical module [Kha17]

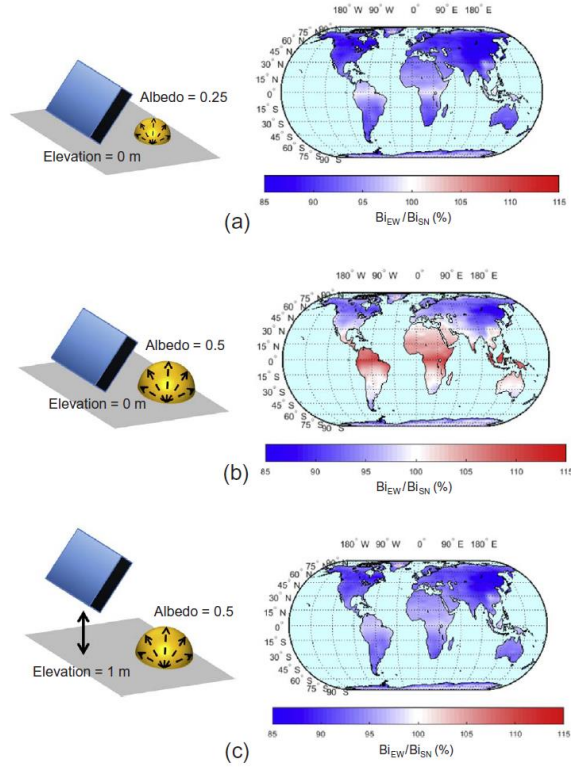


Figure 4.7 Global map showing energy yield ratio of optimally tilted B_{iEW} over B_{iSN} for three different scenarios: a) ground mounted with an albedo of 25%, b) ground mounted with an albedo of 50%, and c) 1 m elevated with an albedo of 0.5 [Sun18]. Tilted angles are optimized for all scenarios i.e. for B_{iEW} is tilt angle 90° ; for B_{iSN} optimum tilt angle is 48° according to Sun, Khan *et al.* [Sun18]

On one hand, according to the simulation performed by Sun, Khan *et al.* 2018 [Sun18], for ground mounting structures and low albedo (Figure 4.7 a), horizontal B_{iSN} can outperform vertical B_{iEW} by up to 15%. This phenomenon can be explained due to the fact that, at a low albedo the collection of the direct light dictates the total production, and vertical B_{iEW} does not absorb any direct light at noon, i.e. when the direct light is the highest.

On the other hand, in comparison with the scenario with a low albedo, in Figure 4.7 b, vertical B_{iEW} produces up to 15% more than horizontal B_{iSN} within 30° latitude. This happens especially for desert environments, where the optimum tilt angle of horizontal B_{iSN} is very low and modules suffer from soiling. With the B_{iEW} soiling is reduced thanks to the high tilt angle, which involves higher energy output and reduced cleaning cost. For higher latitudes, the tilted angle also increases and therefore, soiling losses are reduced and horizontal B_{iSN} outperforms again vertical B_{iEW} .

Nevertheless, as explained in chapters 4.1 and 4.2, high albedo levels and a height between 0.5 and 1 m are to be implemented. Therefore, the most interesting results are the ones shown in Figure 4.7 c, where the depicted result of the simulations shows how the optimal orientation of bifacial modules again becomes B_{iSN} . This change of optimal azimuth angle is explained by the fact that for higher elevations, self-shading of bifacial modules is reduced (see Figure 4.4). Therefore, horizontal B_{iSN} suffers less from self-shading and can produce more power than vertical B_{iEW} . As a result, like Sun, Khan *et al.* 2018 [Sun18] explain in their study, for a certain elevation with minimal self-shading, the optimum orientation is always south-north facing across the entire world.

4.4. Size of the System

Since PV systems are rarely installed singularly or consist of one-row modules and they are rather installed in a field with neighboring modules and several module rows, simulations and experiments with stand-alone modules or single module rows are insufficient to enable an accurate prediction of the energy yield of a bifacial module PV plant.

Bifacial modules, in comparison to monofacial, are influenced by additional neighboring modules creating a shadow on the ground decreasing, this way, the reflected and diffuse irradiance reaching the rear side of the modules. The greater the number of modules in a table, the bigger the impact on the bifacial gain. Asgharzadeh, A. *et al.* studied the impact of the size of the system and found out in their simulations that the yield of the modules in a large array can decrease up to 7 % relative to single module system [Asg17].

However, it is also expected that at a number of adjacent modules, a saturation point in which bifacial gain is no longer negatively affected is achieved. This means, that up to a certain number of modules self-shading does not increase further. Shoukry, I. found in his simulations that the saturation point was reached at a number of five adjacent modules, i.e. starting from the third module in a row, bifacial gain does not decrease anymore [Sho15]. Figure 4.8 depicts this fact.

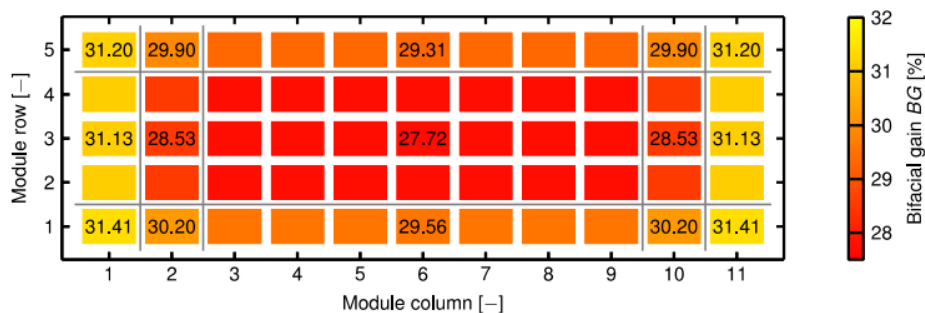


Figure 4.8 Simulated bifacial gain (%) of all modules in a field in El Gouna with an albedo of 50% [Sho15].

4.5. Tilt angle

The optimal tilt angle depends on many factors such as the size of the system, location of the plant and the time of the year. Therefore, no general literature about the optimal tilt angle is available. Consequently, this topic will be deeply analyzed in further chapters through measurements and simulations (chapter 6.2).

4.6. Pitch

Pitch is the distance from the front side of the array to the front side of the array behind. In this chapter, different distances and sizes of tables will be compared.

In the design of bifacial PV plants, besides of the tolerable amount of module front side shading by other modules, also the blocking of the ground-reflected irradiance by the shadowing produced by neighboring module rows has to be taken into consideration. Hence, finding the optimum distance between tables is

a compromise between minimizing the shading losses from both front and rear sides of a module as well as maximizing the number of rows installed for a finite available land surface.

The Ground Coverage Ratio (GCR) is directly correlated with the pitch and is the ratio of the PV modules area and the total ground area and is defined by the following formula:

$$GCR = \frac{A_{module} (m^2)}{A_{entire\ surface} (m^2)} \cdot 100\% \tag{4.1}$$

Where:

A_{module} : module area

$A_{entire\ surface}$: land surface area

Figure 4.9 depicts the effect of the GCR on the bifacial gain of a bifacial PV power plant gain based on internal simulations of LG that were done for 1 MW system with fixed tilt structure and 2 rows of modules in landscape.

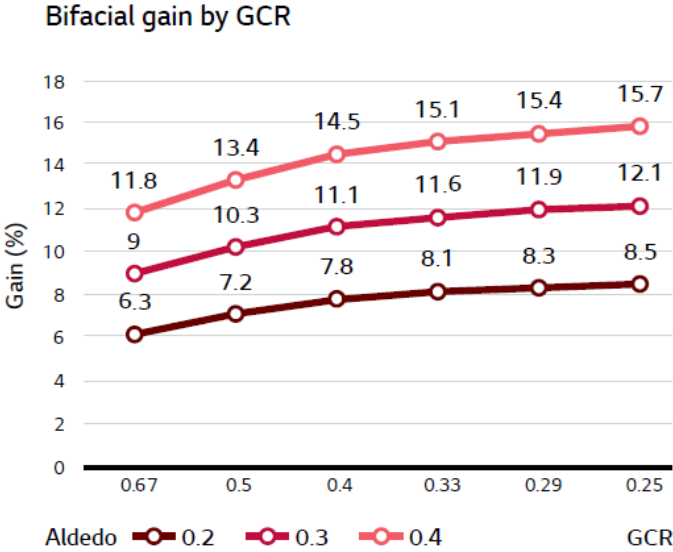


Figure 4.9 Effect of the GCR of the bifacial PV plant on the bifacial gain based on internal simulations of LG. Simulations were done for 1 MW system with fixed tilt structure and 2 rows of modules in landscape [LG].

According to the internal simulations from LG, the smaller the GCR, the higher the bifacial gain. It is also of big interest to point out that the lower the albedo of the land surface, the less the bifacial gain is affected by the GCR. For higher albedos, higher changes in the bifacial gain are expected as a function of the GCR.

4.7. Mounting structure

The mounting structure, especially the mounting rail, can block reflected sunlight that reaches the rear side of the bifacial module if it is not installed carefully. This shading produced by the mounting

structure decreases the BGE. Losses on the rear side of the bifacial module depend on different factors related with the module and the mounting structure such as the rail thickness and width, the number of rails below the module, the rail design and the distance between the rails and the modules.

The best way to minimize the losses is to install a mounting structure optimized for bifacial PV modules i.e. installing the rail edges under the module frames.

4.8. Inverter sizing

Inverter sizing is another of the much-discussed issues when designing a bifacial PV plant. The following section provides recommendations for inverter sizing, which generally depends on the input current and voltage, thermal coefficient and nominal power.

Maximum input current

The current of it is increased by the rear side boost. As a result, the current increases with the bifacial gain (i.e. when the bifacial gain is 20 %, then current increases also around 20 %), data sheet specifications for the electrical values under optimized conditions can be used for this purpose. Hence, the bifacial gain should be estimated in order to know the electrical characteristics to consider the size of the inverter as well as the cables. Therefore, the inverter has to be rated to satisfy the increased current from the bifacial modules.

Usually, modern inverters have higher tolerances with regard to the input currents and can also process the higher currents without problems [Ame17].

Nominal power

When the DC power produced by the PV array exceeds the maximum input level of the inverter, the inverter adjusts the direct current to reduce the DC power. This process involves losses and is also referred as clipping. When sizing the inverter, it is important to consider the DC-AC ratio as well as the clipping loss rate, which will be increased by the power gain.

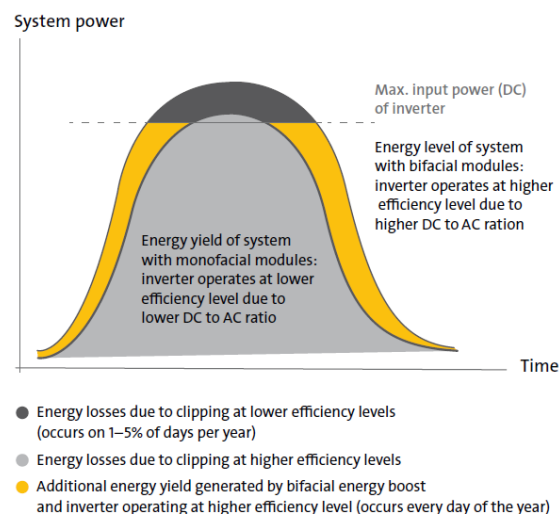


Figure 4.10 Idealized energy yield curves of photovoltaic systems with monofacial and bifacial modules [Ame17].

If the same clipping loss value related to a monofacial module with the same nameplate rating is to be maintained, then either the DC capacity of the system should be scaled down or the AC inverter capacity should be scaled up. Nonetheless, if the clipping loss only increases slightly i.e. below 2 %, it may be more efficient to use the same capacity of inverter without sizing up.

5. Indoor measurements

Indoor experiments allow knowing the I-V characteristics of the bifacial modules as well as parameters such as the bifaciality and the power generation gain. The data provided by the indoor experiments can be used to predict the power output of bifacial solar power plants or for energy rating purposes.

Indoor measurements were carried out in the Energy Practice Laboratory at the University of Applied Sciences Hamburg, faculty Life Sciences located in Bergedorf, Hamburg. The apparatus used for the indoor measurements is a solar simulator with adjustable levels for single-side illumination place. As defined in IEC 60904-9 [IEC07], the solar simulator must be able to provide irradiance levels above 1000 W/m^2 and the simulator's non-uniformity of irradiance must be below 5%.

The device used for the measurement is a sample of the bifacial modules from the manufacturer LongiSolar model LR6-60BP 290M. In Table 5.1 the electrical characteristics of the module are shown:

Table 5.1 Electrical characteristics of the bifacial module used for the indoor measurements from the datasheet of the fabricant and from the laboratory measurements (LR6-60BP 290M).

Type	Side	V_{oc} [V]	I_{sc} [A]	P_{mpp} [W]	V_{mpp} [V]	I_{mpp} [A]	η [%]
Bifacial	Front	39.2	9.36	290	32.6	8.90	17.5
	Back	38.9	7.16	218	33.3	6.54	13.1

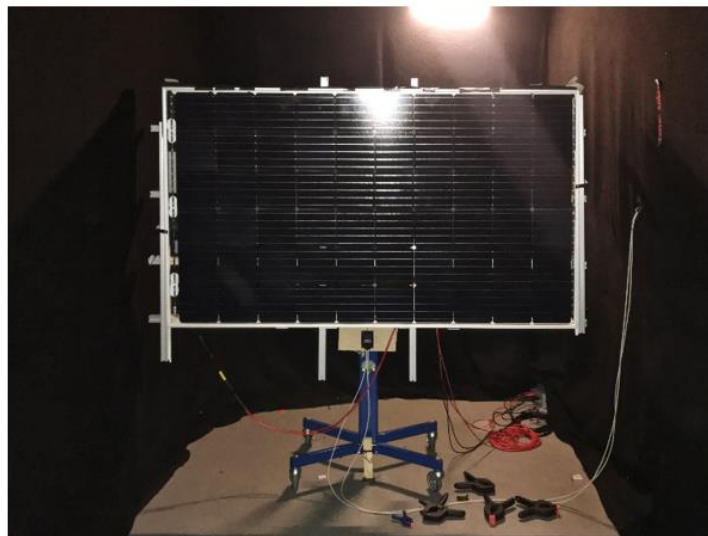


Figure 5.1. Setup for the indoor measurements at the University of Applied Sciences Hamburg.

5.1. General considerations

Measurement results for bifacial devices are more prone to errors than the ones for monofacial devices due to the measurement conditions deviating from the reference conditions. For example, the parasitic reflections from the rear side of the device under test can increase significantly the measurement uncertainty [Dur12].

5.2. Determination of bifaciality coefficient

As described in the standardization of the bifacial I-V characterization, the simulator's non-uniformity of irradiance must be below 5%. Before starting the measurements, with the help of a reference cell, levels of irradiance were measured at different points of the tested module. Figure 5.2 shows the measured percentage non-uniformity of the simulator between the highest irradiance value and the lowest, which is always below 5%.

4.65%	4.34%	3.46%
4.95%	2.94%	2.57%
2.48%	0.00%	1.29%

Figure 5.2. Measured simulator's non-uniformity of irradiance on different points of the bifacial module to be tested.

As the first step for the determination of the bifaciality coefficient ϕ_x , the I-V characteristics of the front side and the back side of the module have to be measured at STC ($G= 1000 \text{ W/m}^2$, $25 \text{ }^\circ\text{C}$). For this purpose, a non-reflecting and non-conducting material had to be used in order to avoid the illumination of the nonexposed side and eliminate then completely the contribution of the other side during the measurement. The background is considered to be non-irradiated if the irradiance is measured to be below 3 W/m^2 , on at least 2 points, on the non-exposed side of the device [DIN17]. Figure 5.3 shows the measurement set-up for the front- and the rear- side for indoor characterization of bifaciality

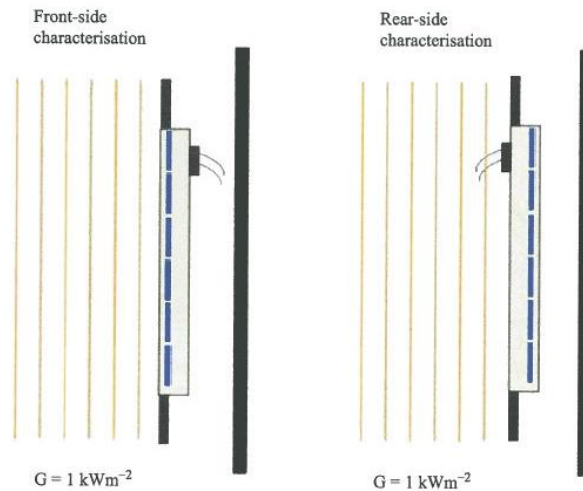


Figure 5.3. Front- and rear-side set-up for indoor characterization of bifaciality [DIN17].

In Figure 5.4, the I-V-curves for the front and rear side are depicted.

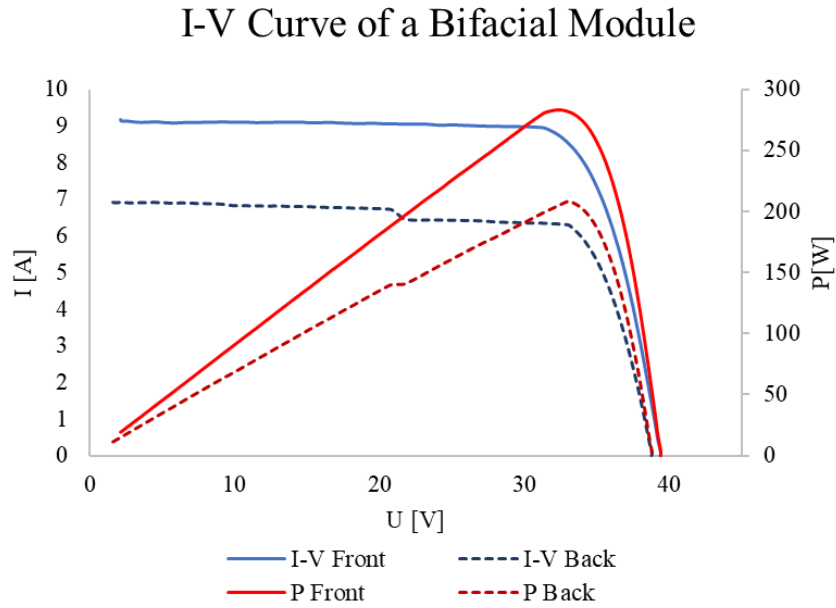


Figure 5.4. Measured I-V curve for the front and the rear side of the bifacial module.

As expected, the front side presents better performance than the rear side. This happens because, in back illumination, most of the charge carriers are generated away from the junction, which is located in the top of the cell, hence collection efficiency is lower than the one of the front side [Dur12]. As most of the bifacial modules, this test module has a distorted rear I-V-curve. This can be explained due to partial shading by the junction box, cabling, frame [Sch17].

Table 5.2 Electrical characteristics of the bifacial module used for the indoor measurements from the datasheet of the fabricant and from the indoor measurements (LR6-60BP 290M).

Source	Side	V_{oc} [V]	I_{sc} [A]	P_{mpp} [W]	V_{mpp} [V]	I_{mpp} [A]	η [%]
Datasheet	Front	39.2	9.36	290	32.6	8.90	17.5
	Back	38.9	7.16	218	33.3	6.54	13.1
Measured	Front	39.3	9.30	289	32.2	8.96	17.4
	Back	38.7	7.12	212	33.0	6.44	12.8

The bifaciality coefficient can be measured and calculated with the short circuit current, open-voltage, or maximum power. The short circuit current bifaciality coefficient φ_{Isc} is the ratio between the short-circuit current generated exclusively by the rear side of the bifacial device and the one generated exclusively by the front side of the bifacial module. The bifaciality coefficient is calculated with the Equation (5.1):

$$\varphi_{Isc} = \frac{I_{sc_r}}{I_{sc_f}} = \frac{7.12 \text{ A}}{9.30 \text{ A}} = 75.14 \% \quad (5.1)$$

Where:

$\phi_{I_{sc}}$: Short circuit current bifaciality coefficient

$I_{sc,r}$: Short-circuit current when the device is illuminated only on the rear side, at STC

$I_{sc,f}$: Short-circuit current when the device is illuminated only on the front side, at STC

As Equation (5.1) shows, the measured bifaciality coefficient of the module matches with the one shown in the data sheet provided by the manufacturer, over 75 %.

The open-circuit voltage bifaciality coefficient and the maximum power bifaciality coefficient are calculated with the same procedure as the short-circuit bifaciality coefficient.

Spectral mismatch correction

For the measurement of the bifacial coefficient, according to the DIN EN 60904-1-2 [DIN17], the spectral mismatch correction has to be applied to the front and back side measurements according to the IEC 60904-7 [IEC08] when the front and back side of the bifacial device have different spectral responsivity, in other words, when the ratio of the number of charge carriers collected by the solar cell and the number of photons of a given energy shining on the solar cell for the front and the back side of the bifacial module are different.

The TÜV Rheinland analyzed the spectral response of bifacial modules, the results of their measurements are shown in Figure 5.5.

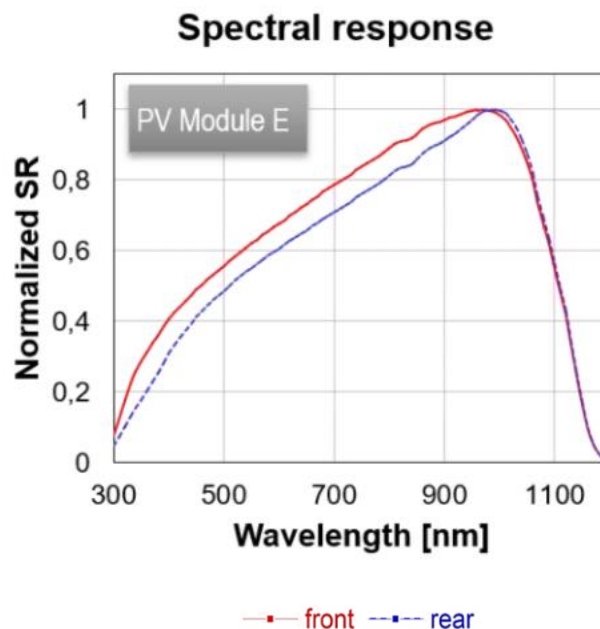


Figure 5.5. Measured spectral response of a bifacial solar module, front and rear side [Bon19a].

As can be seen in Figure 5.5, the spectral responses of the front and rear side of a bifacial module are slightly different. Therefore, a mismatch correction should be applied for the measurement of the bifaciality coefficient. The TÜV Rheinland compared the spectral response from a selection of bifacial modules and calculated the spectral mismatch for the front and the rear side of each module. All were at the millesimal order [Bon19b]. Therefore, the mismatch correction factor will be neglected.

5.3. Indoor power generation gain measurement

Identification of the power generation gain is one of the key parameters for the PV stakeholders in order to propose coherent investments. Power generation gain in bifacial modules is thanks to the rear side irradiance (G_{rear}); typical outdoor conditions involve rear irradiance levels between 5% and 30% of the front side irradiance. The exact value depends on the installation parameters as well as on the diffuse irradiance at the location of the PV plant. Thus, a good and realistic assessment of the gain in generated power of bifacial cells is to measure the IV characteristics with simultaneous irradiance in the front ($G_{front}= 1000 \text{ W/m}^2$) and rear ($G_{rear}= 150 \text{ W/m}^2$ or 300 W/m^2) illumination. Nonetheless, as this would involve two light sources, the new standard for measurements of bifacial cells and modules proposed for indoor measurements the equivalent irradiance (G_E) method.

The equivalent irradiance method considers that the bifacial cells operate at higher total irradiance. In order to perform indoor measurement of the power generation gain, a standard solar simulator with adjustable irradiance levels for one-side illumination had to be used. For this measurement, the rear side of the module had to be covered so that the rear irradiance is not higher than 3 W/m^2 . The power of the device is measured on the front side at equivalent irradiance levels G_{Ei} corresponding to 1000 W/m^2 on the front side plus different rear side irradiance levels G_{Ri} . The equivalent irradiance levels are determined as a function of the bifaciality coefficient φ according to DIN EN 60904-1-2:

$$G_{Ei} = 1000 \frac{\text{W}}{\text{m}^2} + \varphi \cdot G_{Ri} \quad (5.2)$$

$$\varphi = \text{Min} (\varphi_{ISC}, \varphi_{Pmax}) \quad (5.3)$$

Where:

G_{Ei} : one-side equivalent irradiance levels

φ : bifaciality of the module

G_{Ri} : different rear irradiance levels

φ_{ISC} : short-circuit current bifaciality coefficient

φ_{Pmax} : maximum power bifaciality coefficient

The measured φ_{ISC} is 75,14 % and the measured φ_{Pmax} was 73.02 % and for the measurements, the smallest has to be used. Therefore, the used bifaciality coefficient to determine the equivalent irradiance levels G_{Ei} corresponding to 1000 W/m^2 on the front side plus different rear side irradiance levels G_{Ri} is the φ_{Pmax} . In Figure 5.6, the maximum power output as a function of the equivalent one side irradiance levels and the extra rear side irradiance corresponding to 1000 W/m^2 is shown.

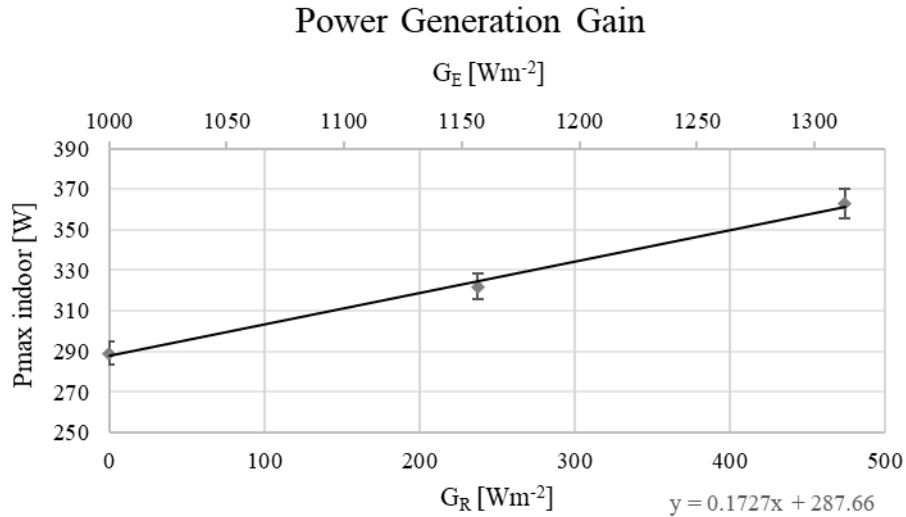


Figure 5.6. P_{max} as a function of irradiance level on the rear side G_R or its 1-side equivalent irradiance G_E

Through the function obtained with the indoor power generation gain measurement, Eq. (5.4), the power of the bifacial module under Bifacial Standard Test Conditions (BSTC) can be calculated.

$$P_{max}(W) = 287.66 + G_{rear} \cdot 0.1727 \quad (5.4)$$

Where:

P_{max} : maximum power

G_{rear} : rear irradiance

The BSTC according to the TÜV Rheinland standard 2PfG 2645/11.17, corresponds to 25 °C device temperature and front side irradiance of 1000 W/m² and rear side irradiance of 135 W/m² with the reference spectral irradiance distribution of AM1.5 as defined in IEC 60904-3 [IEC19, Sch18]. Therefore, the BSTC power is:

$$P_{BSTC} = 287.66 + 135 \cdot 0.1727 = 311 \text{ W} \quad (5.5)$$

Where:

P_{BSTC} : power under Bifacial Standard Test Conditions

6. Outdoor measurements

In order to verify the results of the simulations, a set of measurements under different conditions are carried out. Both short-term experiments, implemented in a PV plant from ENERPARC in Marlow (Germany), and long-term measurements, taken during a period of several months in a PV plant from ENERPARC in Dornstedt (Germany), are used to analyse data and to prove the correctness of the performed simulations and are described in chapters 6.1 and 6.2.

6.1. Long term measurements

Long term measurements have been performed between August 2018 and April 2019. These measurements allow checking the performance of bifacial modules in comparison with standard modules during summer and winter conditions.

6.1.1. Location and setup

The long-term measurements are carried out in a PV power plant from ENERPARC located close to Dornstedt, Germany (N 51.4179). This power plant has a surface of 11.450 m² and an AC power of 726,00 kVA resulting from 2545 PV modules. The PV plant is constructed with three types of modules. However, only two will be of interest, which are the ones that will be compared; both of them have the same power output of 290 Wp (front-side only), with the only difference that one is bifacial and the other is monofacial.

The installed bifacial modules are the LR6-60BP 290M manufactured by LongiSolar, made of monocrystalline silicon. Whereas the monofacial modules are made of multicrystalline silicon, from the REC Twinpeak 2 series 290 Wp manufactured by REC. In Table 6.1, the I-V-curve characteristics of each of them are summarized. The purpose of having two types of modules installed under the same conditions is to calculate the bifacial gain out of the comparison between the taken measurements of each of them.

Table 6.1 Type of modules in the PV plant

Type	Side	V_{oc} [V]	I_{sc} [A]	P_{mpp} [W]	V_{mpp} [V]	I_{mpp} [A]	η [%]
Monofacial		38.8	9.58	290	32.1	9.05	17.4
Bifacial	Front	39.2	9.36	290	32.6	8.90	17.5
	Back	38.9	7.16	218	33.3	6.54	13.1

During the planning of the PV plant, special attention was given to the placement of the modules in order to install them under the same conditions of irradiance reaching the surface of the module as well as the shadowing of the neighboring modules for each type of technology so the fairest comparison could be obtained. In Figure 6.1, the placement of the bifacial and monofacial modules is depicted in red and green respectively.



Figure 6.1. Schematic showing the setup of monofacial and bifacial modules installed at Dornstedt in Germany for the long-term measurements. Red represents bifacial modules, green represents monofacial modules (Enerparc AG).

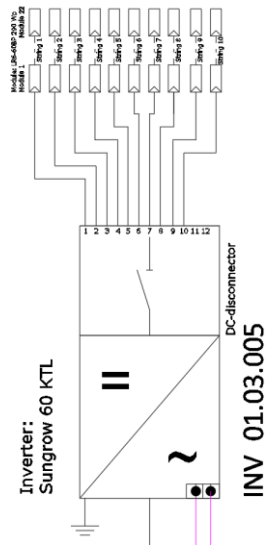
Part of the setup for the long-term measurements is depicted in Figure 6.2, where both monofacial and bifacial modules can be distinguished thanks to the different appearance of the rear side of each of them.



Figure 6.2. Photograph showing part of the setup of monofacial and bifacial modules installed at Dornstedt in Germany (Enerparc AG)

Concerning the electrical description, the inverter concept is the string inverter. Each type of modules is connected to a different inverter so the power output of each type of modules can be separately analyzed with the monitoring system of Enerparc. The type of inverter is the *Sungrow 60 KTL*, with a power of 66 kVA for both types of modules. Each inverter has 10 strings containing 22 modules each of them. The inverter has an MPP tracker, the reason why the analyzed modules are all installed on the upper part of the table, so all of them reach a similar irradiance. Figure 6.3 shows the single line diagram for both modules connected to their respective inverter.

a)



b)

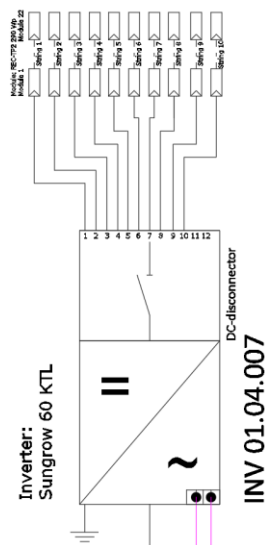


Figure 6.3. Single line diagram for both bifacial **a)** and monofacial **b)** modules (Enerparc AG)

The 10 bifacial PV modules strings are connected to the inverter number 01.03.005, and the strings with monofacial PV modules are connected to the inverter 01.04.007.

As for the module tables, they are constructed at a height of 0,79 m between the ground and the lowest point of the table, this means that strings of modules will be installed at different heights of 2,09, 2,43 and 2,78 m. The distance between tables is 3,5 m and the tilt angle is 20°. Those values are depicted in Figure 6.4.

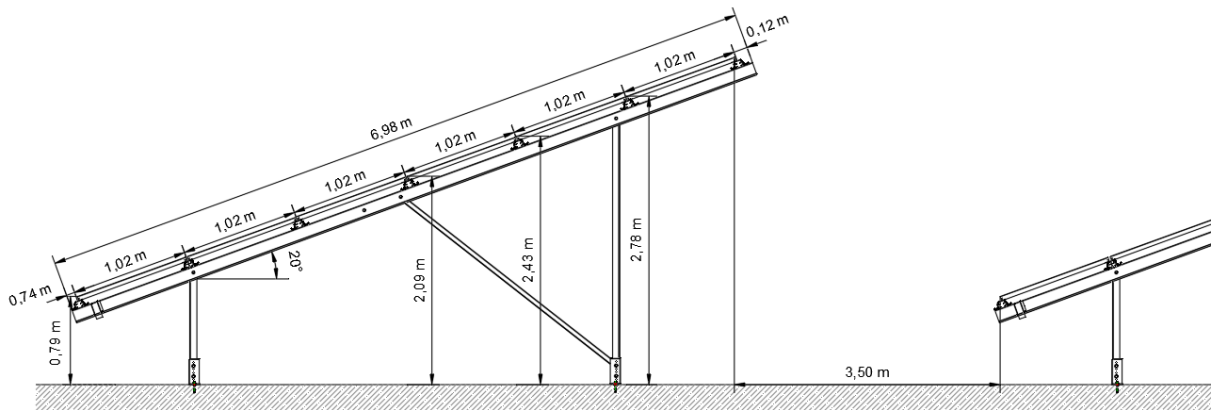


Figure 6.4. Placement of the tables (Enerparc AG).

6.1.2. Data Acquisition System

Temperature – module level

A temperature sensor Pt1000 was installed on half of one monofacial module. The module temperature sensor is accurate to within ± 0.3 % of true module temperature [Gana]. Through the control of the module temperature, some characteristics of the I-V curve can be measured. As S. Kühn-Tomä [Küh19]

demonstrated through measurements in her study, the temperature difference between the monofacial PV modules and the bifacial PV modules is smaller than the dispersion of the bifacial temperature readings at a measurement time point and therefore, it can be assumed for all subsequent measurements that both types of PV modules have the same module temperatures.

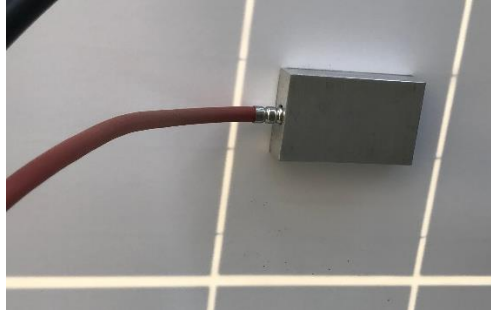


Figure 6.5. Module temperature sensor

Temperature – ambient level

The ambient temperature sensor is equipped with a platinum resistance Pt1000, DIN EN 60751 CI [Ganb]. B. The sensor is placed in a plastic shaft and screwed into the base plate by means of a cable duct. The protection shelter is designed in order to avoid influence from radiation, precipitation, direct irradiance, etc.



Figure 6.6. Ambient temperature sensor

Plane-of-array global irradiance – PV plant level

The PV plant has two plane-of-array irradiance measurement devices: a pyranometer from Kipp and Zonen and a reference cell from IngenieurBüro with an accuracy of $\pm 5\%$.

Pyranometers are specially designed to reach light from all angles and to have a stable output regardless of sky conditions and changing ambient conditions. Whereas reference solar cells are designed to measure the irradiance that is available to a PV module for conversion into electricity rather than being designed to measure the broadband irradiance.

6.1.3. Data Analysis

Thanks to the monitoring system, data collected every 15 minutes is available. In order to quantify the yearly and monthly specific energy yield as well as the bifacial gain, the power output for every month is analyzed. The results are depicted in Figure 6.7.

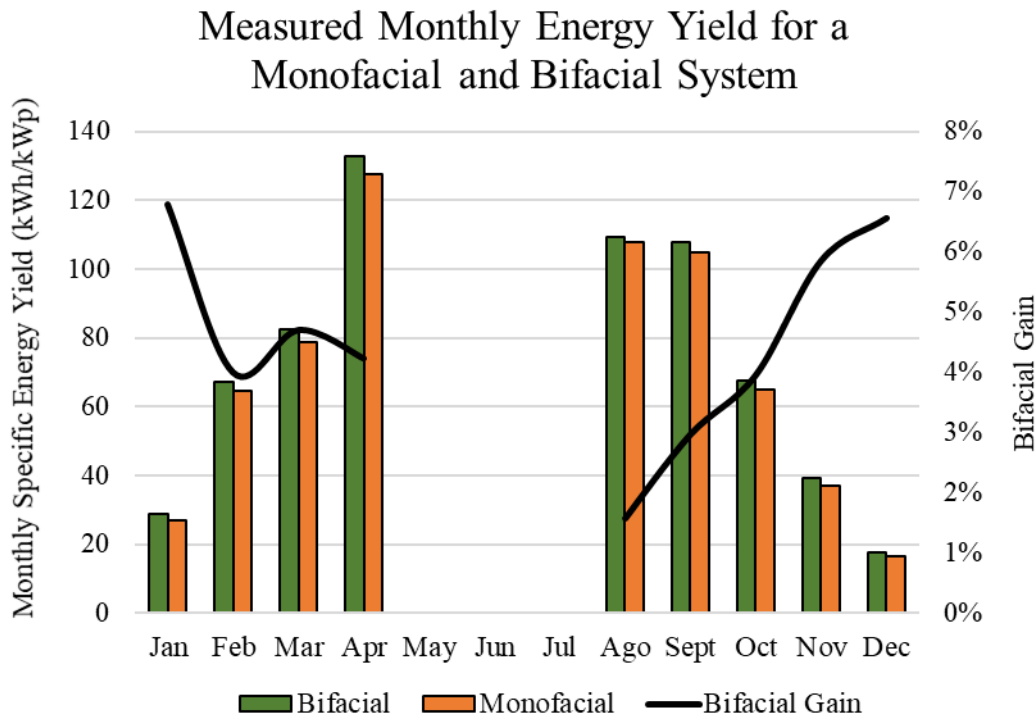


Figure 6.7. Monthly specific energy yield for the entire time of generation of the power plant in Dornstedt (N 51.4179). The PV plant has a fixed tilt angle of 20 °, pitch of 3.5 m, an elevation of 0.8 m and an estimated albedo of 18 %.

According to the measured values, for a PV plant with the geometry of the power plant in Dornstedt a yearly bifacial gain of 4 % is expected. Certainly, this value could be increased if another material with higher albedo was installed underneath the modules as well as if the distance between the rows was extended, both topics will be discussed in further chapters.

Unfortunately, since the power plant started operating in August 2018, there are still some months missing for the analysis of an entire year. Nevertheless, with the available measurements, it was possible to observe that bifacial modules had slightly a higher energy generation than the monofacial modules. Moreover, it was also observed that the bifacial gain was higher during the winter months. This can be due to the fact that bifacial modules benefit from the weather conditions taking part in winter: diffuse irradiance, low temperatures, and high albedo (snow). As mentioned in chapter 4.1, the albedo of the PV plant changes along the day and the year and is dependent on the weather conditions. Snow has a very high albedo, which affects directly to the bifacial gain. In Figure 6.8, the effect of the snow laying on the ground of the PV plant is illustrated; it can be seen that for a day with no snow the bifacial is not as high as for a day with a certain amount of snow on the ground of the PV plant.

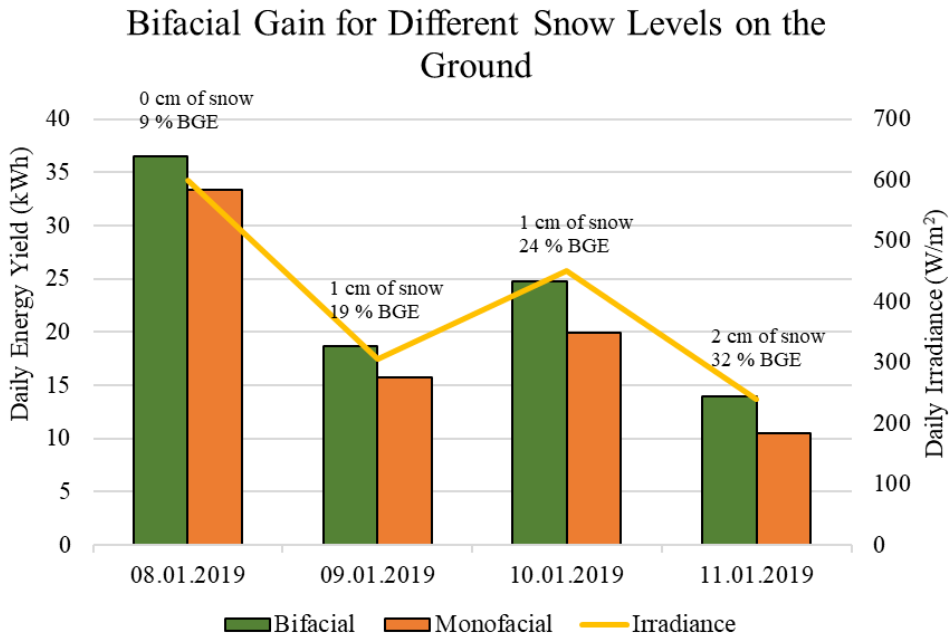


Figure 6.8. Effect of the amount of snow underneath the modules in the bifacial gain. Measurements from a power plant in Dornstedt (N 51.4179) with a fixed tilt angle of 20°, pitch of 3.5 m, an elevation of 0.8 m and an estimated albedo of 18% when there is no snow and 80% with snow.

The snow levels were obtained from the database of “Wetteronline”.

6.2. Short term measurements

The short-term measurements have been carried out during the month of April 2019. These measurements allow comparing the performance of the bifacial modules under different installation conditions.

6.2.1. Location and setup

The measurements are carried out in an Enerparc PV plant located in Marlow, Germany (N 54.16°, E 12.56°). The installation consists of a table with nine adjacent south-facing bifacial modules. The structure is meant to allow the tilt angle to be modified. Therefore, all the support points are in the middle of the structure with a height of 2.00 m. The tilt angle can be modified using the straps attached to each side of the table (see Figure 6.9 and Figure 6.10). The mounting structure has been designed on purpose for bifacial modules, i.e. rail edges are installed under the module frames avoiding the shading on the rear side of the modules.

a)



b)

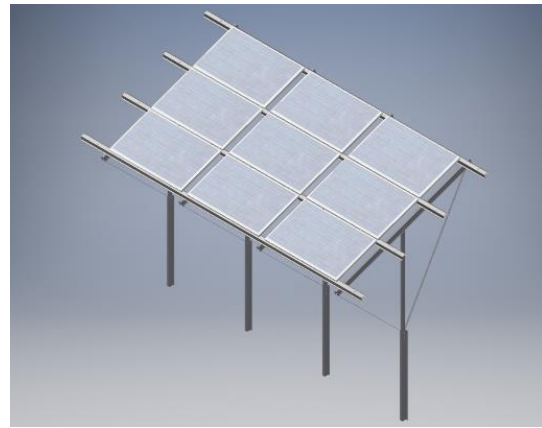


Figure 6.9. Schematic showing the structure designed to carry out the short-term measurements **a)** without modules **b)** with modules. (Enerparc AG).

a)



b)



Figure 6.10. Structure used for the short-term outdoor measurements. Structure designed with four poles in the middle of the width and with four straps at each side in order to modify the tilt angle. **a)** without modules **b)** with modules.

6.2.2. Data Acquisition System - HelioScale ϕ

For the short-term outdoor experiments, a special mobile meteorological station is used. The meteorological station is engineered, assembled and tested by Wilmers Messtechnik, a company based in Hamburg (Germany) that produces data acquisition devices for renewable energy systems.

Rotating Shadowband Irradiometer (GHI, DHI, DNI, Temp)

In order to obtain the required level of accuracy, a Rotating Shadowband Irradiometer (RSI) is used. The RSI consists of a horizontally and north faced mounted pyranometer with a shadowband that rotates automatically at the programmed revolutions per minute – for this study is programmed to rotate every 15 seconds – in order to shortly shade the pyranometer. When the shadowband is in its rest position the global horizontal irradiance (GHI) is measured with a 1-second sampling interval [Wil16]. During the continuous rotation of the shadowband, the pyranometer signal is measured using a high-frequency continuous shooting mode (burst mode). The rotation and the burst mode occur within approximately 1 second. The minimum signal during the burst represents the diffuse horizontal irradiance (DHI). DNI is then calculated from DHI, GHI and the solar zenith angle (SZA). Moreover, the RSI also measures the ambient temperature.

In Figure 6.11 can be seen the Rotating Shadowband Irradiometer installed for the short-term measurements.



Figure 6.11. Rotating Shadowband Irradiometer (RSI) from Hukseflux

Albedometer

It is of great importance to know the exact albedo of the ground surface since it will have a direct impact on the power output. For this purpose, an albedometer that consists of two second-class standard photodiode pyranometers from the manufacturer Hukseflux; one facing the sky and another facing the ground, were used. Then, the albedo was obtained out of the calculation of the ratio of the reflected over the global radiation. Figure 6.12 shows the albedometer used for the short-term outdoor measurements.

According to the fabricant, it is recommended to install it at a distance of 1.5 to 2 m between the ground and the downfacing sensor in order to reduce the shadow effect [HUK18].



Figure 6.12. Set up for the albedo measurement from Hukseflux, composed of two pyranometers; one facing the sky and the other facing the ground.

6.2.1. Data Acquisition System – HT I-V400W

For the measurement of the I-V curve of the modules, the measurement equipment from the company HT ITALIA I-V400W model was used. The accuracy of the digital tester HT ITALIA I-V 400 W is defined as the difference between the reading and the true value for a quantity measured in reference conditions. For the accuracy specification, the abbreviation “rdg” is used, which stands for reading and identifies a percentage error relative to the reading. Another abbreviation used is “dgt” and stands for digits, it indicates the counts on the last significant digit of the digital display.

The I-V400W is equipped with a reference cell to measure the plane-of-array global irradiance – with an accuracy of $\pm(1.0\%rdg+5dgt)$ – and with a module temperature sensor – with an accuracy of $\pm(1.0\%rdg+1^{\circ}C)$ –.

The acquired data are worked out by the measurement equipment and transferred to the reference conditions (STC) in order to be compared, the measurement of the maximum power at STC has a global accuracy of $\pm(5.0\%rdg+1dgt)$.

6.2.2. Methodology for the analysis of the short-term measurements

For the short-term measurements, a table of 9 modules was specially designed in order to take also into account in the measurements the effect of the shadowing of the neighboring modules in the power output and the bifacial gain. For this reason, in the first place, the effect of the size of the system was evaluated and then all measurements were focused on the module in the middle of the table, which represented the worst case and the most realistic one.

Then, the I-V curves for different covering material under the table were carried out during an entire day. After these measurements, the total Wh/day was obtained as well as the best tilt angle for that exact period of the year.

After verifying the measurements, in order to extrapolate them for an entire year, the data of our weather station (GHI, DHI, DNI as well as the exact albedo) will be introduced in the simulation software PVsyst in order to compare the results of the simulation with the measured ones.

Once compared the simulation with the carried-out measurements and validated the simulation, a simulation for an entire year can be done in order to really know the best installation conditions.

6.2.3. Verification of the STC extrapolation from the HT I-V 400 W

Thanks to the I-V curve tracer, the electrical characteristics of the measured module can be known for the moment of the measurement. Even though measurements were done during a short period of time during a day with almost no irradiance and temperature fluctuations, measurements are carried out under different times of the day. Therefore, in order to compare measurements under the same measurement conditions, the values have to be extrapolated to Standard Test Conditions (STC).

The I-V curve tracer software already provides this extrapolation with a global accuracy of $\pm(5.0\%rdg+1dgt)$. Nevertheless, before using the values provided by the measurement equipment, another method is also used in order to compare the values and prove their reliability.

With the following formula the maximum power under STC can be calculated out of the power under OPC, the cell temperature and the irradiance on the module under OPC:

$$P_{STC} = \frac{P_{(E,t_c)}}{1 + \gamma * (t_c - t_{STC})} * \frac{E_{STC}}{E} \quad (6.1)$$

Where:

P_{STC} : Power under STC in W

$P_{(E,t_c)}$: Power at the irradiance and temperature level at the moment of the measurement in W

γ : Temperature coefficient in %/°C

t_c : Cell temperature

t_{STC} : Temperature at STC, 25 °C

E : Irradiance on the plane of the array in W/m²

E_{STC} : Irradiance at STC, 1000 W/m²

With the I-V tracer only the module temperature is measured, for the cell temperature the following formula is used [Boy04]:

$$T_c = T_m + \frac{E}{E_{STC}} * \Delta T \quad (6.2)$$

Where:

T_c : Cell temperature inside the module in °C

T_m : Measured back-surface module temperature in °C

E : Measured solar irradiance on the module in W/m²

E_{STC} : Solar irradiance on the module in STC, 1000 W/m²

ΔT : Temperature difference between the cell and the module back surface at an irradiance level of 1000 W/m² (Table 6.2).

Table 6.2 provides the empirically-determined temperature difference between the cell and the module back surface for different types and mounting configurations. In this study, a glass/cell/glass module type is studied with open rack.

Table 6.2. Empirically determined temperature difference between the cell and the module back surface as a function of the module type mounting structures [Boy04]

Module Type	Mounting structure	ΔT
Glass/cell/glass	Open rack	3
Glass/cell/glass	Close roof mount	1
Glass/cell/polymer sheet	Open rack	3
Glass/cell/polymer sheet	Close roof mount	0

The values under STC from the I-V curve tracer and the ones calculated are compared and an error lower than 5 % was obtained. Table 6.3 depicts the results of the calculations for different temperature and irradiance conditions.

Table 6.3. Pmax under STC comparison between the I-V curve tracer software and the calculated values.

$P_{max_{OPC}}$ (W)	E (W/m ²)	T_{mod} (°C)	T_{cell} (°C)	$P_{max_{STC}}$ I-V 400W (W)	$P_{max_{STC}}$ Calculated (W)	\pm Error (%)
132.04	357	24.10	25.81	374	370	1.27
155.61	498	21.00	31.37	311	312	0.23
159.35	483	25.10	36.37	339	339	2.71
231.89	706	31.80	67.35	336	328	2.51
261.91	813	37.90	38.71	336	320	4.82

6.2.4. Effect of the size of the system in the bifacial gain.

As mentioned in chapter 4.4, the effect of the neighboring modules has a certain impact on the bifacial gain and, therefore, on the entire PV plant yield. In order to quantify this effect, the power output of all modules in the structure is measured and then transferred into Standard Test Conditions (STC). The experiment is carried out with a tilt angle of 20 ° because this is the current tilt angle that ENERPARC uses for their projects in Germany. As for the albedo, a white surface with a measured albedo of 44 % is used in order to make more visible the effect of the neighboring modules on the rear irradiance and thus the bifacial gain.



Figure 6.13. Experimental set-up for the measurements for quantifying the effect of the neighboring modules.

In Figure 6.13 the set up for the experiment is depicted. As can be seen in Figure 6.13, the shadow of the modules is under certain modules. While for those modules less bifacial gain is expected, for the ones that have no shadow on the surface underneath, a higher rear irradiance is expected as well as a higher bifacial gain.

For the measurement of the bifacial gain, only the power output of the front side has to be measured, for this purpose, the rear side of the module is covered with a black cover preventing any irradiance to reach it as depicted in Figure 6.14. When measuring the front-side power output of each module, it is also being ensured that all modules under test are working properly.



Figure 6.14. Experimental set-up for the measurements of the power output of just the front side of the bifacial module.

Results

For the analysis of the measurements, the used nomenclature to refer to each module is from left to right and from the highest row to the lowest. Table 6.4 summarises the results.

Table 6.4. Raw results of the measurements carried out to measure the impact of the shadowing of the neighboring modules for the power output and the bifacial gain.

Module	Time (hh:mm)	$P_{max_{STC}}$ (W)	$P_{max_{STC}}$ (W)	Bifacial gain (%)
		(back side not covered)	(back side covered)	
1	15:03 - 15:06	327	290	13
2	15:09 - 15:11	320	289	10
3	15:15 - 15:19	310	292	7
4	15:00 - 15:02	333	289	15
5	14:52 - 14:53	322	292	11
6	15:13 - 15:20	323	282	11
7	14:57 - 15:58	346	291	19
8	14:54 - 14:55	337	291	16
9	15:17 - 15:17	341	295	17

Measurements were taken on a sunny day with almost no fluctuations on the global irradiance and module temperature within a period of 20 minutes. Nevertheless, irradiance and temperature levels change slightly. For this reason, in order to compare the power output, the measurements are transferred to STC.

Bifacial Gain for each Module in the Measurements Table in the Afternoon

13% ¹	10% ²	7% ³
15% ⁴	11% ⁵	11% ⁶
19% ⁷	16% ⁸	17% ⁹

Length of the structure with three modules in landscape



Figure 6.15. Measured bifacial gain for each module of the measurements table on a sunny day at 15:00 h.

On one side, as expected, since the module number 7 has only two neighboring modules and two sides free of shadowing it has the maximum power output and bifacial gain. Moreover, during the moment of the measurements, this module had no self-shadowing on the surface underneath, which is beneficial for the reflected irradiance. On the other side, a lower bifacial gain is obtained for the module installed in the middle, module number 5, this happens due to the neighboring modules preventing the diffuse irradiance to reach the rear side of the module. Furthermore, part of the surface underneath the module in the middle is shadowed. The module with less bifacial gain is the module number 3, this happens due to the fact that the covering material was not covering the whole surface underneath the module and that the whole surface was shadowed during the moment of the measurement.

As observed, the effect of self-shadowing on the surface underneath the module has a great impact on the power output and bifacial gain. Nevertheless, the shadow moves all over the day and affects first the modules on the left edge and then the modules on the right edge, but the module on the middle is always affected. To show this effect, the same experiment was repeated during the morning. Results are depicted in Figure 6.16.

Bifacial Gain for each Module in the Measurements Table in the Afternoon

6% ¹	12% ²	15% ³
8% ⁴	11% ⁵	19% ⁶
14% ⁷	15% ⁸	21% ⁹

Length of the structure with three modules in landscape →



Figure 6.16. Measured bifacial gain for each module of the measurements table on a sunny day at 10:00 h.

The obtained results match with the study of Asgharzadeh, A. *et al.*, who studied the impact of the size of the system and found out in their simulations that the yield of the modules in a large array can decrease up to 7 % relative to single module system [Asg17]. For the case of this experiment, an average of 4 % of the decrease in the yield is measured and up to 12 % of difference between the highest bifacial gain and the lowest.

Therefore, all further measurements were carried out with the module in the middle of the measurements table, because it is the worst and most realistic case.

6.2.1. Albedo measurement

Defining the exact albedo of the surface of the PV plant is of great importance since the energy generated by the rear side will be mainly due to the reflected irradiance. For this reason, albedo was measured in order to have the most accurate value as possible. There are two ways to measure the albedo:

Monofacial module [Ame17]

One solution for the albedo measurement is the usage of a monofacial module as a measuring instrument. For this purpose, a monofacial module and a voltmeter (multimeter) are needed as test setup. The solar panel should be fixed in a way in which the solar cells of the module face the sky at 180° angle to the ground. The frame should be high enough so that no shadow from the frame, module or person falls directly under the solar module. Then the short circuit current of the module is measured twice for each spot where the albedo has to be measured; one facing up towards the sky ($I_{sc,sky}$) and the other facing towards the ground ($I_{sc,ground}$).

The albedo of each specific spot can then be calculated according to the following formula:

$$\text{Albedo of the spot} = \frac{I_{sc,Ground}}{I_{sc,sky}} \cdot 100\% \quad (6.3)$$

Where:

$I_{SC,sky}$: Measured short circuit current of the module when facing the sky.

$I_{SC,Ground}$: Measured short circuit current of the module when facing the ground.

The overall albedo of the surface is the arithmetic mean of the measured albedo values for each testing spot.

Albedometer

The albedometer is an instrument used to measure the albedo of a surface and it consists of two pyranometers: one facing up towards the sky and the other facing down towards the surface. Albedo can be obtained calculating the ratio of the reflected over the global radiation.

It is recommended to be installed at a distance of 1.5 to 2 m between the ground and the downfacing sensor, this way, the effect of shadows is reduced [HUK18].



Figure 6.17 Albedometer SRA20 [HUK18]

For the experiments carried out in this project, the used meteorological station is composed by two pyranometers (albedometer); one facing the sky and another facing the ground at a distance to the ground of 2,00 m. The pyranometer facing the sky provides Global Horizontal Irradiance (GHI) measurements in 1 second step resolution. Moreover, combined with the pyranometer facing the ground, it also provides the albedo measurements for the ground covering material.

In order to analyze the effect of the reflective surface, different covering materials with different colors were used for the measurements. The colors used were green, silver and white in order to simulate the effect of grass, white plebes and snow respectively.



Figure 6.18. Used covers for the measurement of the effect of the albedo of the ground reflecting material and set-up for the albedo measurement.

On the first place, the measurement of the exact albedo for each covering material was carried out extending the material all over the surface underneath the albedometer as shown in Figure 6.18. The resulting value out of the ratio between the global irradiance measured by the pyranometer facing the ground and the pyranometer facing the sky is the albedo. Table 6.5 shows the results of albedo measurements.

Table 6.5. Measured albedos for each covering material used for the experiments.

<i>Colour of the covering material</i>	<i>Measured Albedo (%)</i>
No cover	12
Green	17
Silver	24
White	44

According to the albedo measurements, a higher generation is expected to be achieved with the white cover underneath the modules than with the green cover.

For further analysis, models and simulations will be compared with the measurements in order to demonstrate its validity and use them to predict the bifacial gain. Thanks to the exact albedo measurement, the validation of the models and simulations will be more precise.

6.2.1. *Effect of the reflective surface*

The covers, with dimensions of 12 m x 16 m each, were extended symmetrically all over the surface that the table of modules encompasses as depicted in Figure 6.19.



Figure 6.19. Experimental set-up for the measurements of the effect of different albedos in the bifacial gain.

Then, the power of the module located in the middle of the measurement table was measured for different albedos and a tilt angle of 15 °. Table 6.6 shows the results of the measurements.

Table 6.6. Measured bifacial gains for a single module with different covering materials underneath and a tilt angle of 15 ° on a sunny day.

Colour of the covering material	Measured Albedo (%)	Total bifacial Gain (%)
No cover	12	4
Green	17	6
Silver	24	9
White	44	17

Measurements were taken between 16:00 and 17:00 h, when the shadow was not located underneath the module in the middle. Reason why the covering material has such a high effect in the bifacial gain. A function is extrapolated out of these values and depicted in Figure 6.20.

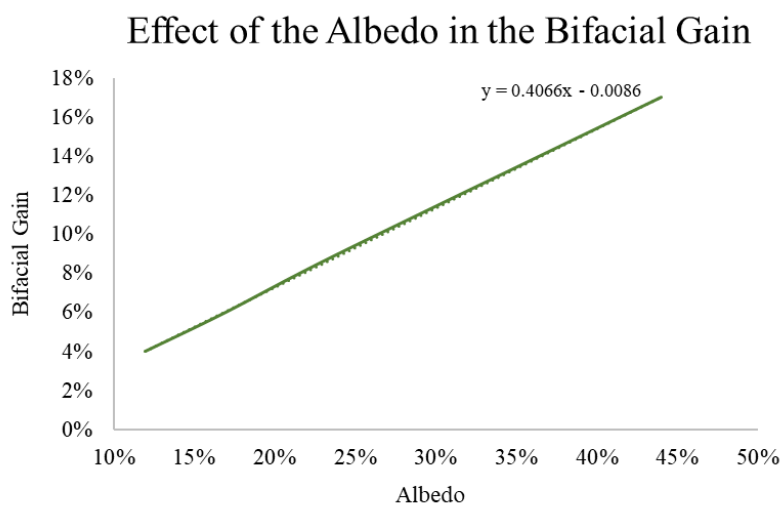


Figure 6.20. Function of the effect of the albedo in the bifacial gain for a single module with no shadow underneath it.

As expected, the higher the albedo, the higher the diffuse horizontal and direct normal irradiance on the rear side of the module and, therefore, the higher the bifacial gain, resulting in the following function:

$$\text{Bifacial Gain [\%]} = 0.4974 \cdot \alpha - 0.0175 \quad (6.4)$$

Where:

α : albedo of the material underneath the measured module

As mentioned in chapter 6.2.4, the effect of the reflection of the covering surface and the effect of shadow have a great impact on the power output. Hae Lim Cha *et al.* used in their paper the view factor to determine the element of back reflection to be predicted. The view factor ($F_{1 \rightarrow 2}$ or F_{12}) is the proportion of the radiation which leaves a surface A_1 and reaches a surface A_2 . F_{12} can be described then as the part of the irradiation that directly strikes from surface A_1 to A_2 .

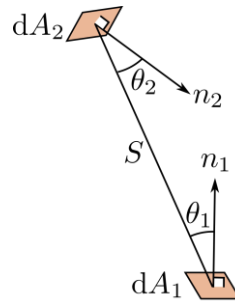


Figure 6.21. View factor between two surfaces.

The view factor from a general surface A_1 to another general surface A_2 at a distance S is given by the following equation:

$$F_{1 \rightarrow 2} = \frac{1}{A_1} \int_{A_1} \int_{A_2} \frac{\cos\theta_1 \cos\theta_2}{\pi S^2} dA_2 dA_1 \quad (6.5)$$

Where:

$F_{1 \rightarrow 2}$: view factor from a general surface A_1 to another general surface A_2

A_1 : Area 1

A_2 : Area 2

θ_1 : angle between the ray between the two differential areas and the surface normal of area A_1

θ_2 : angle between the ray between the two differential areas and the surface normal of area A_2

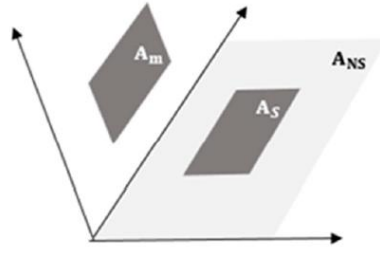


Figure 6.22. The components of the reflected radiation to the rear side [Cha18].

Hae Lim Cha *et al.* assumed that the area of the module is A_m and that the area of the ground where the irradiance affects the back of the module reflected is A_s , both depicted in Figure 6.22. In the Figure, A_{NS} is the area that does not affect directly the back of the module. The total area of the irradiance reaching the rear side of the module can be expressed by the view factor [Cha18]:

$$F_{ms} = \frac{1 - \cos(180^\circ - \beta)}{2} \quad (6.6)$$

Where:

F_{ms} : view factor of area A_s of irradiance affecting the area A_m

β : angle between the module and the ground, tilt angle

Then, it can be assumed that the total irradiance ($I_{Rear,total}$) reaching the rear side of the bifacial module is the sum of the direct irradiance ($I_{Rear,dir}$) and the diffuse irradiance ($I_{Rear,diff}$) on the area of the module (A_m). The albedo coefficient (α) is used for determining the total irradiance reaching the back side of the module [Cha18]:

$$I_{Rear,total} [W/m^2] = \alpha \cdot DNI [W/m^2] \cdot F_{A_s \rightarrow A_m} + \alpha \cdot DHI [W/m^2] \cdot F_{A_s \rightarrow A_m} \quad (6.7)$$

Where:

$I_{Rear,total}$: total irradiance on the rear side of the module

α : albedo coefficient

DNI : Direct Normal Irradiance

$F_{A_s \rightarrow A_m}$: view factor of area A_s of irradiance affecting the area A_m

DHI : Diffuse Horizontal Irradiance

It can already be seen that the albedo is directly proportional to the irradiance reaching the rear side. In order to prove the model, the power output will be calculated for the same conditions under which the measurements were taken and then theoretical and empirical results will be compared.

Thanks to the HelioScale ϕ meteorological station, the irradiance on the rear side of the module can be calculated with the measured values of direct normal irradiance (DNI) and diffuse horizontal irradiance (DHI). In Chapter 5.3, the power generation gain was measured for different irradiance levels on the rear side of the module with 1000 W/m^2 as a reference irradiance for the front side (BSTC). Through the extrapolated function obtained from this experiment, Eq. (5.4), and the measured irradiance values for the moment of the measurements, the output power can be calculated.

It is important not to forget that this model is valid for a single module, in chapter 6.2.4 the effect of the neighboring modules is quantified to be -4% in the power output. Therefore, to the calculations of the modeling a correction of the 4% has to be added. Therefore, the formula used to calculate the power output of a single module contained in a power plant is:

$$P_{Module}[W] = 0.96 \cdot (0.1727 \cdot I_{Rear,total} + 287.66) \quad (6.8)$$

In Figure 6.23 the measured and calculated values are depicted.

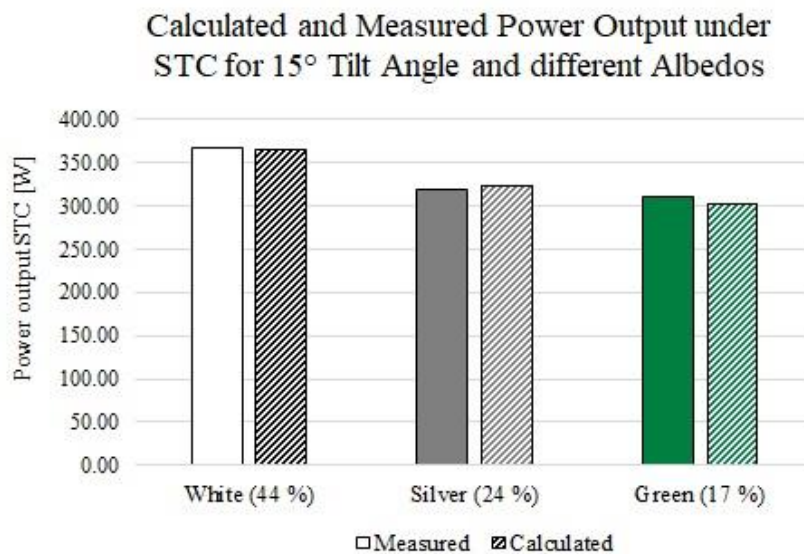


Figure 6.23. Calculated and Measured power output (W) of a single module with 15° tilt angle and for different albedo values.

With an average error of 1.9% between the measured and the calculated values, the model is accepted as valid and, with it, the theoretical explanation of the effect of the albedo of the ground underneath the modules.

6.2.2. Effect of different tilt angle

The sun's latitude and direction of incidence, which vary during the entire year, have a great impact on the amount of sun entering the solar module. Therefore, in order to obtain a result for a long term period, the measurements for an entire day will be compared with the simulation done for the exact same weather conditions measured by the pyranometer and then the simulation will be extrapolated for an entire year. On the 15.04.2019 the power output for a single module was measured every 30 minutes in

order to get the daily generation curve. Measurements were taken for two tilt angles, 20°, and 10° and with a measured albedo of 44 %. Results are depicted in Figure 6.24.

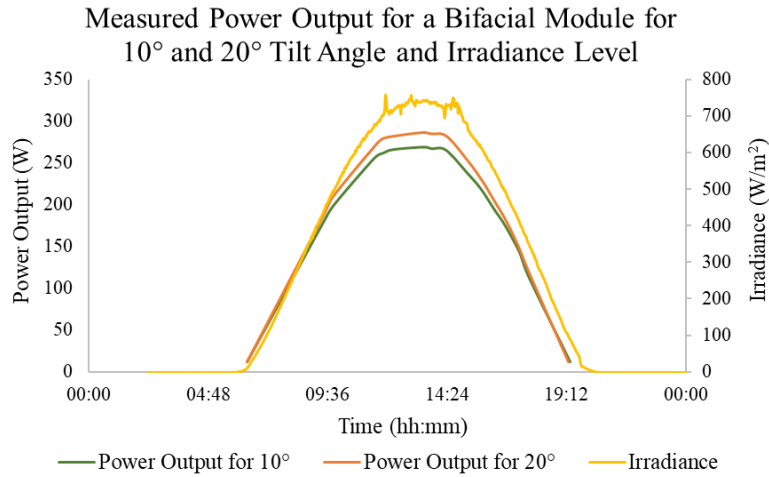


Figure 6.24. Measured power output during an entire day of a bifacial module with a front side power of 290 Wp and measured irradiance level for the same day.

In Figure 6.24 the results of the power output measurements during an entire day can be seen as well as the irradiance level. As it can be observed, more power output was obtained for 20° tilt angle than for 10° tilt angle. It can also be seen a slight shift between power output measurements and irradiance level measurements. This fact happens due to the different spectral responses that the PV cells and pyranometers have. Due to the changing position of the sun, pollution, humidity, clouds, etc, the solar spectrum at ground level varies considerably and, whereas pyranometers measure the total spectrum from 0.3 to 3 micrometers wavelength and give an integrated measurement of the total solar energy available, solar cells can only measure from 0.3 to 1.2 micrometers.

Once obtained the experimental values, a simulation is done for the same installation conditions and weather data. Results are shown in Figure 6.25.

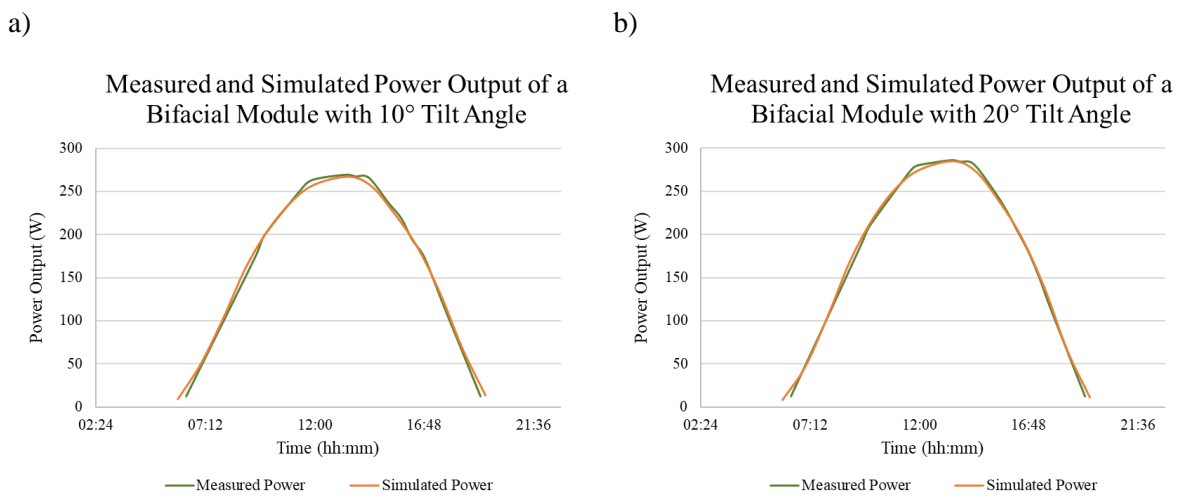


Figure 6.25. Measured and simulated power output for a single module with a front side power of 290 Wp a) for 10° tilt angle and b) for 20° tilt angle.

Once demonstrated the validity of the simulation model, a simulation will be extrapolated for an entire year. The weather data used for the simulation comes from irradiation data of various sources, which are assessed with regard to their data generation and recording period by SolPEG (Solar Power Expert Group) [Sol19], who provides a weighted average of monthly irradiance. This method leads to a high statistical certainty (long averaging period, consideration of different data generation methods) and emphasizes the radiation development of recent years. Figure 6.26 depicts the results of the simulations.

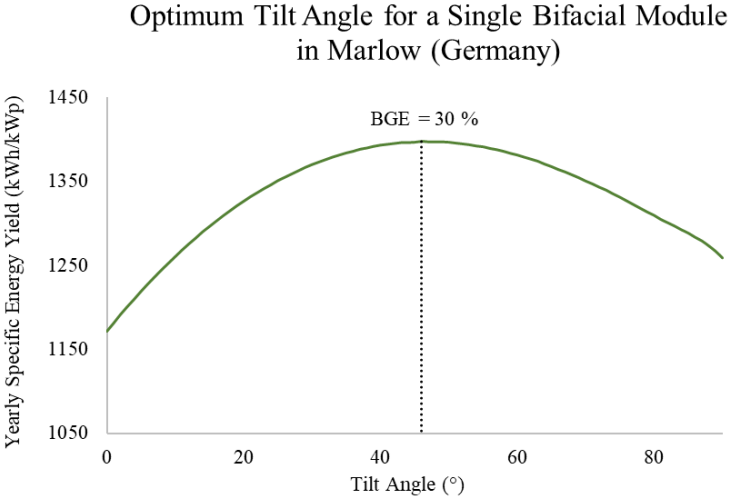


Figure 6.26. Simulated yearly specific energy yield (kWh/kWp) for a single bifacial module with 290 Wp front side power output. With an elevation of 2 m, albedo of 44 % and different tilt angles.

In Figure 6.26, the simulated yearly specific energy yield for the same module used for the outside measurements with no shadowing obstacles in the neighboring and installed in the north of Germany (Marlow, N 54.16°) for different tilt angles. The optimum tilt angle for this case is 46°. If those installation conditions are compared with a monofacial module installed in a typical power plant with 20° tilt angle, 6 rows of modules per table and 2.3 m of distance between rows, a bifacial gain up to 30 % is obtained.

Certainly, this is a nonrealistic case since PV systems are rarely installed singularly and they are rather installed in a field with neighboring modules and several module rows. Since Enerparc bets for a high usage of the available surface, with a collector width of 6 m and a distance between rows of 2.3 m, resulting in a GCR of ~ 75 %, simulations have been carried out for a 766 kWp bifacial power plant with a GCR of 75 % and different tilt angles.

Optimum Tilt Angle for a Bifacial Power Plant in Marlow (Germany)

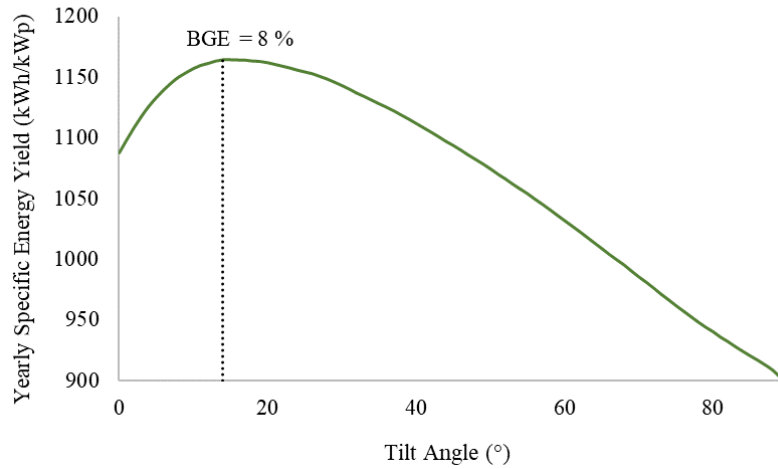


Figure 6.27. Simulated yearly specific energy yield (kWh/kWp) for a power plant in Marlow (Germany) with an albedo of 44 %, a height between the lower side of the module and the ground of 0.7 m, a distance between rows of 2.3 m and different tilt angles [0°,90°]

In this case, the tilt angle that provides a maximum energy yield and, therefore, a maximum bifacial gain, is 14 °. Nevertheless, for this tilt angle is the soil effect is higher than for higher tilt angles and in the long term it would also affect the yearly generation. Higher tilt angles up to 25 ° would also mean higher output without such a great impact on the soiling effect.

7. Simulations

In chapter 6, first the power output of a bifacial power plant installed under the typical conditions of a conventional power plant with monofacial modules, i. e. same tilt angle (20°) and same albedo (estimated 17 %) is analysed for a long term period (August 2018 – April 2019) in part 6.1. Once known that the bifacial gain obtained in a power plant with no modification in the system parameters is 4 %, the individual effect of each system parameter has been analysed through short term measurements and simulation models validated with measurements in part 6.2, where it has been found that modules in large scale systems generate lower energy levels due to large shadowing areas cast by neighboring modules, that the albedo of the ground underneath the modules has a proportional impact on the bifacial gain and that the tilt angle is dependent on the distance between rows.

7.1. Parameters contribution rate

It has been known that parameters such as the albedo, tilt angle, size of the system and GCR have an impact on the energy yield. However, this is not enough to design a bifacial power plant, since almost every parameter depends on each other, moreover, not all of them have the same impact on the bifacial gain. In order to show the respective contribution rates of the significant design elements on the energy yield, different simulations with the simulation model proved with measurements have been carried out for different values of each significant design element and the variance of the resulting yearly specific energy yield has been calculated. The higher the variance, the more the yearly specific energy yield varies as a function of its respective design element and, therefore, the higher the contribution rate of it. Table 7.1 shows the analysis of variance:

Table 7.1. Analysis of variance (ANOVA).

<i>Parameter</i>	<i>DF</i>	σ^2	ρ
Albedo (%)	2	1374.35	51.47 %
Tilt angle (°)	2	902.16	33.79 %
GCR (%)	2	375.78	14.07 %
Elevation	2	17.86	0.67 %
Total	8	2670.14	100.00 %

DF: Degrees of Freedom, σ^2 : variance, ρ : contribution ratio.

The respective variance has been calculated with the following equation:

$$\sigma^2 = \frac{1}{N - 1} \cdot \sum_{i=1}^N (x_i - \bar{x})^2 \quad (7.1)$$

Where:

σ^2 : variance

N : number of samples

$N - 1$: degrees of freedom

x_i : discrete value

\bar{x} : mean

And the respective contribution rates of every system design parameter are calculated according to the following formula as the variance divided by the sum of all the variances.

$$\rho (\%) = \frac{\sigma^2_i}{\sigma^2_{tot}} \cdot 100 \quad (7.2)$$

Where:

ρ : contribution rate

σ^2_i : variance of the system design parameter i

σ^2_{tot} : sum of all variances

According to the analysis of variances, the parameter that has the most impact on the bifacial power plant performance is the albedo, followed by the tilt angle and then, the GCR. The parameter that affects the less to the energy yield is the height of the module, this is due to its saturated behavior at heights up to 0.7 m as shown in Figure 4.5.

Once known the contribution rates of the significant design elements on the energy yield, simulations are carried out with the validated model in order to analyze the combined effect of the design elements.

7.2. Combined effect of the design elements

Tilt angle, distance between rows and module rows per table

As shown in chapter 6.2.2, the optimum tilt angle is totally dependent on the size of the system and distance between rows. Therefore, various simulations are carried out for a bifacial power plant located in Marlow (Germany) in order to find out the effect of the system size in the optimum tilt angle. The simulations were designed for a power plant with a constant installed capacity of 766 kWp and different distances between rows as well as a different number of module rows in the table with landscape orientation, resulting in different GCR. The results of the simulations are depicted in Figure 7.1.

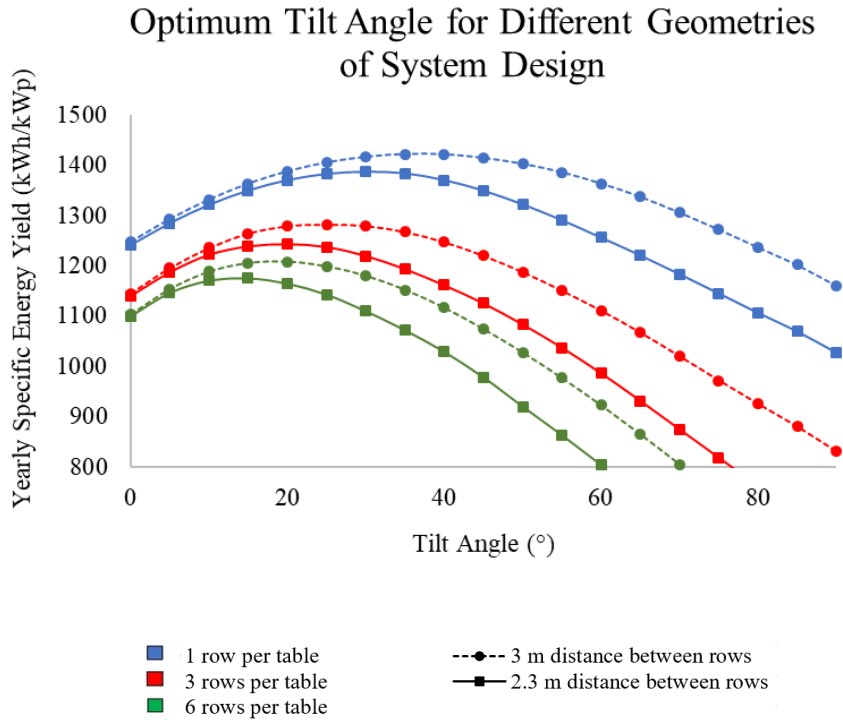


Figure 7.1. Yearly specific energy yield (kWh/kWp) for different tilt angles of a bifacial power plant installed in Marlow (Germany) with different distances between rows and different number of module-rows per table, a ground albedo of 44 % and a height between the lowest side of the table and the ground of 0.7 m.

For more visual information, Table 7.2 and

Table 7.3 Table 7.3 show the optimum tilt angle and the bifacial gain respectively for different distances between rows and a variety of number of module-rows on the table.

Table 7.2. Simulated optimum tilt angle for different distances between rows and different number of module-rows with landscape orientation on the table. The simulated power plant has a nominal front-side-power of 766 kWp, an albedo of 44 % and a height over the ground of 0.7 m.

Rows of modules per table	2 m	2.3 m	3 m	3.4 m
1	30 °	30 °	35 °	35 °
3	20 °	20 °	25 °	25 °
6	10 °	15 °	15 °	15 °

Table 7.3. Simulated bifacial gain for different distances between rows and different number of module-rows with landscape orientation on the table. The simulated power plant has a nominal front-side-power of 766 kWp, an albedo of 44 % and a height over the ground of 0.7 m.

Rows of modules per table	2 m	2.3 m	3 m	3.4 m
1	19 %	19 %	20 %	21 %
3	11 %	11 %	12 %	13 %
6	8 %	8 %	9 %	9 %

As it can be observed, the yearly energy yield, as well as the optimum tilt angle, vary for every geometry design of the power plant; the closer the modules are to each other, the lower the optimum tilt angle and the less the energy yield and, therefore, the lower the bifacial gain.

The Ground Coverage Ratio (GCR) is a useful concept to depict this effect. The GCR is defined as the ratio of module area to land area, the more the module-rows are separated from each other, the lower the GCR and, therefore, the less advantage taken from the land area. In Figure 7.2 the Bifacial Gain in Energy (BGE) is plotted as a function of the GCR.

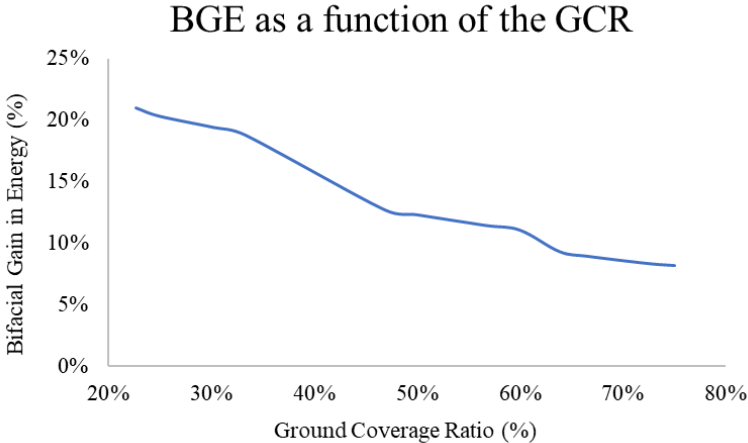


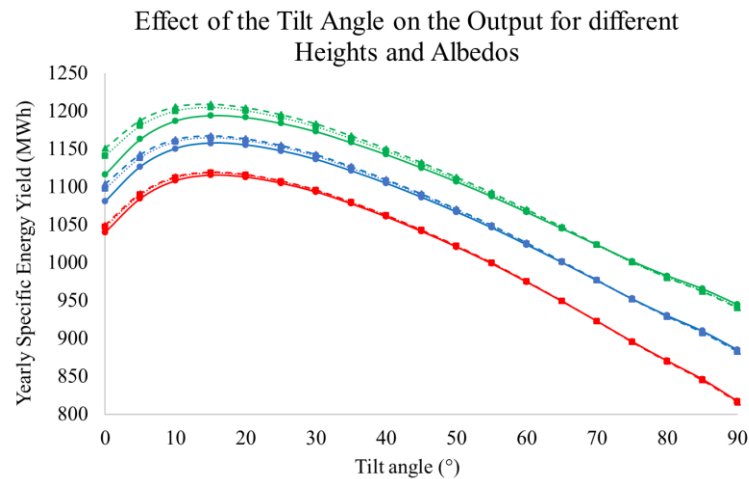
Figure 7.2. Measured and simulated power output for a single module with a front side power of 290 Wp a) for 10° tilt angle and b) for 20° tilt angle.

Therefore, the decision of which tilt angle should be used in a bifacial power plant is a compromise between finding the maximum bifacial gain and energy yield as possible without misusing the available land area.

Tilt angle, albedo and elevation

In chapter 6.2.2 the optimum tilt angle for a bifacial PV power plant was found to be 14° even though higher tilt angles up to 25° would also provide a high bifacial gain with less soiling losses. In order to find out if the albedo and elevation of the modules also have an impact on the optimum tilt angle, several simulations are carried out. The results are depicted in Figure 7.3.

a)



b)

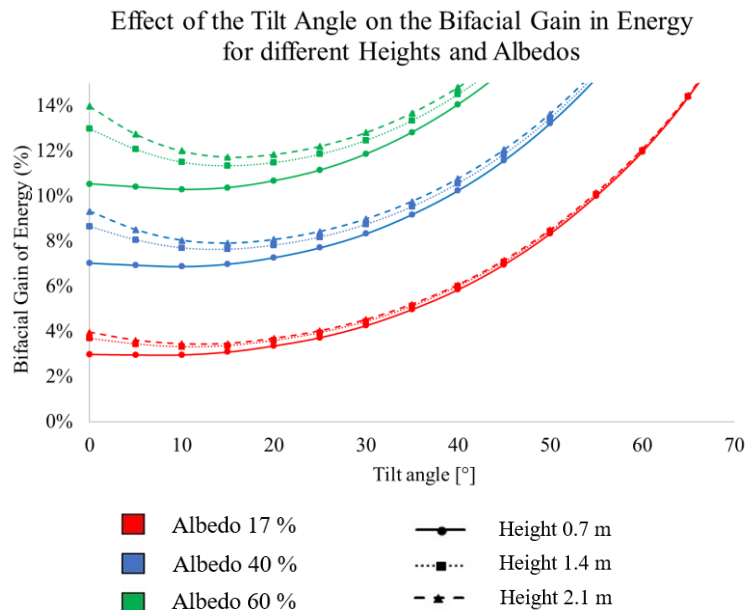


Figure 7.3 Effect of the tilted angle on a) energy yield and b) bifacial gain of energy. Data obtained from several simulations done with the program PVSyst for the period of a whole year for a 766 kWp PV plant located in Marlow (Germany) for south-north orientation, 6 modules per row, 2.3 m of distance between rows and different albedos and heights.

In Figure 7.3, on one side, it can be seen that the optimum tilt angle for a bifacial power plant stays constant for different albedos and heights, this means there is no correlation between the height and the albedo and the tilt angle. On the other side, it can also be seen that the higher the elevation of the

modules, slightly higher gets also the energy yield and the bifacial gain for tilt angles lower than 20° for lower albedos and for angles up to 35° for higher albedos.

8. Summary

The task of the present work was to find out the optimum geometry of system design for bifacial PV power plants in order to get the maximum performance out of a limited land area. Thus, research of the current status of the bifacial technology was done. Many recent developments in the bifacial PV industry were found (chapter 2); transparent backsheets and optimization for the interconnection of bifacial cells are ones of the examples of recent developments that will help to bring PV systems to lower Levelized Cost of Energy (LCOE) and thus, to help the bifacial market grow.

In addition, a review of recently published literature for bifacial systems installed under many different design geometries was done (chapter 3) in order to identify all the significant design elements and the expected bifacial gain for different combinations of each of them. This compilation of different works has shown that the energy yield for bifacial modules is heavily influenced by the rear side conditions.

Thus, indoor experiments have been carried out with a sample of bifacial module following the instructions given in the DIN EN 60904-1-2 in order to get the power generation gain as a function of the rear side irradiance and, therefore, the power output under bifacial standard test conditions (BSTC) (chapter 5). The BSTC are defined by the TÜV Reinhard as the power output for 1000 W/m² front side irradiance, 135 W/m² rear side irradiance, with the reference spectral irradiance distribution of AM1.5 and a device temperature of 25 °C. The BSTC is a very new concept and it is planned to become a standard in the future in order to help to predict the energy yield of a bifacial power plant.

Furthermore, through long term outdoor measurements carried out from August 2018 to April 2019, it was found that the bifacial gain is higher for the winter period than for the summer period, and that the yearly bifacial gain for a power plant with 20 ° tilt angle and an estimated albedo of 17 % is 4 % (chapter 6.1.3). A ground surface with high albedo would be desirable as it is one of the key parameters for bifacial module electrical performance.

To get to know the individual effect of the system design parameters, an experiment set up for outdoor measurements has been designed and built up. This set up allows to change the tilt angle and is equipped with an albedometer and a weather station that measures the Global Horizontal Irradiance (GHI), Diffuse Horizontal Irradiance (GHI) as well as the Direct Normal Irradiance (DNI). Hence, out of the short term measurements, it has been found out that modules in large scale systems generate up to 12 % lower energy levels than other modules in the same structure due to large shadowing areas cast by neighboring modules (Figure 6.15). In addition, it has also been shown that the albedo is directly proportional to the energy yield and that for an albedo of approx. 45 % for a power plant of the same characteristics as the power plant used for the long term measurements a bifacial gain of 8 % is obtained (Figure 6.27).

Since the optimum tilt angle varies with the sun's latitude and direction of incidence, which varies during the entire year, the analysis of the optimum tilt angle and the impact of it combined with other system design parameters is done by several simulations. The simulation model has been validated comparing it with the carried out measurements. The simulation showed that the albedo is the parameter that has the most impact on the bifacial power plant performance, followed by the tilt angle and then, the Ground Coverage Ratio (GCR). It has been found that for lower GCR, higher bifacial gains are obtained (Figure 7.2). Nevertheless, in order to get 10 % extra bifacial gain, just 1/3 of the land surface of what currently Enerparc AG uses would be used (Figure 7.2). It could also be seen through simulations analysis that

the tilt angle is on one side, totally dependent on the GCR (Figure 7.1) but totally independent on the height of the modules and the albedo of the ground underneath them (Figure 7.2).

It is necessary to mention that all bifacial gains were measured and calculated for a specific module with 75 % bifaciality. Certainly higher gains would be expected if a module with higher bifaciality is used.

Outlook

As the execution time for this master thesis was limited, it is recommended to take more measurements for an entire year in order to have the complete behavior of the bifacial gain during all the periods of the year. Furthermore, since a weather station that is capable to measure the DHI is available, it would also be interesting to find the correlation between the diffuse irradiance fraction and the bifacial gain.

In addition, according to published literature, it has been found that tracking bifacial PV systems can decrease the LCOE even further, a detailed analysis of the benefits of tracked bifacial systems would also be advisable as the second face of this work.

9. Bibliography

- [Alt17] Althoff, M. W. "Verschattungsanalyse und Ertragsprognose einer Photovoltaikanlage mit geringem Neigungswinkel und in der Modulebene diagonal gedrehten Modulen". Bachelorarbeit im Studiengang Umwelttechnik, 2017.
- [Ame17] Americas, S. "Calculating the Additional Energy Yield of Bifacial Solar Modules", 2017.
- [Asg17] Asgharzadeh, A. et al. "Analysis of the Impact of Installation Parameters and System Size on Bifacial Gain and Energy Yield of PV Systems", 2017.
- [Biz17] Bizzarri, F. ENEL "Innovative tracked bifacial PV plant at la Silla observatory in Chile", *presented at the Bifacial PV Workshop*, Konstanz, Germany, 26 Oct., 2017.
- [Bon19a] Bonilla, J., "Bifacial PV Modules: Performance Characterization and Energy Yield Measurements. PV magazine Webinar: New approach for bifacial modules and yield expectations", *presented at the PV magazine Webinar*, 29 April, 2019.
- [Bon19b] Bonilla Castro, J. N.; Herrmann, "Energy Yield Comparison between Bifacial and Monofacial PV Modules", *published at the PV Module Forum 2019*, 2019.
- [Boy04] Boyson, W. E.; King, D. L.; Kratochvill, J. A. "Photovoltaic Array Performance Model", 2004.
- [BSW19] BSW-Solar, "Bundesverband Solarwirtschaft". <https://www.solarwirtschaft.de/pressegrafiken/>.
- [Cas16] Castillo-Aguilella, J. E.; Hauser, P. S. Multi-Variable Bifacial Photovoltaic Module Test Results and Best-Fit Annual Bifacial Energy Yield Model. In *IEEE Access*, 2016, 4; pp. 498–506.
- [Cha18] Cha, H. et al. Power Prediction of Bifacial Si PV Module with Different Reflection Conditions on Rooftop. In *Applied Sciences*, 2018, 8; p. 1752.
- [Chi15] Chiodetti, M. "Bifacial PV plants: performance model development and optimization of their configuration", 2015.
- [Chu18] Chunduri, S. K.; Schmela, M., "TAIYANGNEWS: Bifacial Solar Module Technology", 2018.
- [Chu19] Chunduri, S., "What's hot in Advanced Module Technologies", *presented on the TaiyangNews Webinar on Advanced Module Technologies 2019 - How to Optimize PV Panels for Higher Output*, 2019.
- [Com14] Comparotto, C. et al., "Bifacial n-type solar modules: indoor and outdoor evaluation", in *Proceedings to the 29th European Solar Energy Conference EUPVSEC*, Amsterdam, 2014.

- [Cze18]** Czernie, F. TÜVRheinland "Measurement and Validation of Bifacial Modules' Power Output", *presented at the Solar Asset Management Europe*, 2018.
- [DIN17]** DIN EN 60904-1-2 "Photovoltaic devices. Part 1-2: Measurement of current-voltage characteristics of bifacial photovoltaic (PV) devices", 2017.
- [DiS17]** DiStefano, A.; Leotta, G.; Bizzarri, F. E. ENEL "La Silla PV Plant as a Utility-Scale Side-By-Side Test for Innovative Modules Technologies", *presented at the 33rd European Photovoltaic Solar Energy Conference and Exhibition (EUPVSEC)*, Amsterdam, 2017.
- [Dur12]** Duran, C. "Bifacial Solar Cells: High Efficiency Design, Characterization, Modules and Applications", 2012.
- [EPE19]** EPEXSPOT, <https://www.epexspot.com/en/>, *access date: 11.03.2019*, 2019.
- [Gana]** Gantner instruments "Surface Temperature Sensor Pt1000".
- [Ganb]** Gantner instruments, "Ambient Temperature Sensor Pt1000".
- [Gar19]** Garreau, L., Technology Innovation and Risk Mitigation of Solar Assets, *presented at the PV Operations Europe*, Munich, 28th February, 2019.
- [Gul18]** Gul, M. et al. "Enhancement of Albedo for Solar Energy Gain with Particular Emphasis on Overcast Skies". In *Energies*, 2018, 11; p. 6.
- [Guo13]** Guo, S.; Walsh, T. M.; Peters, M. "Vertically mounted bifacial photovoltaic modules: A global analysis". In *Energy*, 2013, 61; pp. 447–454.
- [Hil17]** Hildebrandt, H. Next2Sun "3 MWp vertical E-W oriented system in Germany", *presented at the bifi PV Workshop*, Konstanz, Germany, 25 Oct. 2017, 2017.
- [HUK18]** HUKSEFLUX "User Manual SRA02". Second class albedometer, 2018.
- [IEA19]** IEA, I. E. A., "Total Final Consumption (TFC) by source". <https://www.iea.org/statistics/?country=WORLD&year=2016&category=Energy%20consumption&indicator=TFCbySource&mode=chart&dataTable=BALANCES>, accessed 6 May 2019.
- [IEC07]** IEC 60904-9, "Photovoltaic devices - Part 9: Solar simulator performance requirements", 2007.
- [IEC08]** IEC 60904-7, "Photovoltaic devices - Part 7: Computation of the spectral mismatch correction for measurements of photovoltaic devices", 2008.
- [IEC19]** IEC 60904-3, "Photovoltaic devices - Part 3: Measurement principles for terrestrial photovoltaic (PV) solar devices with reference spectral irradiance data", 2019.

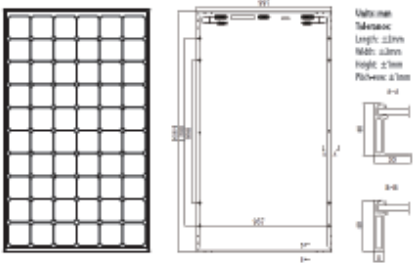
- [Ish16]** Ishikawa, N.; Nishiyama, S., "World First Large Scale 1.25 MW Bifacial PV Power Plant on Snowy Area in Japan", *presented at the 3rd bifi PV workshop*, Miyazaki, Japan, 29 Sep., 2016.
- [Joa17]** Joanny, M. et al., Bifacial Systems Overview, *presented at the Bifi PV workshop*, Konstanz, Germany, 25 Oct., 2017.
- [Jon18]** Jong, M. de, "Presentation", 2018.
- [Kha17]** Khan, M. R. et al. "Vertical bifacial solar farms: Physics, design, and global optimization". In *Applied Energy*, 2017, 206; pp. 240–248.
- [Kop16]** Kopecek, Radovan, et al., "Summary and Second day, 3rd BIFI Workshop", *presented at the 3rd BIFI Workshop*, Myazaki, Japan, 2016.
- [Kop18]** Kopecek, R.; Libal, J., "Bifacial PV world 2018. Technology, applications and economics", *presented at the Bifacial PV workshop*, Denver, USA, 10 Sep., 2018.
- [Kre11]** Kreinin, L. et al., "Experimental Analysis of the Increases in Energy Generation of Bifacial over Mono-Facial PV Modules", *presented in the 26th European Photovoltaic Solar Energy Conference and Exhibition*, Hamburg., 2011.
- [Kre17]** Kreiter, R. S. Sunfloat "Floating bifacials. Reflections on power", *presented at the bifi PV Workshop*, Konstanz, Germany, 25 Oct., 2017.
- [Küh19]** Kühn-Thomä, S. I. "Messungen und Simulationen von Mehrerträgen beim Vergleich von bifazialen zu konventionellen Photovoltaikmodulen", 2019.
- [LG]** LG Electronics Inc. "Bifacial Design Guide".
- [Lib18]** Libal, J.; Kopecek, R. "Bifacial Photovoltaics. Technology, applications and economics". IET, Stevenage, pp. 190-205, 2018.
- [Lic19]** Lichner, C. PV magazine. Next2Sun finanziert dritten bifazialen Solarpark über Energiegenossenschaft, 2019.
- [Mey18]** Meyer, C., "Vertical Bifacial: Grid-friendly and competitive agrophotovoltaic concept. New project of Dirmingen", 2018, Paris.
- [NAS02]** NASA, "Visible Earth catalog", accessed 8 Jan 2019.
- [Pod17]** Podlowski, L.; Wendlandt, S., "Yield Study on Identical Bifacial Rooftop Systems Installed in the USA and in Germany, *presented at the bifi PV Workshop*, Konstanz, Germany, 25 Oct., 2017.
- [SAN16]** SANYO, Data Sheet "SANYO HIT-210_205_200 DNKHE1 (EN)_modositott1", 2016.

- [Sch17]** Schmid, A., "IV measurement of bifacial modules: bifacial vs. monofacial illumination", *Presented at the 33rd European PV Solar Energy Conference and Exhibition, 25-29 September, Amsterdam, 2017.*
- [Sch18]** Schweiger, M., "Bifacial Modules - Verifying Module Power and Output". Next Generation Solutions for Solar Renewables and Energy Storage, *Presented at the Intersolar Europe Side Event, Munich, 21 June, 2018.*
- [Sho15]** Shoukry, I. "Bifacial Modules: Simulation and Experiment", 2015.
- [Sol18]** Solar Builder, "Tracking Trackers: We look at what's new with these seven solar trackers"" 5 Jul., 2018.
- [Sol19]** SolPEG, "Ertragsgutachten PV-Freiflächenanlagen bis 750 kWp Marlow. Ermittlung der anfänglichen durchschnittlichen Stromproduktion einer Photovoltaik Freiflächenanlage nahe Marlow in Mecklenburg-Vorpommern", 2019.
- [Ste17]** Stein, J. S.; Burnham, L.; Lave, M. "One Year Performance Results for the Prism Solar Installation at the New Mexico Regional Test Center: Field Data from February 15, 2016 - February 14, 2017". SANDIA REPORT, 2017.
- [Sug13]** Sugibuchi, K.; Ichikawa, N.; Obara, S., "Bifacial-PV Power Output Gain in the Field Test Using 'EarthON' High Bifaciality Solar Cells", *presented at the 28th European Photovoltaic Solar Energy Conference and Exhibition, Paris, 2013.*
- [Sun18]** Sun, X. et al. "Optimization and performance of bifacial solar modules: A global perspective". In *Applied Energy*, 2018, 212; pp. 1601–1610.
- [Thu18]** Thurston, C. W., "Tracker market is adapting to bifacial module technology", *PV magazine*, 17 Feb., 2018.
- [Ver17]** Vermeulen, W., "400kW bifacial system in NL and comparison with two other systems", *presented at the bifacial PV workshop, Konstanz, October 25th, 2017.*
- [Vol16]** Volker Quaschnig "Understanding Renewable Energy Systems", 2016.
- [Wah19]** Wahl, W., "Latest Advanced Module Product Developments from LONGi Solar", *presented at the TaiyangNews Webinar on Advanced Module Technologies 2019 - How to Optimize PV Panels for Higher Output, 2019.*
- [Wil16]** Wilbert, S. et al. Eds. "Uncertainty of Rotating Shadowband Irradiometers and Si-Pyranometers Including the Spectral Irradiance Error". Author(s), 2016.
- [Win18]** Winfried Wahl "Bifacial Modules with Hi.MO2 Technology", 2018.

[Yan08] Yang, F. et al. "Dependence of Land Surface Albedo on Solar Zenith Angle: Observations and Model Parameterization". In *Journal of Applied Meteorology and Climatology*, 2008, 47; pp. 2963–2982.

Appendix A: Bifacial module LR6-60BP 290M datasheet

LR6-60BP 290~310M

Design (mm)	Mechanical Parameters	Operating Parameters
 <p> Ultra-thin Silencioac Length: 33mm Width: 33mm Height: 2.5mm Pitch: 2.5mm </p>	Cell Orientation: 60 (6×10) Junction Box: IP67, three diodes Output Cable: 4mm ² , 300mm in length, length can be customized Connector: MCA or MCA comparable Weight: 22kg Dimension: 1664×997×40mm Packaging: 26pcs per pallet	Operational Temperature: -40℃ ~ +85℃ Power Output Tolerance: 0 ~ +5 W Voc and Isc Tolerance: ±3% Maximum System Voltage: DC1500V (IEC) Maximum Series Fuse Rating: 20A Nominal Operating Cell Temperature: 45±2℃ Application Class: Class II Bifaciality: ≥75%

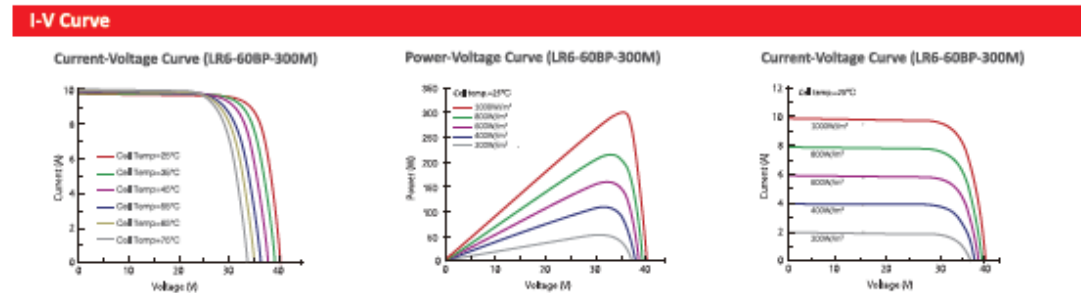
Electrical Characteristics	Test uncertainty for Pmax: ±3%									
	Model Number	LR6-60BP-290M		LR6-60BP-295M		LR6-60BP-300M		LR6-60BP-305M		LR6-60BP-310M
Testing Condition	Front	Back	Front	Back	Front	Back	Front	Back	Front	Back
Maximum Power (Pmax/W)	290	218	295	222	300	226	305	229	310	233
Open Circuit Voltage (Voc/V)	39.2	38.9	39.4	39.1	39.6	39.3	39.8	39.5	40.0	39.7
Short Circuit Current (Isc/A)	9.36	7.16	9.47	7.25	9.58	7.33	9.69	7.42	9.80	7.50
Voltage at Maximum Power (Vmp/V)	32.6	33.3	32.7	33.5	32.9	33.7	33.1	33.8	33.2	34.0
Current at Maximum Power (Imp/A)	8.90	6.54	9.01	6.63	9.11	6.71	9.22	6.77	9.33	6.85
Module Efficiency(%)	17.5	13.1	17.8	13.4	18.1	13.6	18.4	13.8	18.7	14.0

STC (Standard Testing Conditions): Irradiance 1000W/m², Cell Temperature 25℃, Spectra at AM1.5

Electrical characteristics with different rear side power gain (reference to 300W front)

Pmax /W	Voc/V	Isc /A	Vmp/V	Imp /A	Pmax gain
315	39.6	9.94	32.9	9.58	5%
330	39.6	10.40	32.9	10.04	10%
360	39.7	11.35	32.8	10.98	20%
375	39.7	11.82	32.8	11.44	25%

Temperature Ratings (STC)	Mechanical Loading		
Temperature Coefficient of Isc	+0.060%/℃	Front Side Maximum Static Loading	5400Pa
Temperature Coefficient of Voc	-0.300%/℃	Rear Side Maximum Static Loading	2400Pa
Temperature Coefficient of Pmax	-0.380%/℃	Hailstone Test	25mm Hailstone at the speed of 23m/s

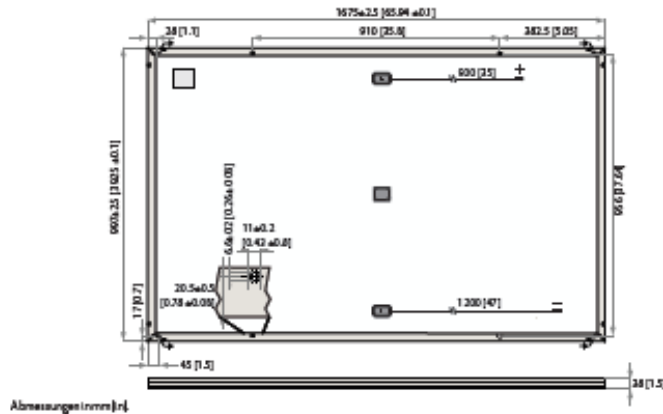


Room 201, Building 8, Sandhill Plaza, Lane 2290, Zuchongzhi Road, Pudong District, Shanghai, 201203
 Tel: +86-21-61047332 Fax: +86-21-61047377 E-mail: module@longi-silicon.com
 Facebook: www.facebook.com/LONGi Solar

Note: Due to continuous technical innovation, R&D and improvement, technical data above mentioned may be of modification accordingly. LONGi Solar have the sole right to make such modification at anytime without further notice; Demanding party shall request for the latest datasheet for such as contract need, and make it a consisting and binding part of lawful documentation duly signed by both parties.

Appendix B: Monofacial reference module REC Twinpeak 290 datasheet

REC TWINPEAK 2 SERIES



Abmessungen (mm) [in]

ELEKTRISCHE DATEN @ STC*	Produktbezeichnung: RECxxxTP2				
Nennleistung - P_{MPP} (Wp)	275	280	285	290	295
Leistungstoleranz - (W)	0/+5	0/+5	0/+5	0/+5	0/+5
Nennspannung im MPP - U_{MPP} (V)	31,5	31,7	31,9	32,1	32,3
Nennstrom im MPP - I_{MPP} (A)	8,74	8,84	8,95	9,05	9,14
Leerlaufspannung - U_{OC} (V)	38,2	38,4	38,6	38,8	39,0
Kurzschlussstrom - I_{SC} (A)	9,30	9,39	9,49	9,58	9,65
Modulwirkungsgrad (%)	16,5	16,8	17,1	17,4	17,7

Werte unter Standardtestbedingungen: STC (Luftmassa AM 1.5, Einstrahlung 1000 W/m², Zelltemperatur: 25°C).
 Bei geringerer Einstrahlung von 200 W/m², AM 1.5 und Zelltemperatur 25°C wird mindestens 95% der STC Moduleffizienz (1000 W/m²) erreicht.
 *xxx bezieht sich auf die angegebene Leistung P_{MPP} @ STC, und wird durch die Buchstaben BLK für Module mit schwarzem Rahmen ergänzt.

ELEKTRISCHE DATEN @ NOCT*	Produktbezeichnung: RECxxxTP2				
Nennleistung - P_{MPP} (Wp)	206	210	214	218	221
Nennspannung im MPP - U_{MPP} (V)	29,2	29,4	29,6	29,8	30,0
Nennstrom im MPP - I_{MPP} (A)	7,07	7,15	7,24	7,32	7,37
Leerlaufspannung - U_{OC} (V)	35,4	35,6	35,8	36,0	36,2
Kurzschlussstrom - I_{SC} (A)	7,52	7,59	7,68	7,75	7,81

Nennbetriebs Temperatur der Zelle NOCT (800 W/m², AM 1.5, Windlast 1 m/s, Umgebungstemperatur 20°C).
 *xxx bezieht sich auf die angegebene Leistung P_{MPP} @ STC, und wird durch die Buchstaben BLK für Module mit schwarzem Rahmen ergänzt.

ZERTIFIKATE
IEC 61215, IEC 61730 & UL 1703, IEC 62804 (PID Free), IEC 61701 (Salz nebeltest Schirfregende), IEC 62716 (Ammoniakbeständigkeit), 6011925-2 (Ignitability Class E), UNI 8457/074 (Class I), ISO 9001:2015, ISO 14001, OHSAS 18001

takeaway
 for an easy way
 Recyclingpartnerschaft Konformizer
 WEEE-Richtlinie mit take-away

GARANTIE
10 Jahre Produktgarantie
25 Jahre lineare Leistungsgarantie (eine maximale Leistungsdegradation von 0,7% p.a.)
Siehe Garantiebedingungen für weitere Details.

17,7% EFFIZIENZ
10 JAHRE PRODUKTGARANTIE
25 JAHRE LINEARE LEISTUNGSGARANTIE

TEMPERATUREIGENSCHAFTEN	
Nennbetriebs Temperatur der Zelle (NOCT)	44,6°C (±2°C)
Temperaturkoeffizient P_{MPP}	-0,36 %/°C
Temperaturkoeffizient V_{OC}	-0,30 %/°C
Temperaturkoeffizient I_{SC}	0,066 %/°C

ALLGEMEINE INFORMATIONEN	
Zelltyp:	120 REC HC multikristallin 6 Strings mit 20 Zellen
Glas:	3,2 mm Solarglas mit spezieller, antireflektiver Oberflächenbehandlung
Rückseitenfolie:	Hochbeständiges Polyester Polyolefin Konstruktion
Rahmen:	Eloxiertes Aluminium (Mit silberner oder schwarzer Rahmenanfertigung)
Junction box:	Dreitellig mit 3 Bypass Dioden, IP67 konform 4 mm ² Solarkabel, 0,9 m + 1,2 m
Stecker*:	Stäubli MC4 PV-KBT4/PV-KST4 (4 mm ²) Tonglin TL-Cable 015FR (4 mm ²) *Je nach Produkttyp

MAXIMALWERTE	
Betriebstemperatur:	-40 .. +85°C
Maximale Systemspannung:	1000 V
Maximale Schneelast:	550 kg/m ² (5400 Pa)
Maximale Windlast:	244 kg/m ² (2400 Pa)
Max. Versicherungswert:	25 A
Max. Rückstrom:	25 A

MECHANISCHE DATEN	
Maße:	1675 x 997 x 38 mm
Fläche:	1,67 m ²
Gewicht:	18,5 kg

Hinweis! Technische Änderungen vorbehalten.







Rev: REC-0507-07 Rev: E-04-17

Aus einer Norwegischen Gründung im Jahr 1996 heraus hat sich REC zu einer führenden, vertikal integrierten Solarenergiefirma entwickelt. Mit der eigenen Herstellung von Silizium, Wafern, Zellen und Modulen versorgt REC die Welt verlässlich mit sauberer Energie. Dank unserer bekannten Produktqualität erfreuen wir uns einer der niedrigsten Reklamationsraten in der Industrie. REC gehört zu Bluestar Elkem mit Hauptsitz in Norwegen und operativen Geschäftssitz in Singapur. Mit mehr als 2.000 Mitarbeitern weltweit produzieren wir jährlich Qualitätsmodule mit 1,4 GW.

REC
 www.recgroup.com

Appendix C: Helios Scale Phi

HelioScale Φ [phi]

HELIOSCALE PHI		TECHNICAL SPECIFICATIONS	
Rotating Shadowband Irradiometer (RSI) DNI, GHI & DIF [W/m ²]		Sensing element	Silicon photodiode (LI-COR LI-200)
		Output signal global irradiance	0 to 1500 [W/m ²] – 0 to 135 μ A
		Output signal diffuse irradiance	0 to 1500 [W/m ²] – 0 to 135 μ A
		Output temperature	-40 to +60 °C – 2.3315 to 3.3315 V- (10 mV/K)
		Spectral response	400 to 1100 nm
		Longterm accuracy of DNI	\pm 3 %
		Response time	10 μ s
		Operating temperature	-40 to +70 °C
		Relative humidity	0 to 100%
		Silicon Based Pyranometer [W/m ²]	
Zero offset – Thermal rad. (200 W/m ²)	0 W/m ²		
Spectral range	400 to 1100 nm		
Operating temperature range	-30 to +70 °C		
Non-stability (change/year)	\pm 2%		
Thermo Hygro Sensor Air-temperature [°C]		Sensing element	Semi-conductor temperature with capacitive humidity sensor
		Transducer	Electronical with serial output
		Output signal	RS485
		Accuracy	\pm 0.5 °C from 0 to 40 °C
		Operating temperature	-40 to +80 °C
		Accuracy	\pm 2% from 10 to 90 %RH
		Typical long-term stability	\pm 1 %RH/a
		Response time	<10 s
		Radiation shield	Naturally aspirated multi-plate radiation shield
		Barometric Pressure Sensor Barometric Pressure [hPa]	
Measuring range	400 to 1100 hPa		
Resolution	0.1 hPa		
Long-term stability	\pm 0.5 hPa/a		
Data Logging System blueberry COMPACT		Digital inputs	10
		Analogue inputs	6 differential or 12 single ended
		Additional inputs	Via RS485 and INPUT modules
		Serial inputs	RS485, half-duplex, RS232 for modem
		Analogue measuring range	0 to 10 V
		Resolution	16 bit, autoranging
		Measuring interval	1 s to 24 h
		Statistical interval	1 s to 24 h
		Statistical functions	Mean value, standard deviation, max, min, sum
		Data memory	1 GB (non-volatile ring buffer)
		Data interface	RS232 interface, 1200 to 115200 baud, RS485 interface, half duplex, 1200 to 115200 baud
		Remote data transfer	Ethernet interface (LAN), 10 MBit/s, GSM, GPRS, DSL, ISDN router
		External power supply	15 to 30 VDC or solar panel (optional 120/220)
		Power consumption	Typ. 600 mW (50 mA at 12 V)
		Sensor excitation	12 VDC switched, max. 100 mA
Temperature range	-40 to +70 °C		
Technical Surrounding		Autonomous power supply	
		Lightning protection & grounding kit	
		Waterproof enclosure	

Appendix D: I-V 400 W



I-V400w

Rel. 1.09 – 09/10/15

I-V curve tracer and IVCK tester up to 15A

Pag 2 of 3

2. ELECTRICAL SPECIFICATIONS

Accuracy is calculated as \pm [% reading + (number of dgts) x resolution] at 23 °C \pm 5 °C, <80%HR

VDC Voltage @ OPC

Range (V) (***)	Resolution (V)	Accuracy
5.0 ÷ 999.9	0.1	$\pm(1.0\%rdg+2dgt)$

(***) The I-V curve and Rs measurements start for VDC > 15V and the accuracy is defined for VDC > 20V

IDC Current @ OPC

Range (A)	Resolution (A)	Accuracy
0.10 ÷ 15.00	0.01	$\pm(1.0\%rdg+2dgt)$

Max Power @ OPC (Vmpp >30V, Impp >2A)

Range (W) (*, **)	Resolution (W)	Accuracy
50 ÷ 9999	1	$\pm(1.0\%rdg+6dgt)$

Vmpp = Maximum power voltage, Impp = Maximum Power Current

(*) Max measurable value of Power must include FF value (~ 0.7) $\rightarrow P_{max} = 1000V \times 10A \times 0.7 = 7000W$

(**) Test is stopped and the message "Thermal instability" occurs if the instrument detects Voltage > 700V and Current I > 3A, I > -0.038V + 37.24 - 0.5

VDC Voltage (@ STC and OPC), IVCK

Range (V) (***)	Resolution (V)	Accuracy (*, **)
5.0 ÷ 999.9	0.1	$\pm(4.0\%rdg+2dgt)$

IDC Current (@ STC and OPC), IVCK

Range (A)	Resolution (A)	Accuracy (**)
0.10 ÷ 15.00	0.01	$\pm(4.0\%rdg+2dgt)$

Max Power @ STC (Vmpp >30V, Impp >2A)

Range (W) (*, **)	Resolution (W)	Global accuracy (**)
50 ÷ 9999	1	$\pm(5.0\%rdg+1dgt)$

Vmpp = Maximum power voltage, Impp = Maximum Power Current

(*) Measurements start for VDC > 15V and the accuracy is defined for VDC > 20V

(**) Test conditions:

- Test cond.: Steady Irrad. $\geq 700W/m^2$, spectrum AM 1.5, solar incidence vs perpendicular. $\leq \pm 25^\circ$, Cells Temp. [15..65°C]
- Global accuracy include contribute of solar sensor and its measuring circuit

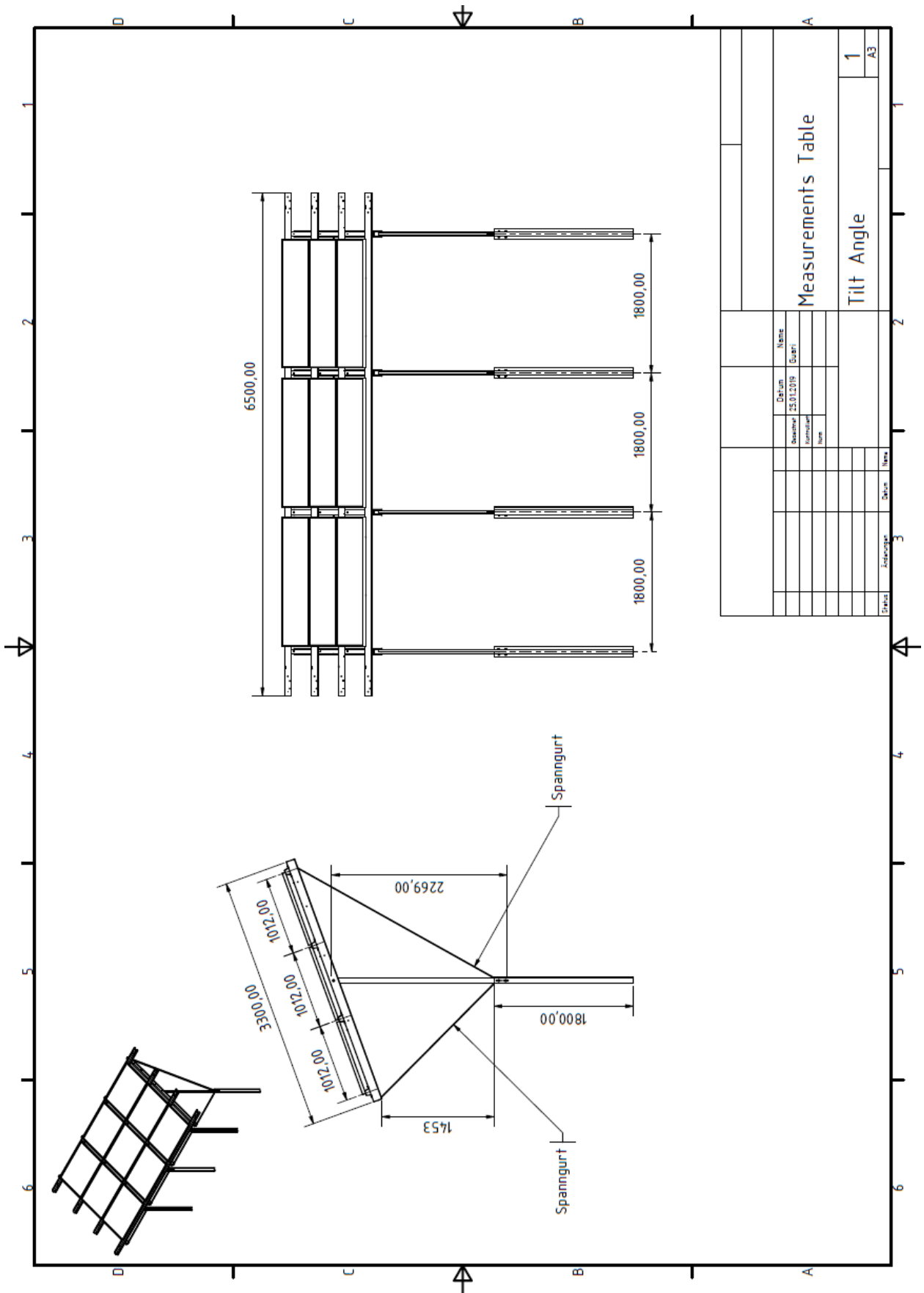
Irradiance (with reference cell)

Range (mV)	Resolution (mV)	Accuracy
1.0 ÷ 100.0	0.1	$\pm(1.0\%rdg+5dgt)$

Temperature of module (with auxiliary PT1000 probe)

Range (°C)	Resolution (°C)	Accuracy
-20.0 ÷ 100.0	0.1	$\pm(1.0\%rdg+1^\circ C)$

Appendix E: Measurements Table



Appendix F: Simulations

System:

Global System configuration

Number of kinds of sub-arrays:

Simplified Schema

Global system summary

Nb. of modules	2640	Nominal PV Power	766 kWp
Module area	4375 m ²	Maximum PV Power	689 kWdc
Nb. of inverters	12	Nominal AC Power	720 kWac

Sub-array #1

Sub-array name and Orientation

Name:

Orient: **Unlimited sheds**

Tilt: **20°**
Azimuth: **0°**

Presizing Help

No sizing Enter planned power kWp

... or available area(modules) m²

Select the PV module

Available Now: Filter:

Bifacial module Bifacial system

Longi Solar | 290 Wp 27V Si-mono LR6-60BP-290M-frame | Longi 201804

Sizing voltages: V_{mpp} (60°C) **27.6 V**
V_{oc} (-10°C) **44.0 V**

Use Optimizer

Select the inverter

Available Now: Output voltage 400 V Tri 50Hz 50 Hz 60 Hz

Sungrow | 60 kW 570 - 950 V TL 50/60 Hz SG60KTL | Since 2014

Nb. of inverters:

Operating Voltage: **570-950 V** Global Inverter's power **720 kWac**
Input maximum voltage: **1000 V** **"String" inverter with 14 inputs**

Design the array

Number of modules and strings

Mod. in series: between 21 and 22

Nbre strings:

Overload loss: **0.0 %**
P_{nom} ratio: **1.06**

Nb. modules: 2640 Area: 4375 m²

Operating conditions

V _{mpp} (60°C)	607 V
V _{mpp} (20°C)	720 V
V _{oc} (-10°C)	968 V

Plane irradiance: **1000 W/m²**

I_{mpp} (STC): 1089 A
I_{sc} (STC): 1151 A
I_{sc} (at STC): 1151 A

Max. in data STC
Max. operating power at 1000 W/m² and 50°C: **692 kW**

Array nom. Power (STC) 766 kWp

Results:

PVSYST V6.77		Enerparc AG (Germany)		15/05/19		Page 1/4	
Grid-Connected System: Simulation parameters							
Project :		Marlow Measurements Comparisson					
Geographical Site		Marlow		Country		Germany	
Situation		Latitude 54.16° N		Longitude 12.56° E			
Time defined as		Legal Time Time zone UT+1		Altitude 36 m			
Meteo data:		Marlow		SolPEG 2019 - Künstlich			
Simulation variant :		Marlow 766 kWp final					
		Simulation date		15/05/19 04h20			
Simulation parameters		System type		Unlimited sheds			
Collector Plane Orientation		Tilt 20°		Azimuth		0°	
Sheds configuration		Nb. of sheds 30		Unlimited sheds			
		Sheds spacing 8.03 m		Collector width 6.05 m			
Inactive band		Top 0.02 m		Bottom 0.02 m			
Shading limit angle		Limit profile angle 41.7°		Ground cov. Ratio (GCR) 75.3 %			
Shadings electrical effect		Cell size 15.6 cm		Strings in width 1			
Models used		Transposition Perez		Diffuse Perez, Meteonom			
Horizon		Free Horizon					
Near Shadings		Mutual shadings of sheds		Electrical effect			
Bifacial system		Model		Unlimited sheds, 2D calculation			
		Sheds spacing 8.03 m		Sheds width 6.09 m			
		Limit profile angle 42.1°		GCR 75.8 %			
		Ground albedo 44.0 %		Height above ground 1.50 m			
		Module bifaciality factor 75 %		Rear shading factor 0.0 %			
		Module transparency 12.8 %		Rear mismatch loss 3.0 %			
User's needs :		Unlimited load (grid)					
PV Array Characteristics							
PV module		Si-mono Model		LR6-60BP-290M-frame			
Custom parameters definition		Manufacturer		Longi Solar			
Number of PV modules		In series 22 modules		In parallel 120 strings			
Total number of PV modules		Nb. modules 2640		Unit Nom. Power 290 Wp			
Array global power		Nominal (STC) 766 kWp		At operating cond. 692 kWp (50°C)			
Array operating characteristics (50°C)		U mpp 636 V		I mpp 1089 A			
Total area		Module area 4375 m²		Cell area 3892 m²			
Inverter		Model		SG60KTL			
Original PVsyst database		Manufacturer		Sungrow			
Characteristics		Operating Voltage 570-950 V		Unit Nom. Power 60.0 kWac			
Inverter pack		Nb. of inverters 12 units		Total Power 720 kWac		Pnom ratio 1.06	
PV Array loss factors							
Array Soiling Losses				Loss Fraction 1.0 %			
Thermal Loss factor		Uc (const) 29.0 W/m²K		Uv (wind) 0.0 W/m²K / m/s			
Wiring Ohmic Loss		Global array res. 4.6 mOhm		Loss Fraction 0.7 % at STC			
LID - Light Induced Degradation				Loss Fraction 1.0 %			
Module Quality Loss				Loss Fraction -0.8 %			
Module Mismatch Losses				Loss Fraction 0.5 % at MPP			
Strings Mismatch loss				Loss Fraction 0.10 %			

Copyright Licensed to Enerparc AG (Germany)

Grid-Connected System: Simulation parameters

Incidence effect (IAM): User defined profile

0°	20°	30°	40°	50°	60°	70°	80°	90°
1.000	1.000	1.000	1.000	1.000	1.000	0.950	0.760	0.000

System loss factors

AC wire loss inverter to transfo	Inverter voltage	400 Vac tri		
	Wires: 3x700.0 mm ²	79 m	Loss Fraction	1.0 % at STC
External transformer	Iron loss (24H connexion)	680 W	Loss Fraction	0.1 % at STC
	Resistive/Inductive losses	1.9 mOhm	Loss Fraction	0.9 % at STC

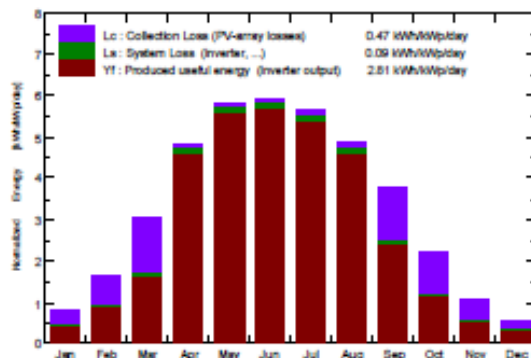
Grid-Connected System: Main results

Project : Marlow Measurements Comparisson
Simulation variant : Marlow 766 kWp final

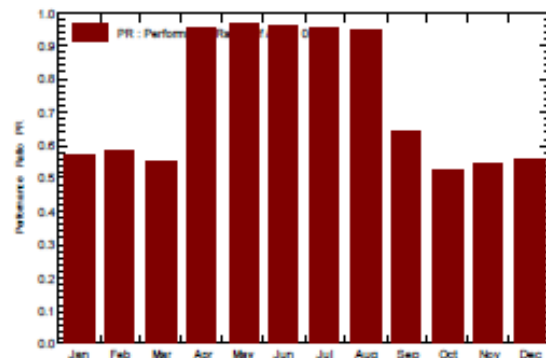
Main system parameters		System type	Unlimited sheds	
PV Field Orientation	Sheds disposition, tilt	20°	azimuth	0°
PV modules	Model	LR6-60BP-290M-frame	Pnom	290 Wp
PV Array	Nb. of modules	2640	Pnom total	766 kWp
Inverter	Model	SG60KTL	Pnom	60.0 kW ac
Inverter pack	Nb. of units	12.0	Pnom total	720 kW ac
User's needs	Unlimited load (grid)			

Main simulation results		Produced Energy	785.0 MWh/year	Specific prod.	1025 kWh/kWp/year
System Production		Performance Ratio PR	83.32 %		

Normalized productions (per installed kWp): Nominal power 766 kWp



Performance Ratio PR



Marlow 766 kWp final Balances and main results

	GlobHor kWh/m ²	DiffHor kWh/m ²	T_Amb °C	GlobInc kWh/m ²	GlobEff kWh/m ²	EArray MWh	E_Grid MWh	PR
January	16.6	11.40	1.30	25.4	18.7	12.0	11.1	0.569
February	32.8	20.90	1.60	45.4	37.0	21.2	20.2	0.582
March	75.7	40.90	3.90	95.1	85.6	41.5	40.1	0.551
April	126.0	57.60	8.40	145.1	137.3	108.8	105.9	0.953
May	167.5	73.30	13.00	179.5	169.6	136.3	132.7	0.965
June	172.6	81.30	16.00	178.2	167.9	135.1	131.4	0.963
July	168.8	82.30	18.80	176.2	165.7	131.9	128.4	0.952
August	136.6	67.60	18.00	151.4	142.7	112.6	109.6	0.946
September	93.4	48.80	14.70	113.5	104.6	57.9	56.2	0.846
October	51.5	29.70	10.10	70.1	58.6	29.4	28.2	0.525
November	20.8	13.60	5.90	32.3	23.7	14.4	13.5	0.545
December	11.6	8.40	2.60	18.3	13.0	8.7	7.8	0.557
Year	1073.9	535.79	9.58	1230.5	1124.6	809.8	785.0	0.833

Legends:	GlobHor	Horizontal global irradiation	GlobEff	Effective Global, corr. for IAM and shadings
	DiffHor	Horizontal diffuse irradiation	EArray	Effective energy at the output of the array
	T_Amb	Ambient Temperature	E_Grid	Energy injected into grid
	GlobInc	Global incident in coll. plane	PR	Performance Ratio

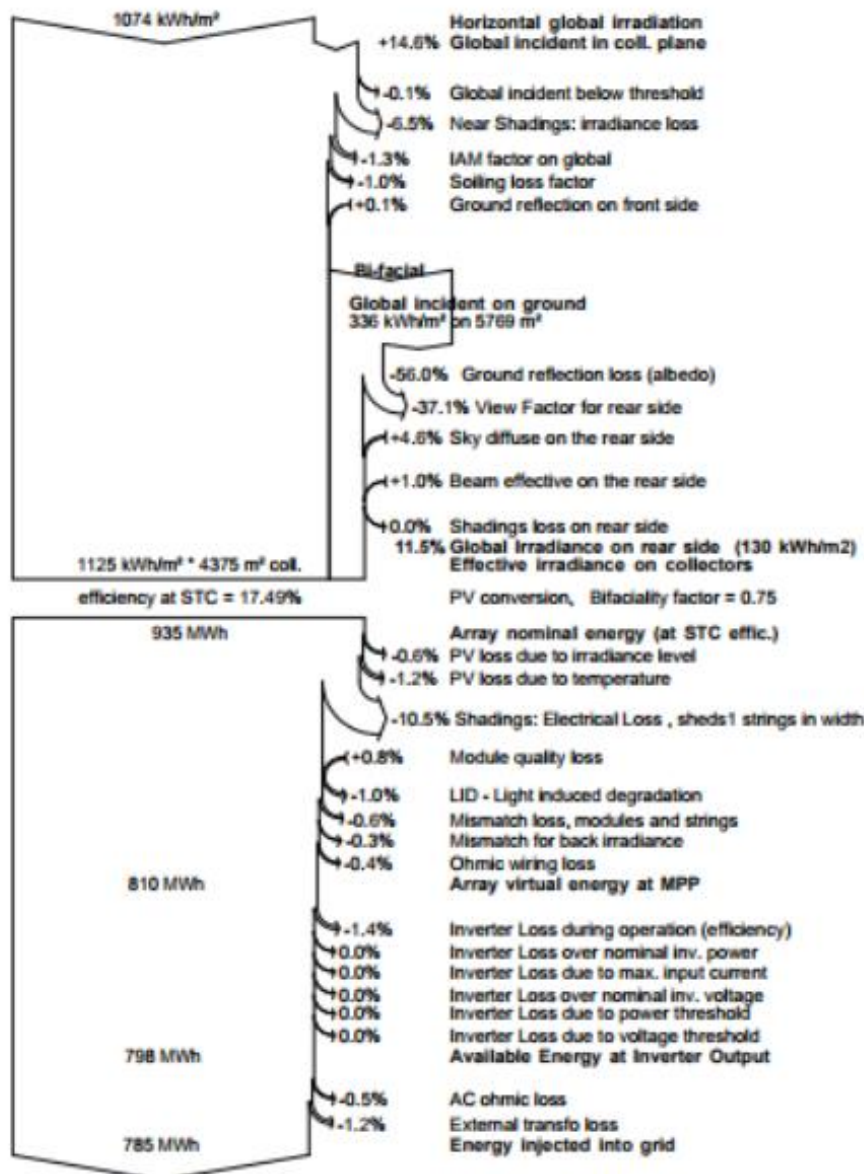
Grid-Connected System: Loss diagram

Project : Marlow Measurements Comparisson

Simulation variant : Marlow 766 kWp final

Main system parameters	System type	Unlimited sheds		
PV Field Orientation	Sheds disposition, tilt	20°	azimuth	0°
PV modules	Model	LR6-60BP-290M-frame	Pnom	290 Wp
PV Array	Nb. of modules	2640	Pnom total	766 kWp
Inverter	Model	SG60KTL	Pnom	60.0 kW ac
Inverter pack	Nb. of units	12.0	Pnom total	720 kW ac
User's needs	Unlimited load (grid)			

Loss diagram over the whole year



Project Licensed to Enerparc AG (Germany)